Development of Microactuator Technologies for Space Applications

Dr. Eui-Hyeok (EH) Yang

Nano and Micro Systems
NASA Jet Propulsion Laboratory

NASA's JPL Operated by Caltech

National Aeronautics and Space Administration
Jet Propulsion Laboratory
California Institute of Technology

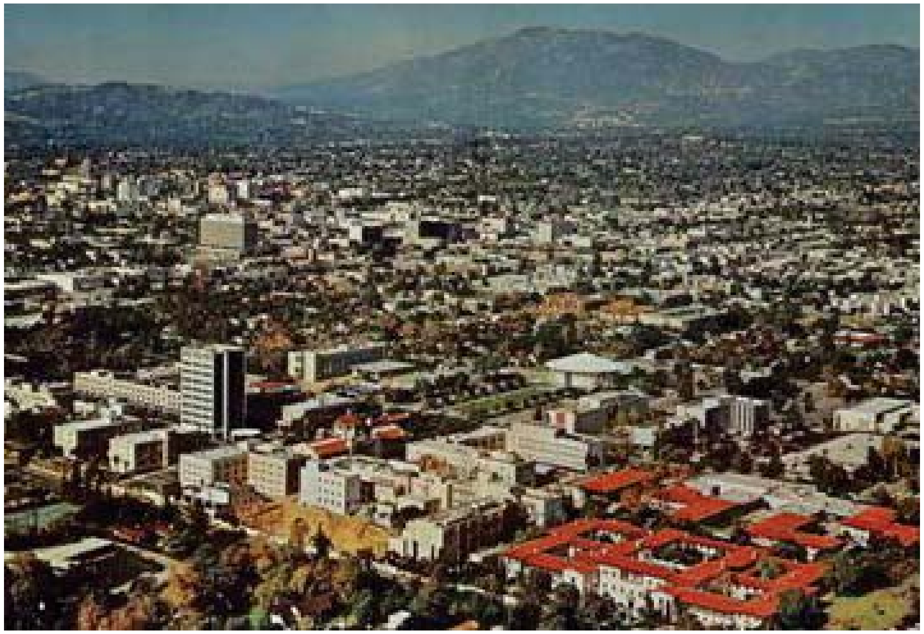

- Has a dual character:
  - A Federally-Funded Research and Development Center (FFRDC) under NASA;
  - A division of Caltech, staffed with 5500 employees;
- Is a major national research and development (R&D) capability supporting:
  - NASA programs;
  - Defense programs and civilian programs of national importance.

•JPL led the development of US rocket technology in WWII.

•JPL was transferred to NASA upon its creation in 1958.

•Developed the first U.S. satellite, Explorer I.

•JPL spacecraft have explored all the planets of the solar system except Pluto.

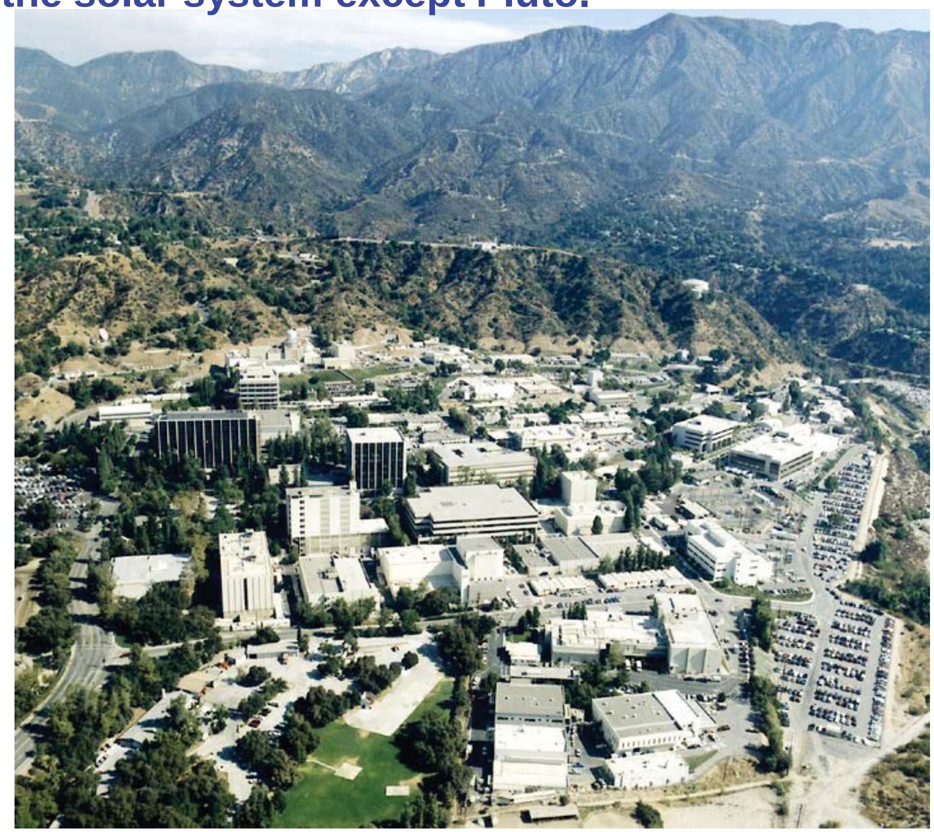

National Aeronautics and Space Administration
Jet Propulsion Laboratory
California Institute of Technology

Seventeen JPL Spacecraft, and Three Major Instruments, Operating across the Solar System

Spitzer studying stars and galaxies in the infrared

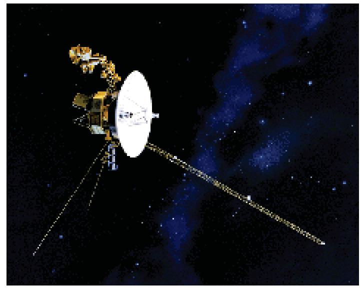

Two Voyagers on an interstellar mission

Cassini studying Saturn

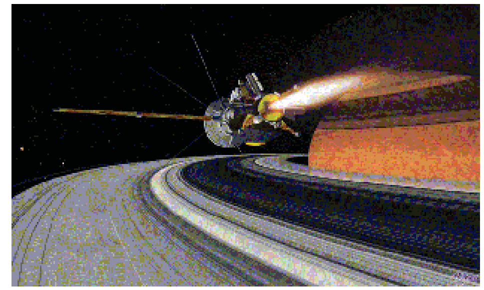

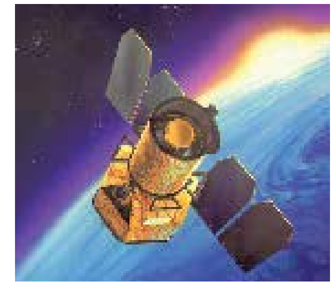

GALEX studying UV universe

Ulysses, Genesis, and ACRIMSAT studying the sun

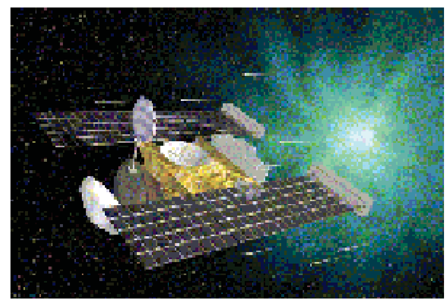

Stardust returning comet dust

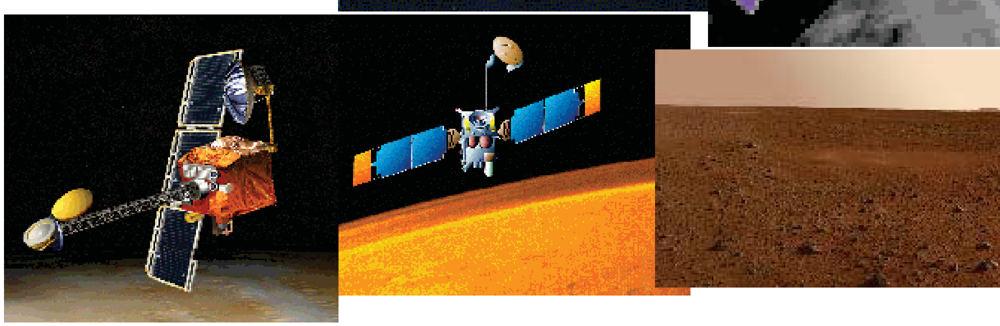

Mars Global Surveyor and Mars Odyssey orbiters; “Spirit” and “Opportunity” on Mars

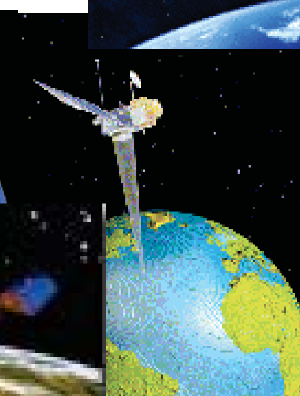

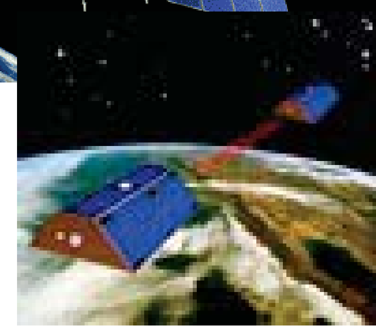

Topex/Poseidon, QuikSCAT, Jason 1, and GRACE (plus ASTER, MISR, and AIRS instruments) monitoring Earth

Micro and Nano Devices for Space Applications

National Aeronautics and Space Administration
Jet Propulsion Laboratory
California Institute of Technology

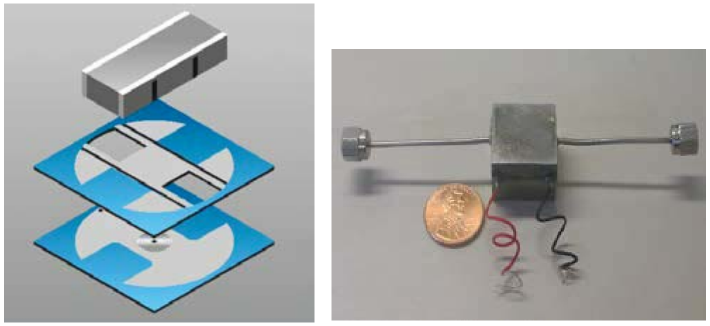

High-pressure, leak-tight microvalve for proportional flow control

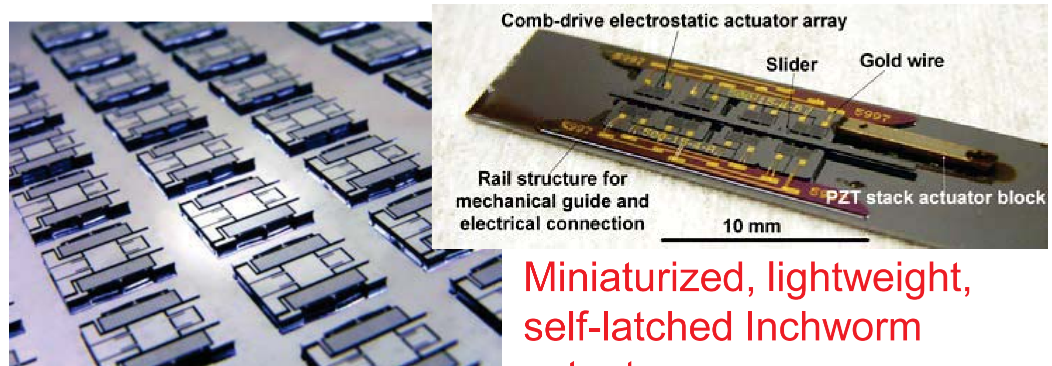

Miniaturized, lightweight, self-latched Inchworm actuator

Microactuator Technology

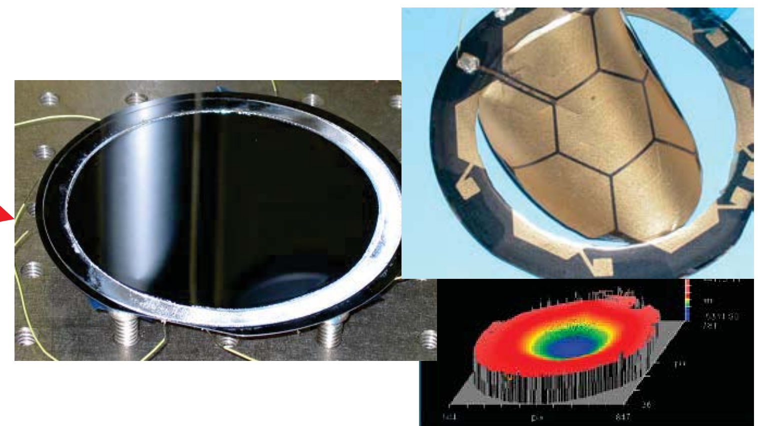

Electroactive polymer mirror membrane

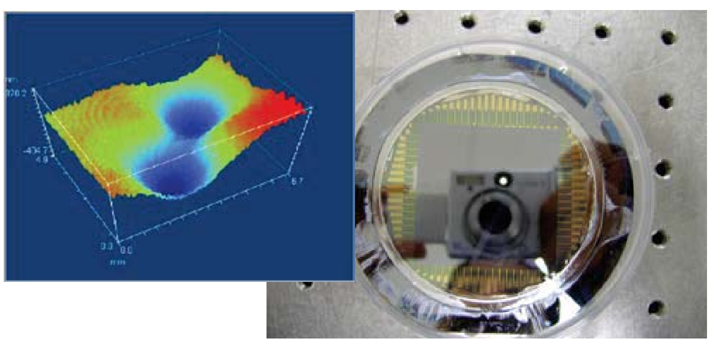

Large-stroke, large-area membrane deformable mirror for ultra-large telescopes

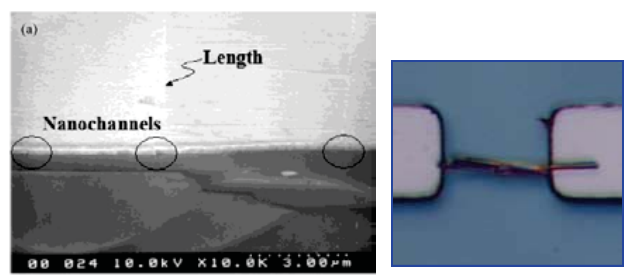

Nano-manufacturing Technology

Outline

- MEMS Deformable Mirror
- Inchworm Microactuator

Adaptive and active optics for space telescopes

- Piezoelectric Microvalve

Micropropulsion for microspacecrafts

Adaptive Optics, Why?

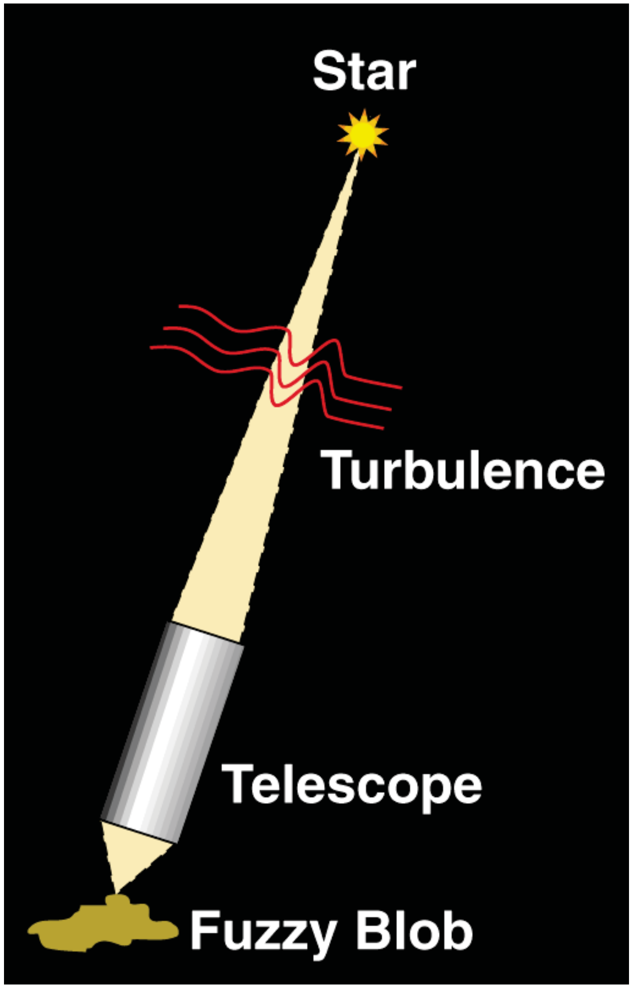

•Turbulence in earth's atmosphere spreads out light; makes it a blob rather than a point.

- Temperature fluctuations in small patches of air cause changes in index of refraction.
- When they reach telescope they are no longer parallel; rays can't be focused to a point:

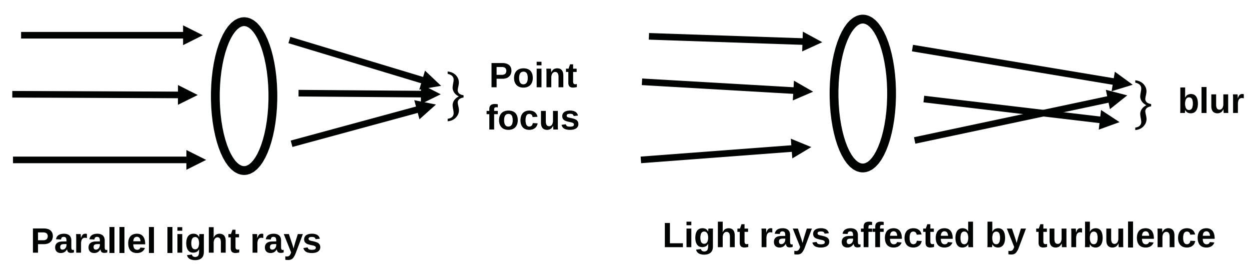

http://www.ucolick.org/%7Emax/289C/

Adaptive Optics

National Aeronautics and Space Administration
Jet Propulsion Laboratory
California Institute of Technology

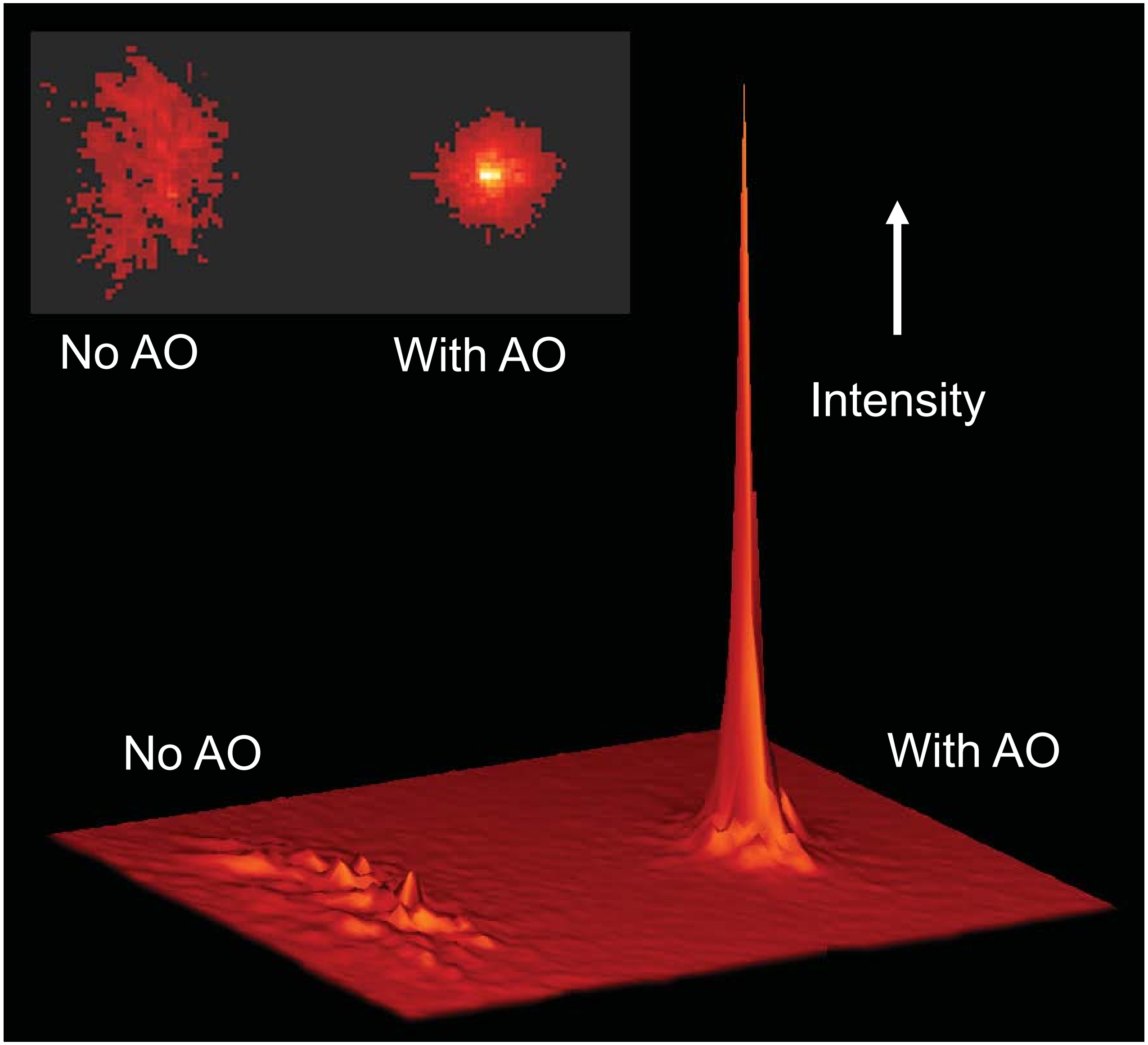

Courtesy: Lick Observatory

61-element deformable mirror on a ground-based 3-m telescope

Ultra Large Space Telescope

National Aeronautics and Space Administration
Jet Propulsion Laboratory
California Institute of Technology

Do we still need AO in Space?

Future ultra-large space telescope mirrors - Ultra-lightweight, flexible materials
➔Large, localized surface errors

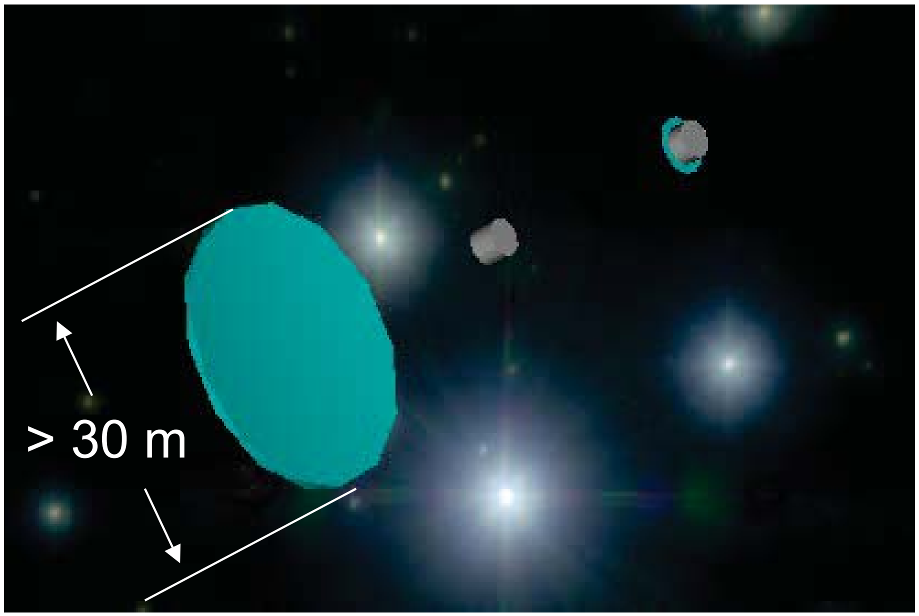

The resolution of an optical system is limited by the diffraction of light waves.

$$\alpha = 1.22\frac{\lambda}{D}$$

(Dekany *et al. "Advanced Segmented Silicon Space Telescope (ASSiST)", Proc. of SPIE, V.4849, p.103*)

1. Adaptive wavefront correction at tertiary optics: Requiring deformable mirrors (DMs) scalable to large-area, large-stroke.

2. Active control of mirror surface: Requiring miniaturized inchworm actuators.

National Aeronautics and Space Administration
Jet Propulsion Laboratory
California Institute of Technology

Existing Deformable Mirrors (DMs)

Most deformable mirrors today have thin glass face-sheets.

MEMS DMs - (electrostatic)

BMC (Boston Univ.),
Flexible Optical BV (Delft Univ.),
Agil-Optics, Inc. (Stanford Univ.)

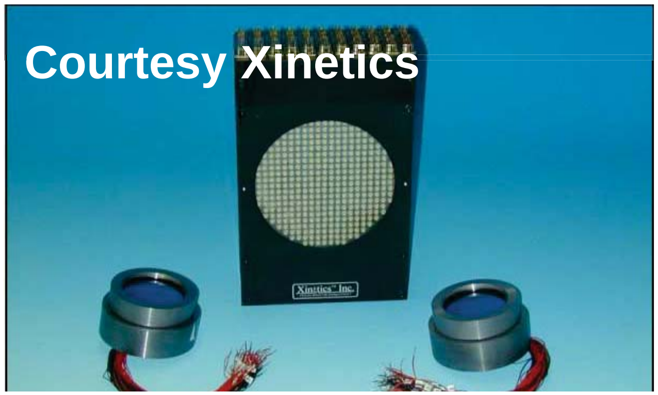

Xinetics photonics module
Cost: ~$800K (64x64)
Stroke 0.1~0.2 μm

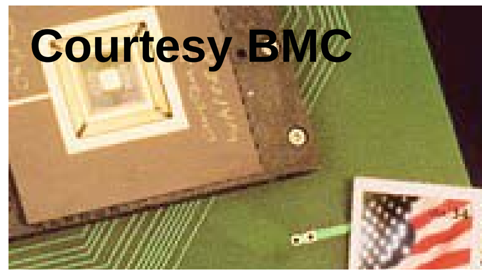

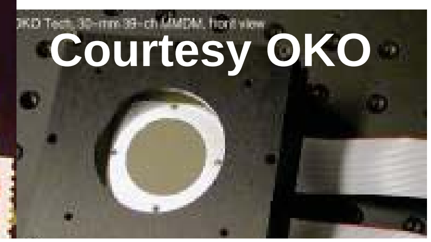

Limitation in stoke, mirror size, or influence function

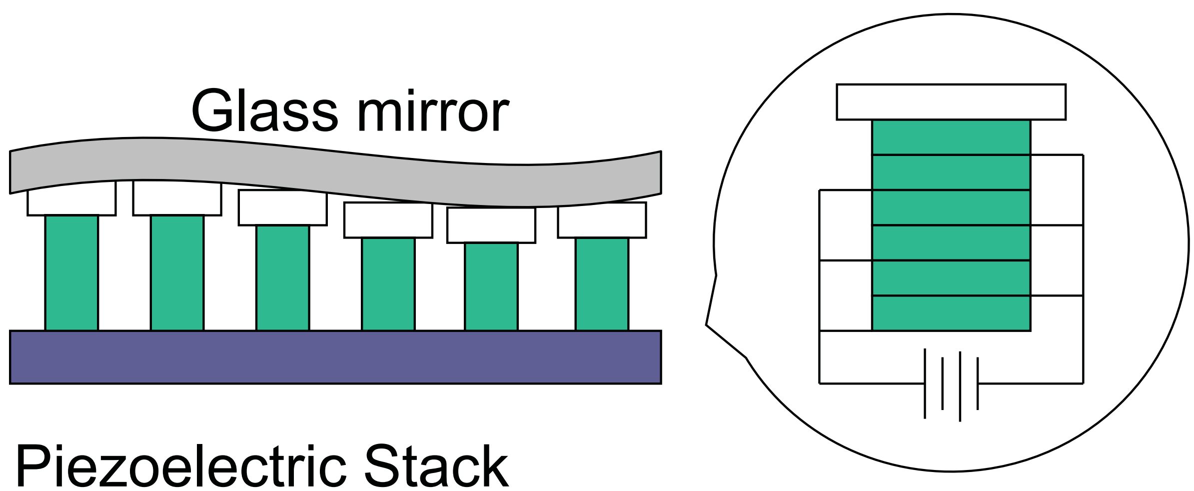

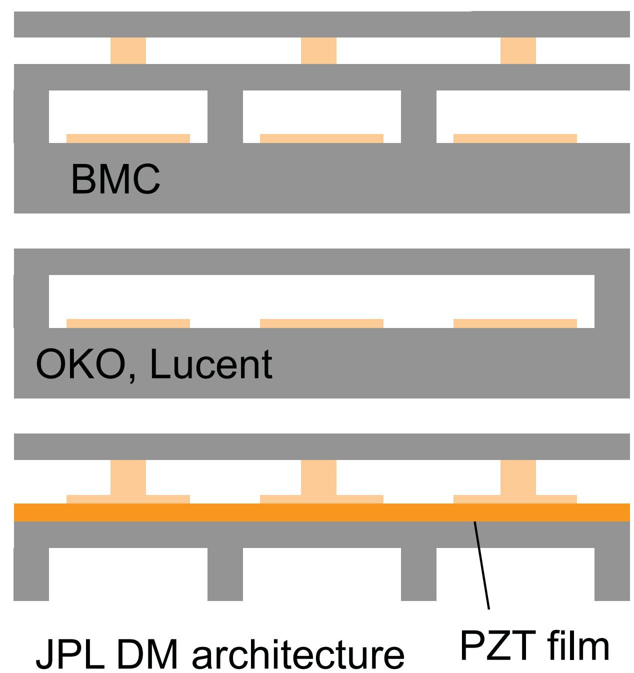

Actuators for DMs

Electrostatic Actuators

Advantages

No hysteresis

Disadvantages

Limited stroke (~2 μm)
High voltage (few 100's V)
Snap-down (deflection < ~1/3 of gap)

Piezoelectric Unimorph Actuators

Advantages

Low voltage (~50V)
Stroke proportional to actuator size
High bandwidth (for our design)

Disadvantages

10~20% Hysteresis
PZT film process needs further improvement.
(many unknown parameters)

National Aeronautics and Space Administration
Jet Propulsion Laboratory
California Institute of Technology

Piezoelectric Unimorph Actuator: Actuation Principle

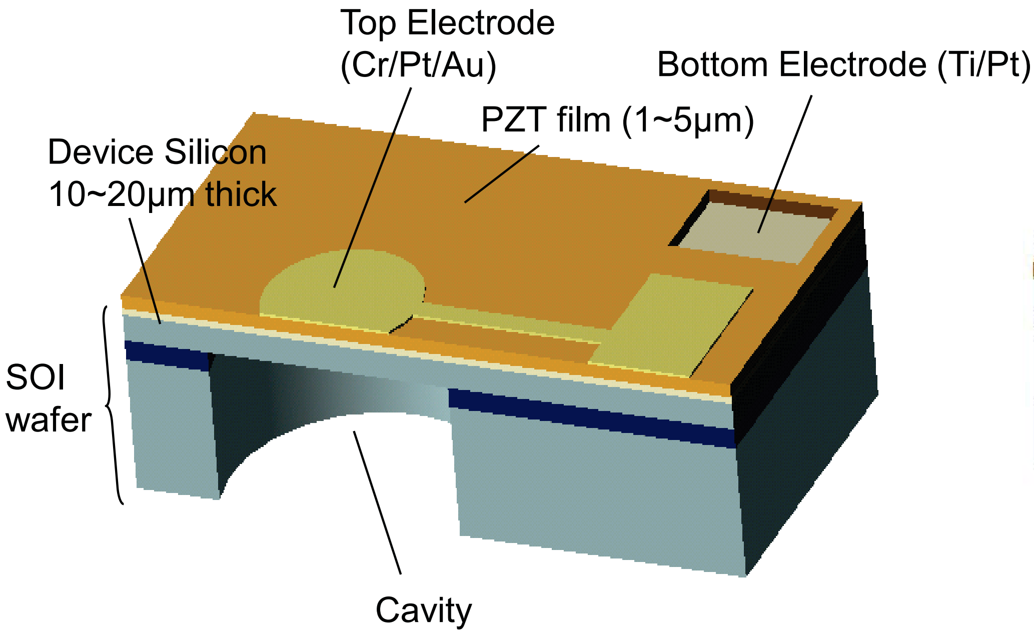

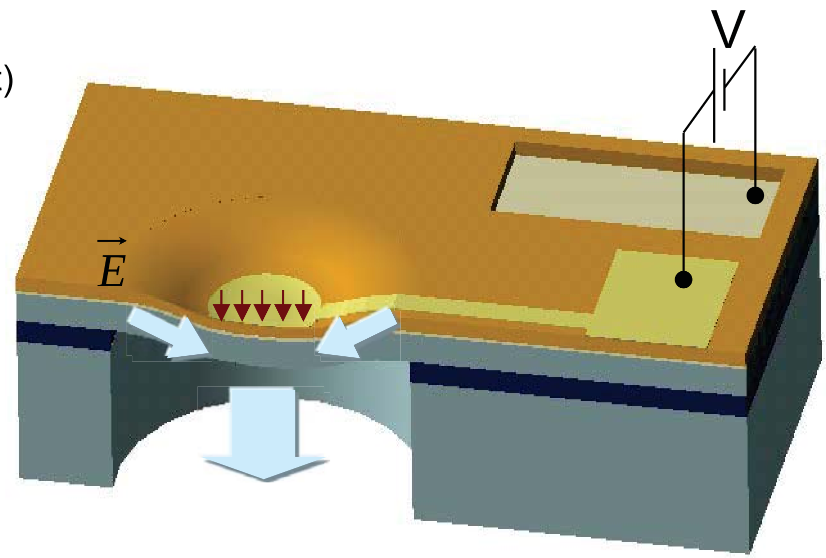

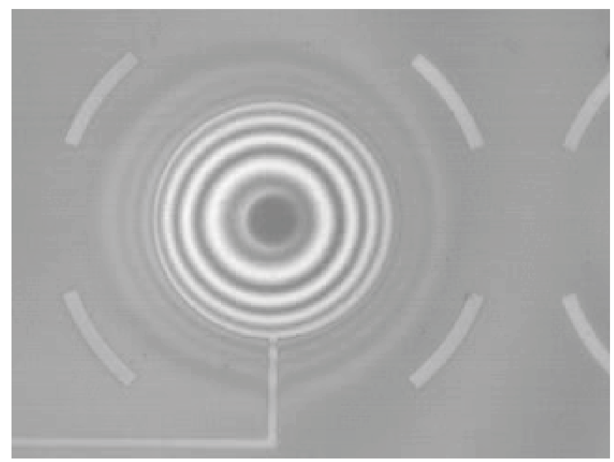

- Scalable to large-stroke for large-wavefront correction.
- Highly scalable actuator count, potentially up to 10^6 actuators.
- Fast response and low power (30 μs/cycle, 4 nF)

Example: d31 mode actuation, 2.5 mm in diameter, the Si/PZT thickness ratio of 6, the electrode size 60%.

Fabrication Process

National Aeronautics and Space Administration
Jet Propulsion Laboratory
California Institute of Technology

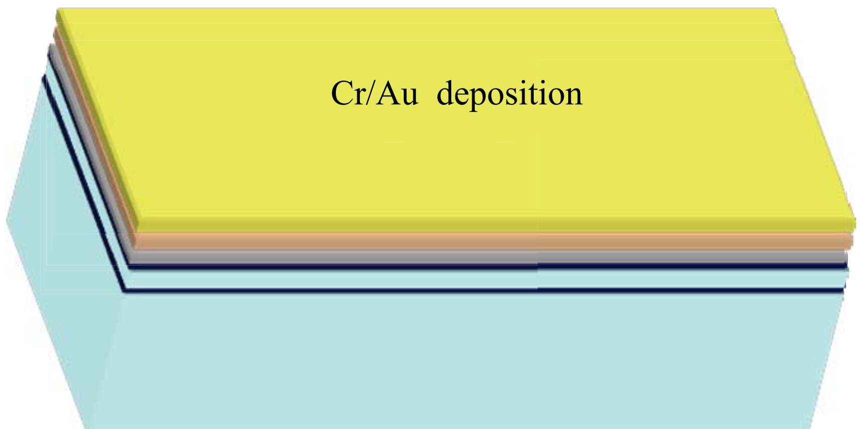

National Aeronautics and Space Administration
Jet Propulsion Laboratory
California Institute of Technology

Fabrication Process

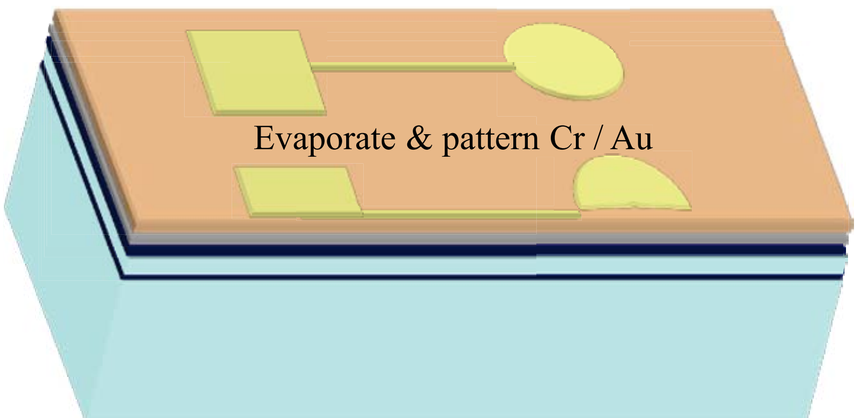

Fabrication Process

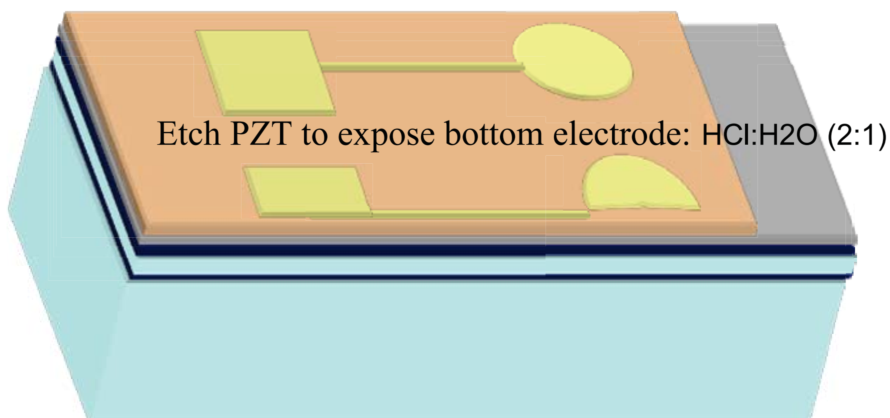

Fabrication Process

National Aeronautics and Space Administration
Jet Propulsion Laboratory
California Institute of Technology

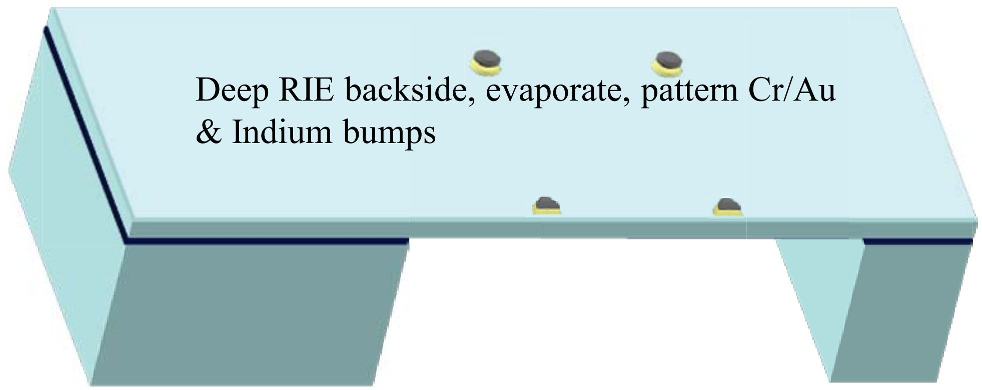

Mirror wafer

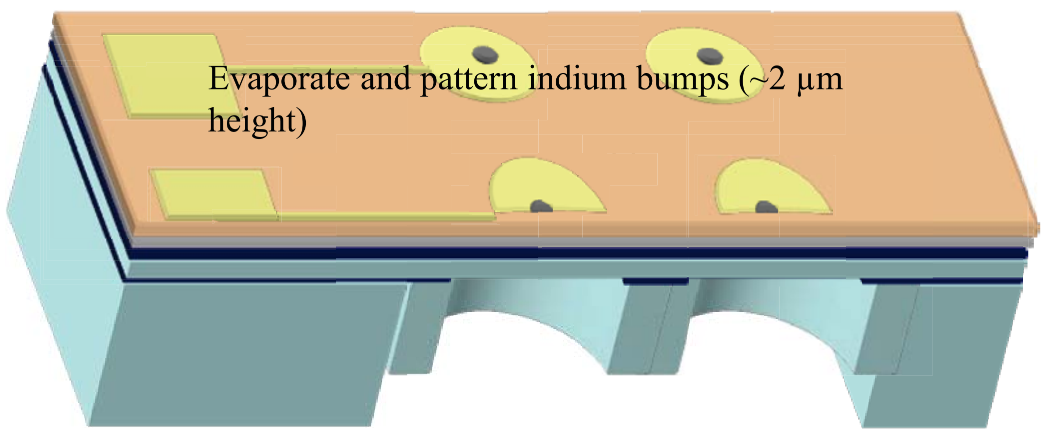

Actuator wafer

Fabrication Process

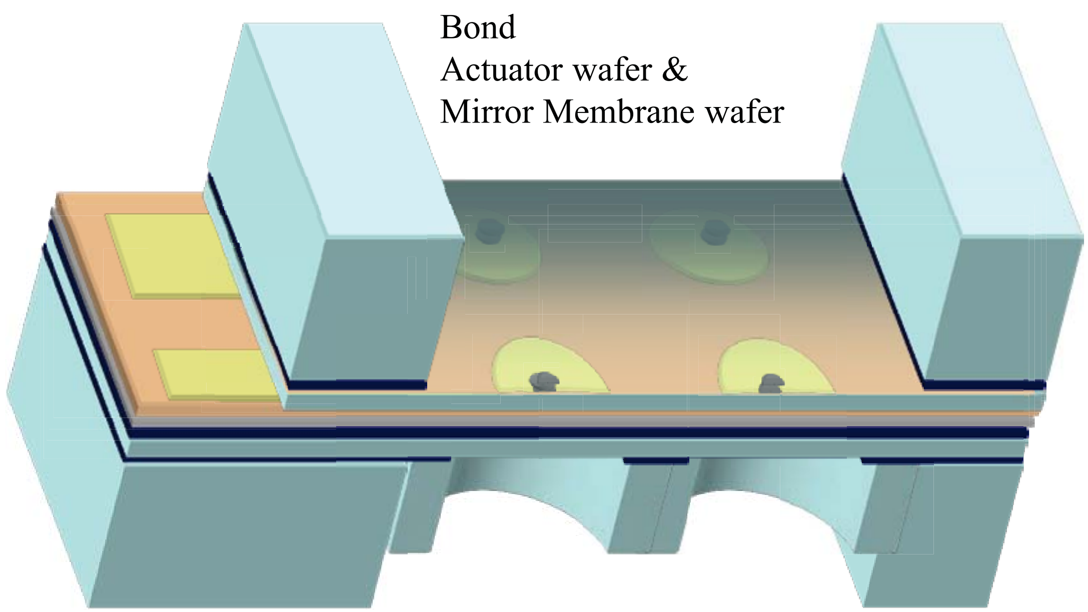

National Aeronautics and Space Administration
Jet Propulsion Laboratory
California Institute of Technology

Preliminary DM: Testing

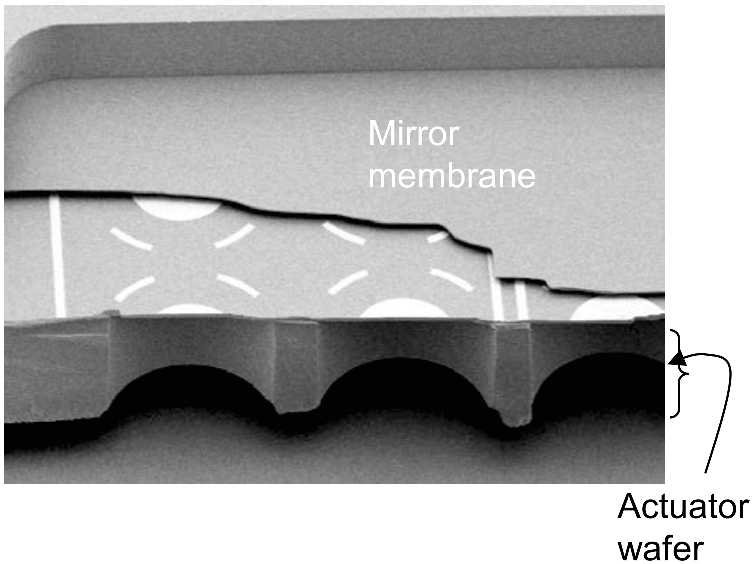

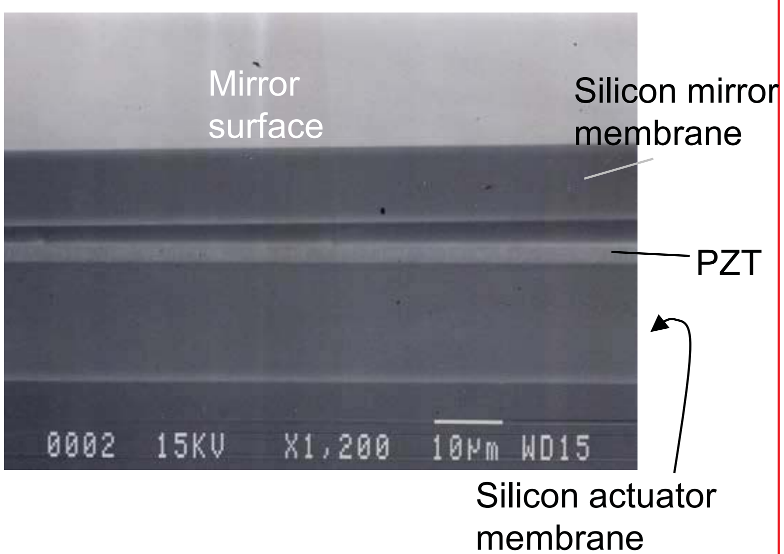

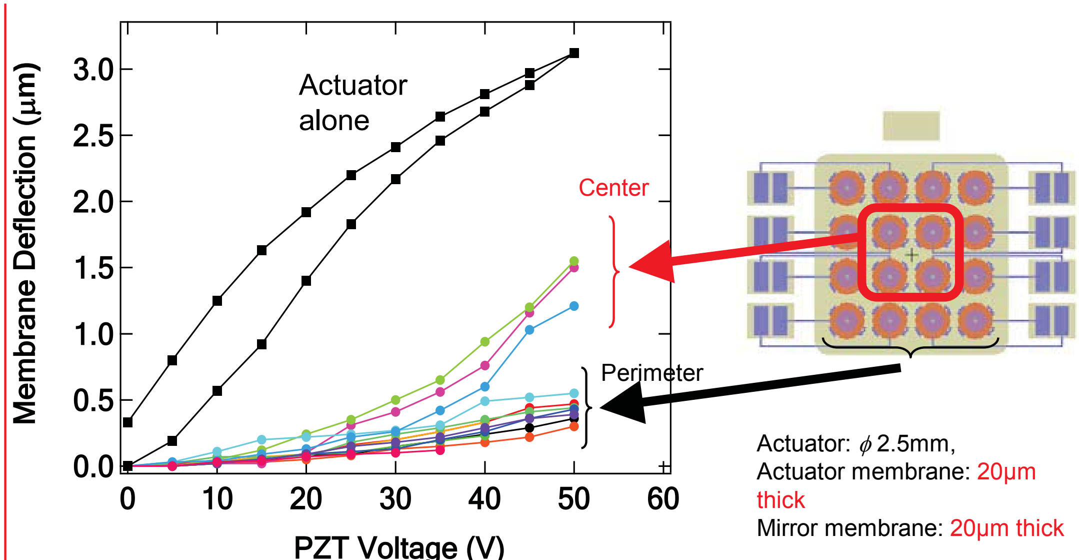

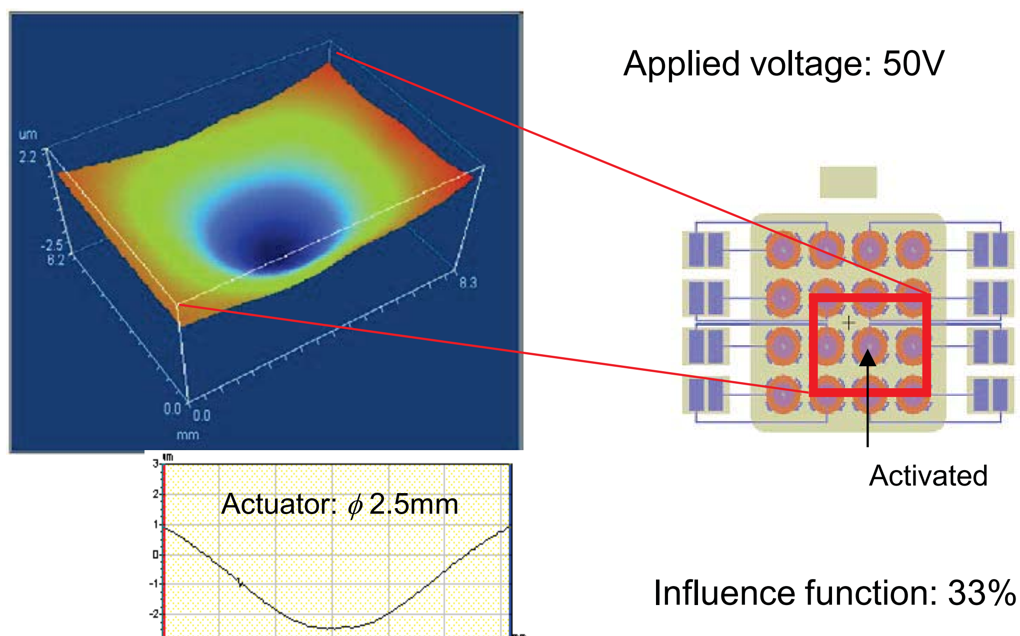

Y. Hishinuma and **E. H. Yang**, "Piezoelectric Unimorph Microactuator Arrays for Single-Crystal Silicon Continuous Membrane Deformable Mirror," *IEEE/ASME Journal of Microelectromechanical Systems, Vol. 15, No. 2, April 2006.*

NASA logo
National Aeronautics and Space Administration
Jet Propulsion Laboratory
California Institute of Technology

Preliminary DM: Testing

DM: Actuator: ϕ 1.0mm, 20μm thick Si membrane

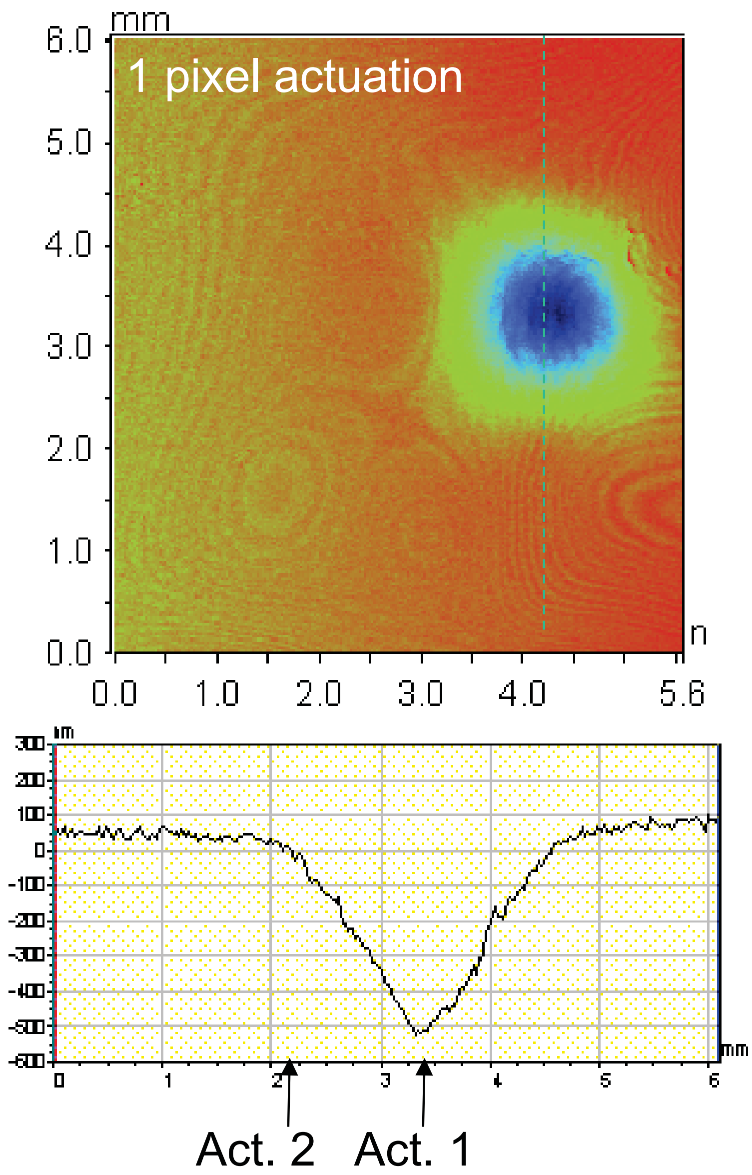

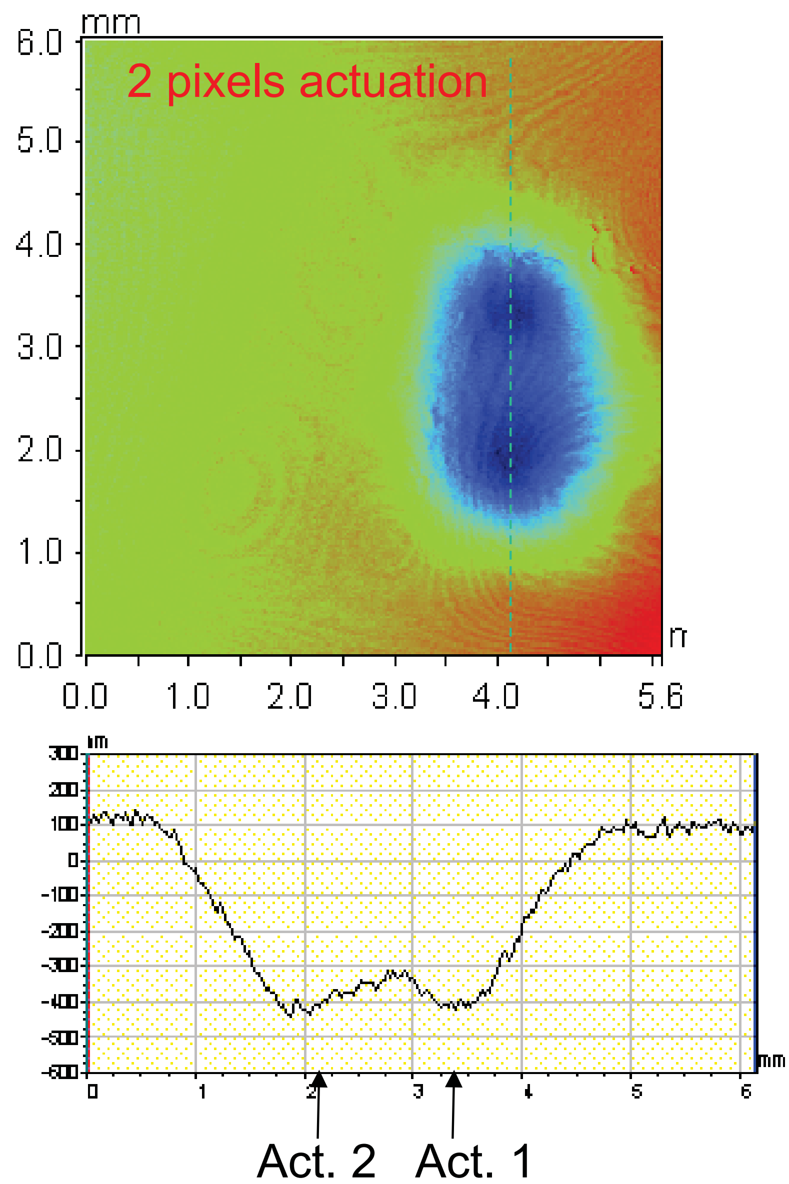

Unimorph Actuator Modeling

National Aeronautics and Space Administration
Jet Propulsion Laboratory
California Institute of Technology

Membrane deflection function

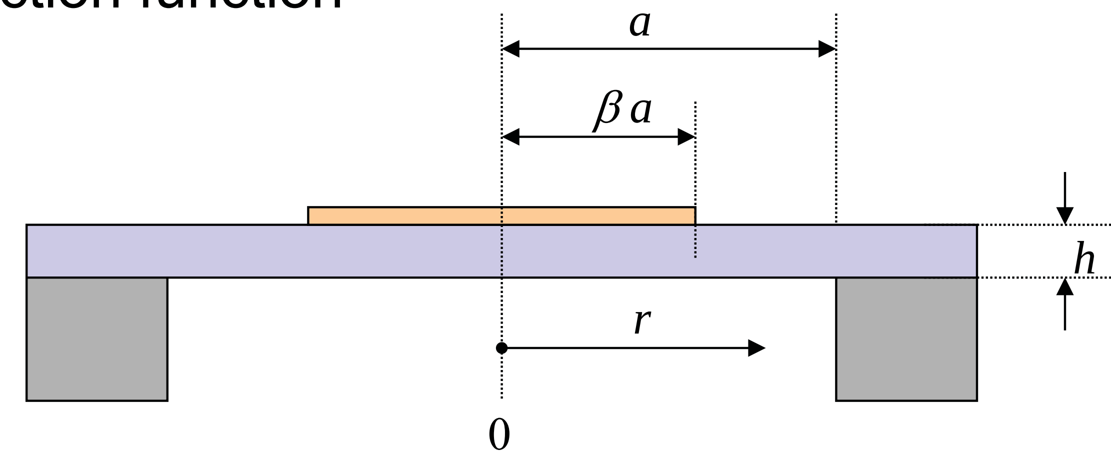

From Thin Plate Theory*

$$w(r) = \begin{cases} \lambda\left(\frac{c_1}{4}r^2 + c_2 \ln\frac{r}{a} + c_3\right), & 0 < r < \beta a \\ \lambda\left(\frac{d_1}{4}r^2 + d_2 \ln\frac{r}{a} + d_3\right), & \beta a < r < a \end{cases}$$

$$w(r) = \lambda F(r)$$

λ: Lagrange multiplier
Find unknown coefficients using boundary conditions

*Timoshenko and Woinowsky-Krieger, “Theory of Plates and Shells”, 1959

Unimorph Actuator Modeling

National Aeronautics and Space Administration
Jet Propulsion Laboratory
California Institute of Technology

Total energy of membrane under deflection

$$U_{tot} = U_{el} + U_s + U_M$$

(1) Elastic energy

$$U_{el} = \frac{1}{2} D\lambda^2 \int_0^a 2\pi r \left[\left(\frac{d^2F}{dr^2} + \frac{1}{r}\left(\frac{dF}{dr}\right) \right)^2 - 2(1-\nu)\frac{1}{r}\frac{dF}{dr}\frac{d^2F}{dr^2} \right] dr$$

(2) Stretching energy due to tensile stress

$$U_s = \frac{1}{2} S\lambda^2 \int_0^a 2\pi r \left(\frac{dF}{dr}\right)^2 dr$$

(3) Potential energy due to bending moment

$$U_M = \frac{1}{2} M\lambda \int_0^{\beta a} 2\pi r \left(\frac{d^2F}{dr^2} + \frac{1}{r}\frac{dF}{dr} \right)$$

Y = 107 GPa : Young's Modulus of Silicon

ν= 0.22 : Poisson's ratio

e_{31} = -6 C/m^2

$\sigma_{Ti, Pt}$= 300 MPa

σ_{PZT}= 260 MPA

$$D = \frac{Yh^3}{12(1-\nu^2)}$$

Flexural rigidity

$$S = \beta\sigma_p t_p + \sum_i \sigma_i t_i$$

Stretching force per unit length

$$M = \sigma_p(E_3) t_p \frac{h_{eff}}{2}$$

Bending moment

$$\sigma_p = -\tilde{e}_{31} \cdot E_3$$

Stress due to PZT

Energy minimum condition

$$\frac{\partial U_{tot}}{\partial \lambda} = 0$$

Ref: P. Muralt, et al., *Sensors and Actuators A* 53 p398 (1996)

Unimorph Actuation

National Aeronautics and Space Administration
Jet Propulsion Laboratory
California Institute of Technology

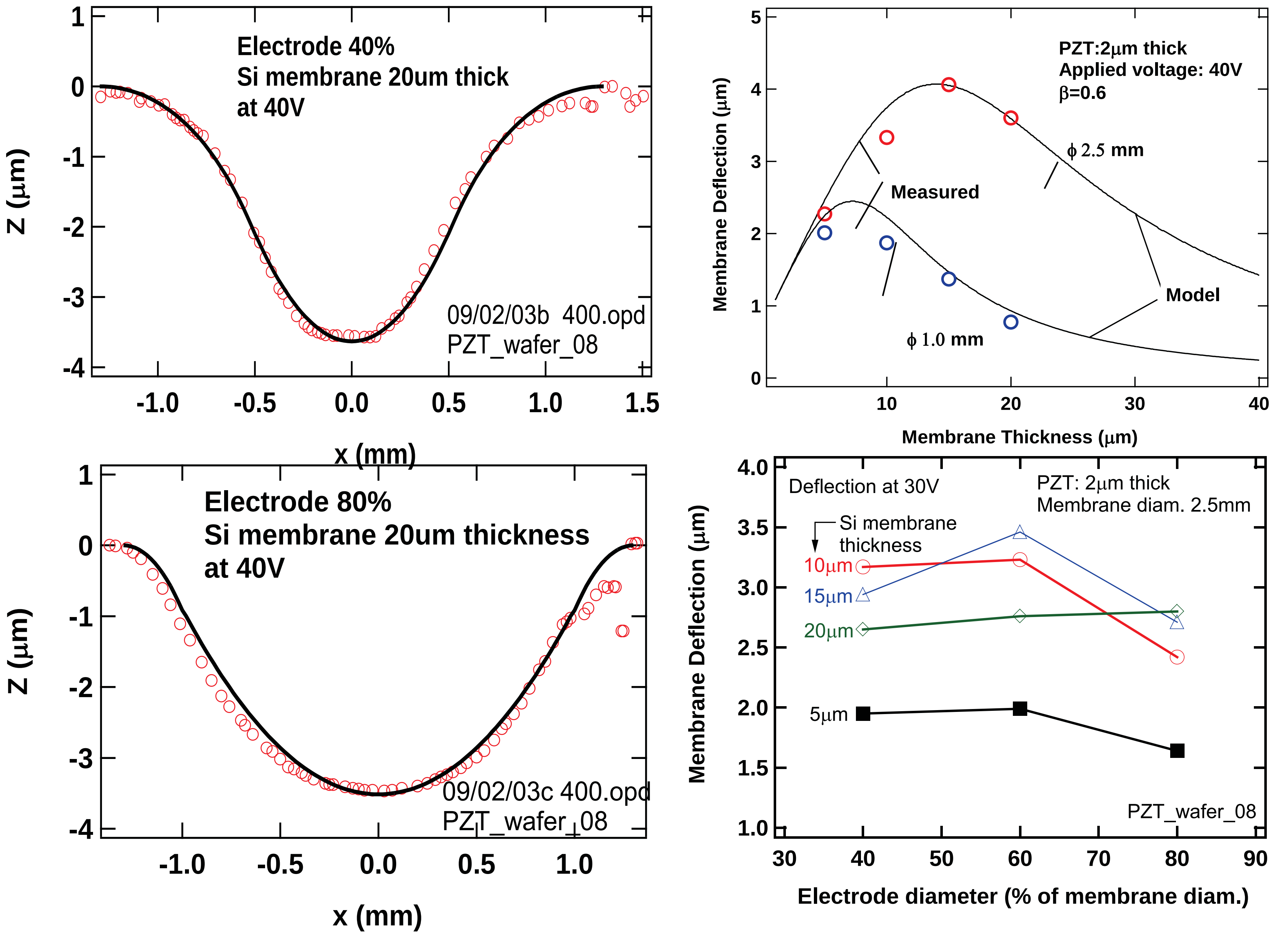

National Aeronautics and Space Administration
Jet Propulsion Laboratory
California Institute of Technology

Dynamic Response

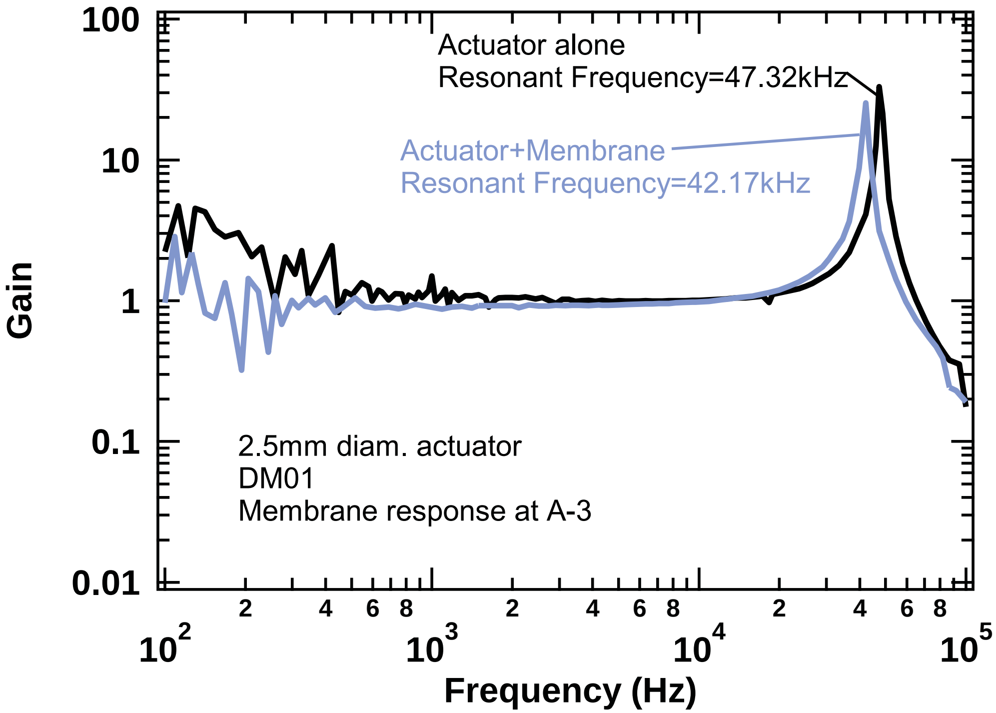

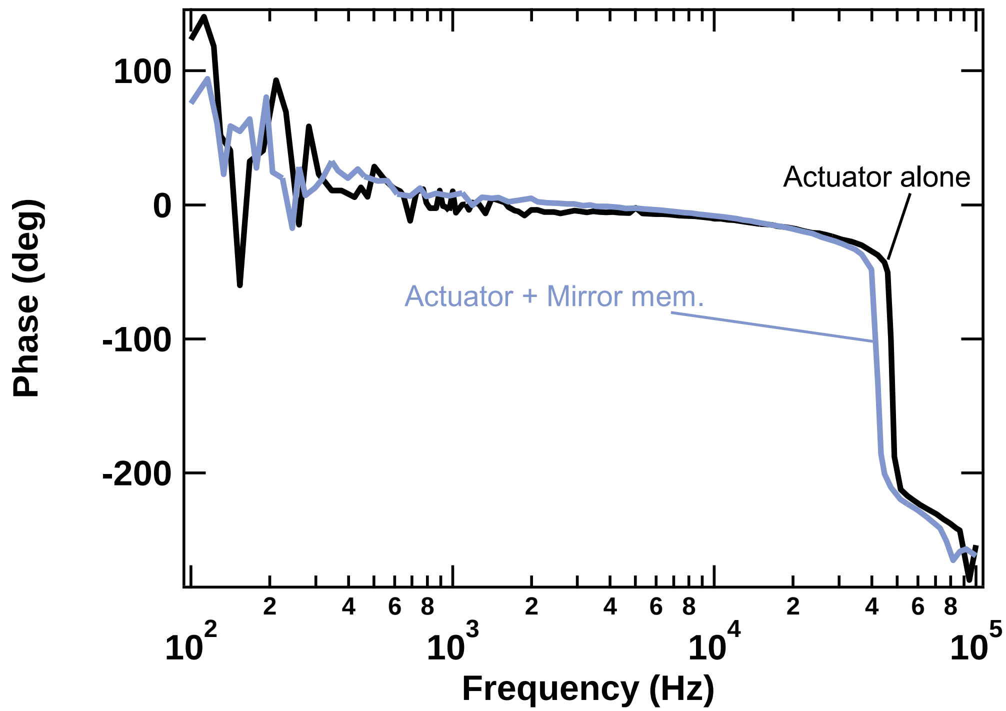

Frequency Bandwidth: ~30 kHz

Bandwidth limited by mechanical response

Large-Stroke Unimorph Actuator

National Aeronautics and Space Administration
Jet Propulsion Laboratory
California Institute of Technology

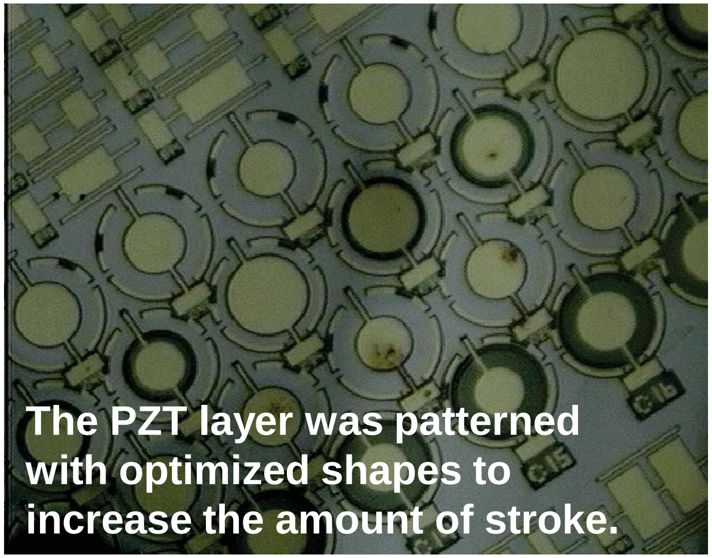

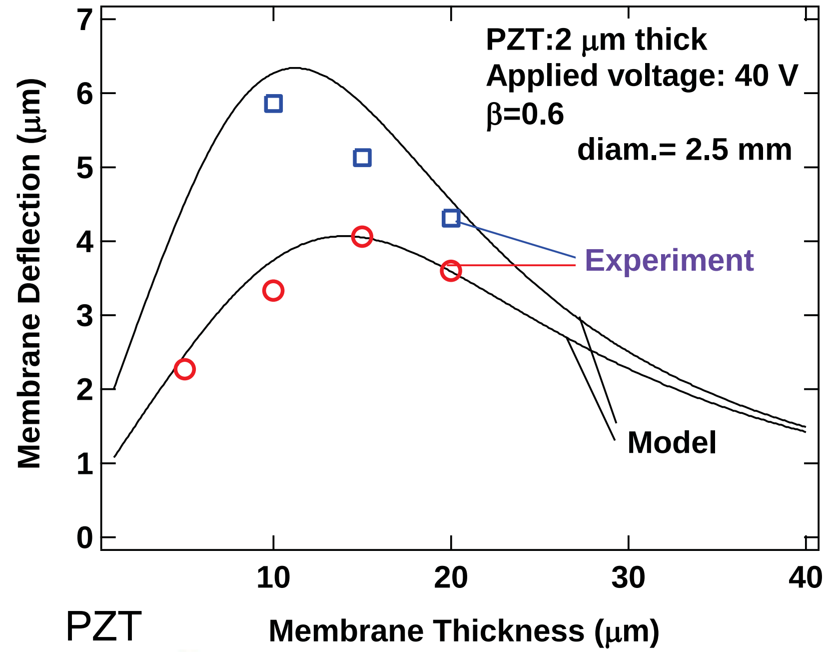

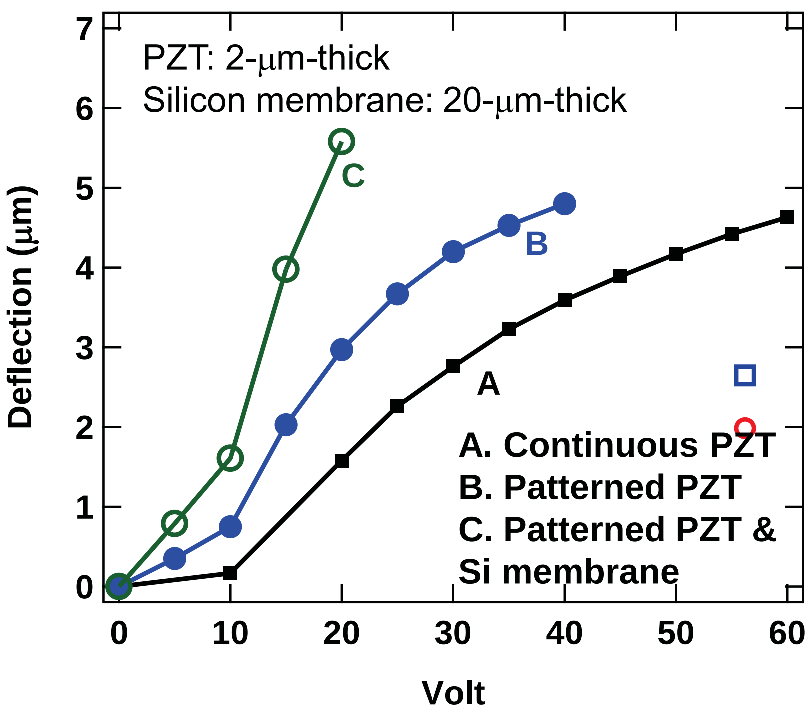

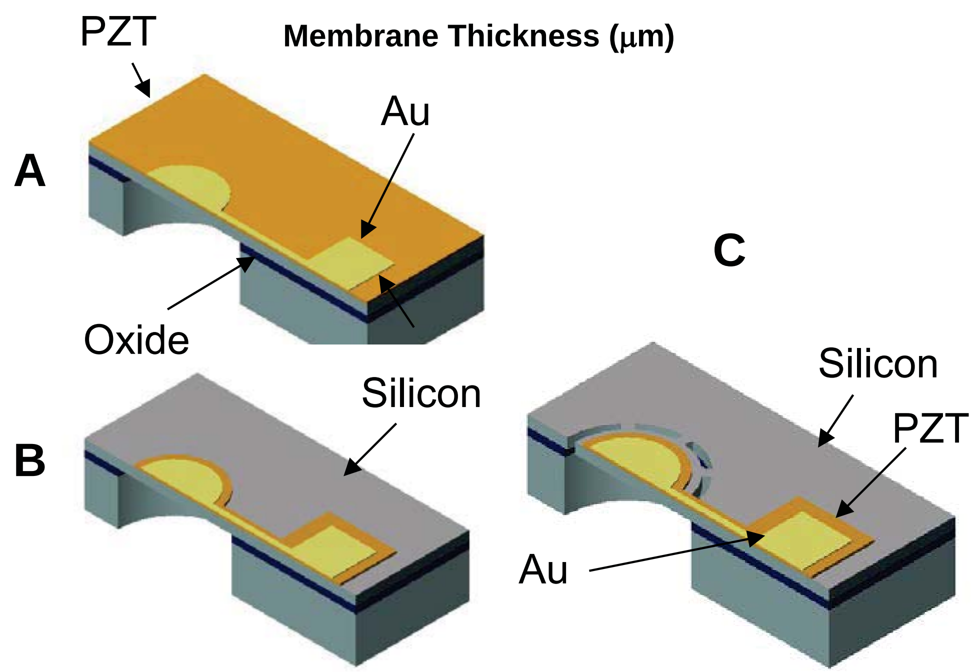

Current Status

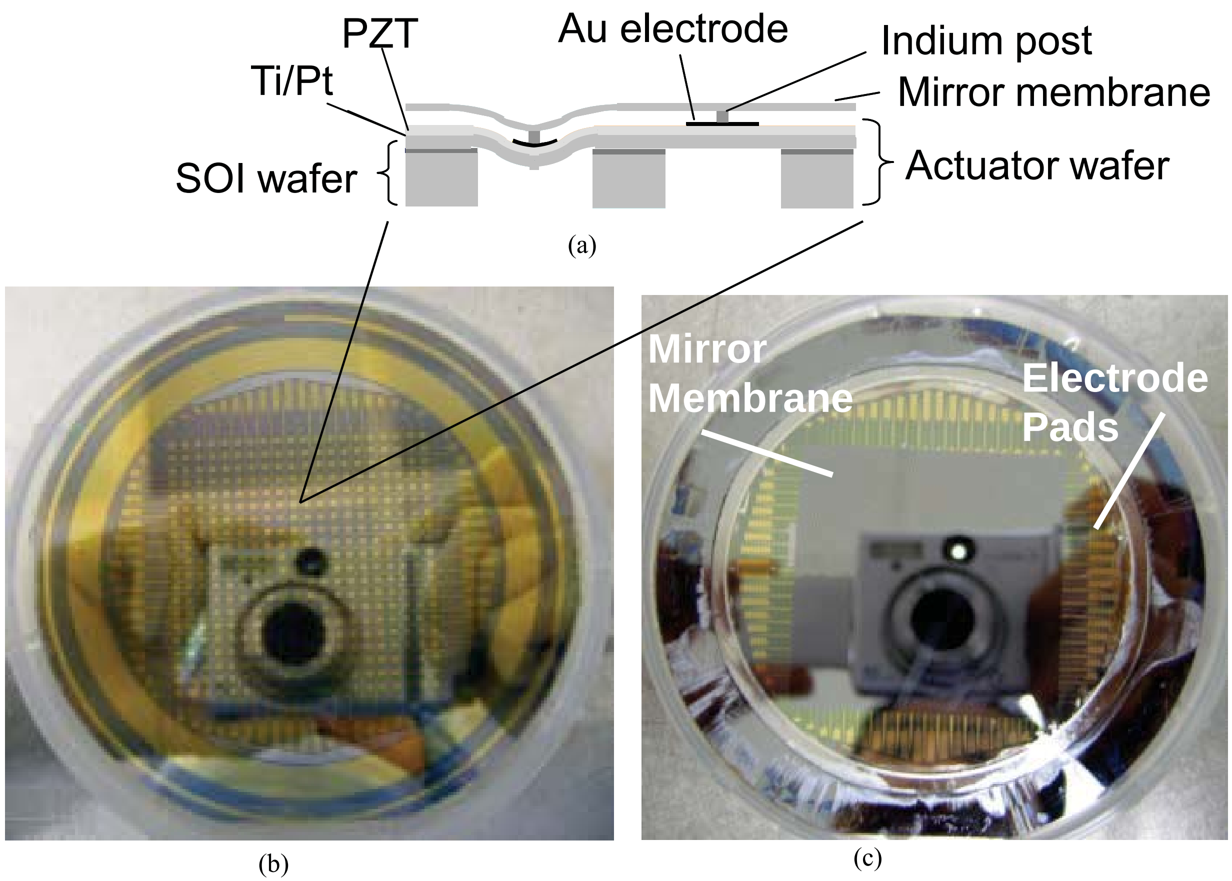

Fabricated DM with 20 x 20 piezoelectric unimorph. (a) Cross-sectional schematic (b, c) Photographs of the actuator arrays and the DM.

- Optimization of the actuator structure and PZT films.
- Stress compensation (both for actuators and mirrors)
- Actuator hysteresis compensation.
- Reliable fabrication to improve the mirror quality and the actuator stroke.

E. H. Yang, Y. Hishinuma, J.-G. Cheng, S. Trolier-McKinstry, E. Bloemhof, and B. M. Levine, "Thin-Film Piezoelectric Unimorph Actuator-based Deformable Mirror with a Transferred Silicon Membrane," *IEEE/ASME Journal of Microelectromechanical Systems, 2006. in-press*

Outline

- MEMS Deformable Mirror
- **Inchworm Microactuator**

For space telescopes

- Piezoelectric Microvalve

Inchworm Microactuator: Why?

National Aeronautics and Space Administration
Jet Propulsion Laboratory
California Institute of Technology

•Is an AO system at tertiary optics sufficient? Do we still need direct correction in mirror shape in addition to AO?

•Deformable mirrors at tertiary optics cannot correct wavefront errors exceeding several microns.

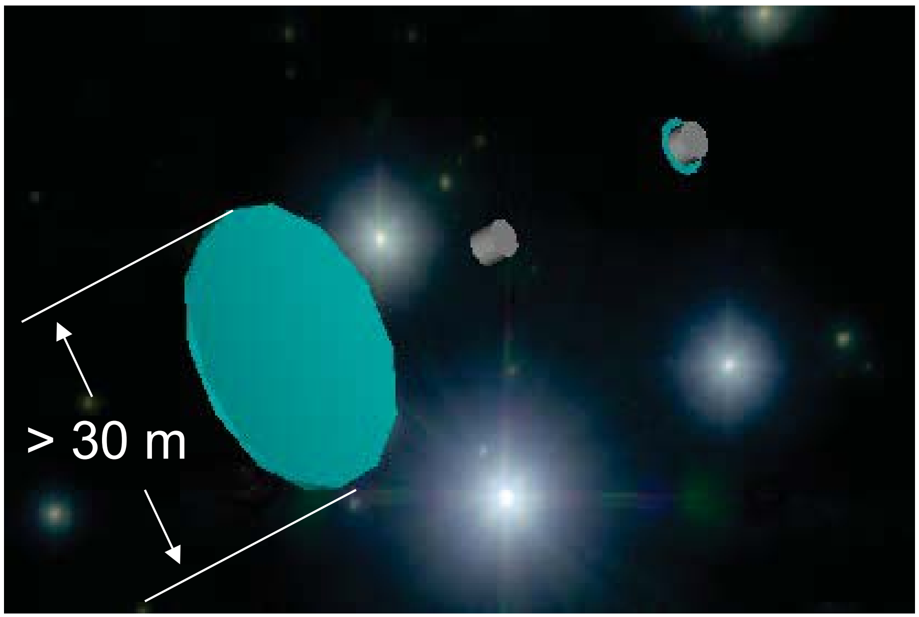

Generic Requirements

• Max. Freq.	~1 kHz
• Stroke	**> 1 mm**
• Resolution	<30 nm
• Force	**> 30 mN**
• Power	100 μW
• Mass	~ 100 mg

1. Adaptive wavefront correction at tertiary optics: Requiring deformable mirrors with large-area, large-stroke.

2. Active control of mirror surface: Requiring miniaturized inchworm actuators.

Ultra-Large Monolithic Mirror

National Aeronautics and Space Administration
Jet Propulsion Laboratory
California Institute of Technology

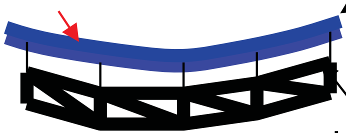

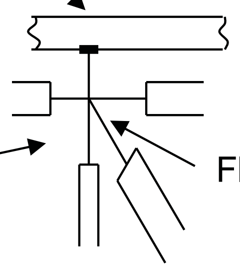

Ultra-large, ultra-lightweight, nanolaminate-based space telescope mirror concept.

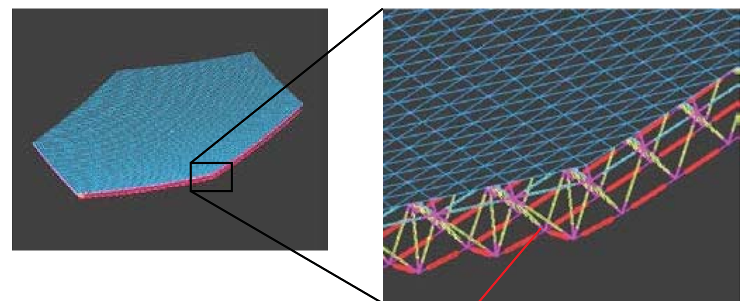

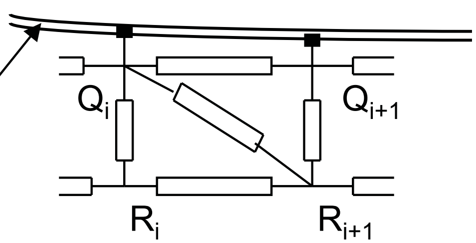

The flexures are bonded at the points $\{Q_i\}$ and $\{R_i\}$, and the angles between the tangents to flexures at the points remain constant.

A possible actuated beam concept:

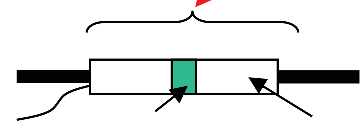

Concept of thin mirror face sheet with hinged supporting lightweight actuating truss structures. (Gullapalli *et al*.)

S. N. Gullapalli, **E. H. Yang** and S. –S. Lih, “ New technologies for the actuation and control of large aperture lightweight optical quality mirrors,” *IEEE Aerospace Conference*, Big Sky, Montana, USA, 2003.

Existing Inchworm Actuators

National Aeronautics and Space Administration
Jet Propulsion Laboratory
California Institute of Technology

- MEMS Inchworm actuators [1~3]: 50~500μN max push force. No self-latching (zero-power latching).
- Conventional inchworm actuators [4]: 100g (mass)

[1] R. Yeh, *et al.,* MEMS 01, Interlaken, Switzerland, Jan. 21-25, pp.260-264, 2001.
[2] H. N. Kwon, J. H. Lee, MEMS 02, Las Vegas, pp. 586-593, 2002.
[3] M. P. de Boer, *et al.,JMEMS*, Vol. 13, pp. 63-74, 2004.
[4] Q. Chen, *et al.,* MEMS 98, Heidelberg, Germany, pp. 384-389, 1998.

Target Performance

• Max. Freq.	~1 kHz
• Stroke	> 1 mm
• Resolution	<30 nm
• Force	> 30 mN
• Power	100 μW
• Mass	~ 100 mg

•This actuator has been designed for correcting the surface shape of a segmented or thin-monolithic mirror after deployment in space.

•If microactuators weighing a100-mg are available, a hundred such microactuators per square meter will add only about 0.01 kg/m^2.

Self-Latched Inchworm Microactuator

Before slider insertion

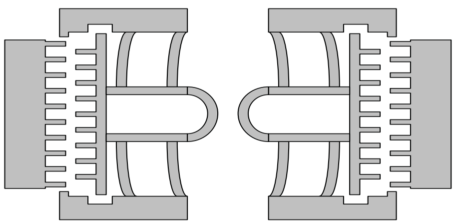

After slider insertion

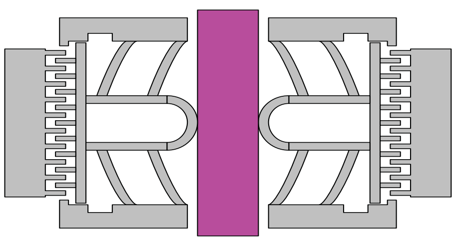

Comb drive powered,
Clutches separated

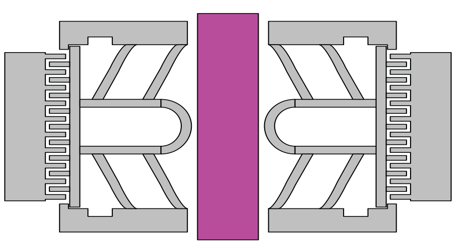

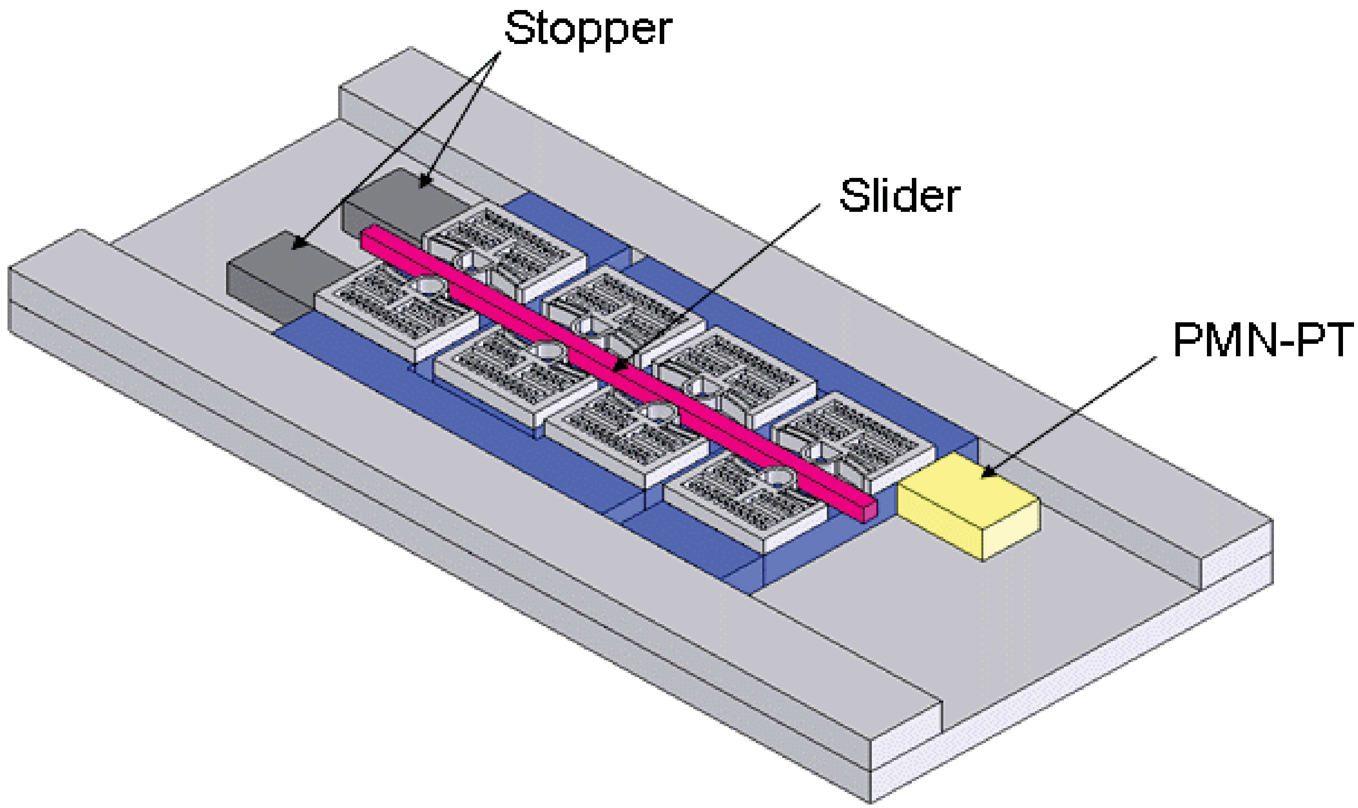

R. Toda and **E. H. Yang**, "Zero-Power Latching, Large-stroke, High-precision Linear Microactuator for Lightweight Structures in Space," *IEEE Micro Electro Mechanical Systems (MEMS) Conference*, Istanbul, Turkey, January, 2006.

2-Point Clamping to 4-Point Clamping

National Aeronautics and Space Administration
Jet Propulsion Laboratory
California Institute of Technology

2-point clamp actuator is prone to slider tilt

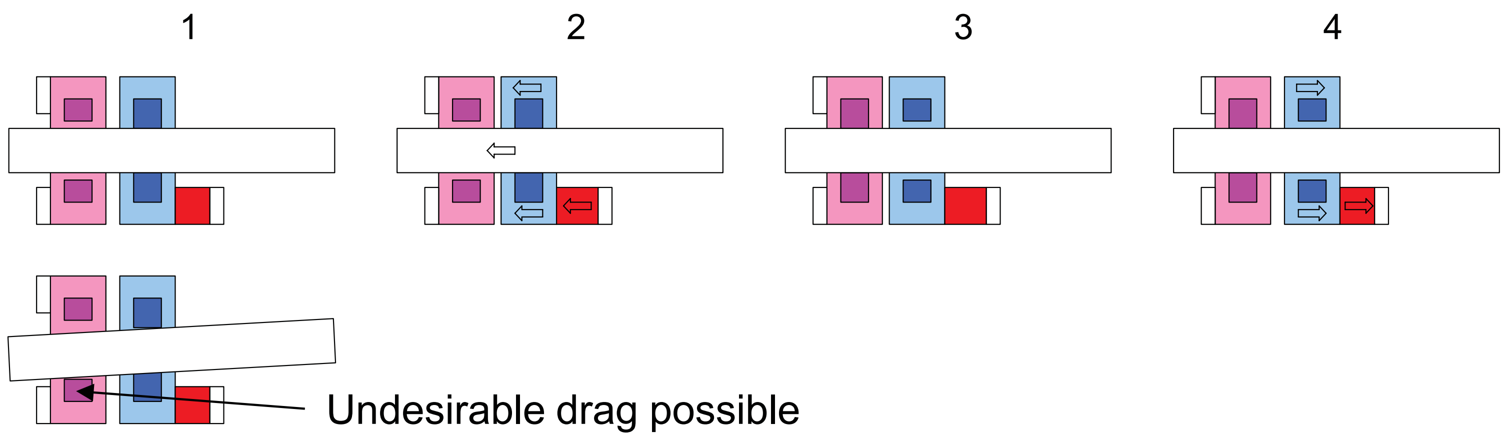

4-point clamp actuator is more stable

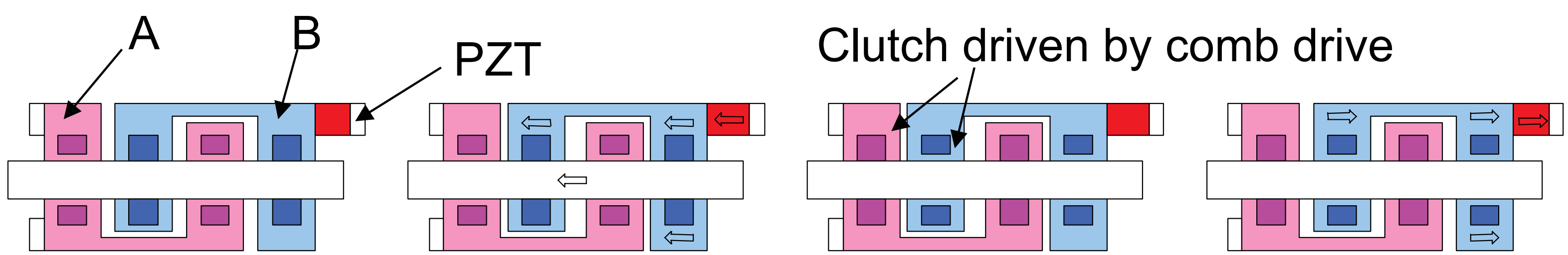

(a) Unit A released. Unit B clutched.

(b) Unit B laterally moved.

(c) Unit A clutched. Unit B released.

R. Toda and **E. H Yang**, "Four Point Latching Microactuator," *(NPO-42041)*

Comb Drive Design: Electrostatic Force

National Aeronautics and Space Administration
Jet Propulsion Laboratory
California Institute of Technology

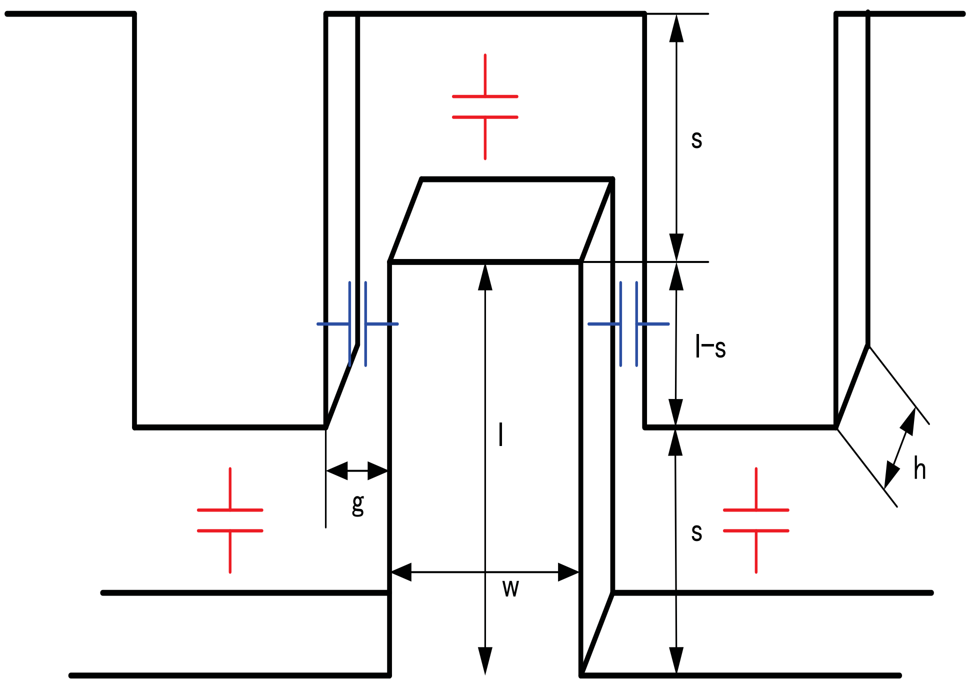

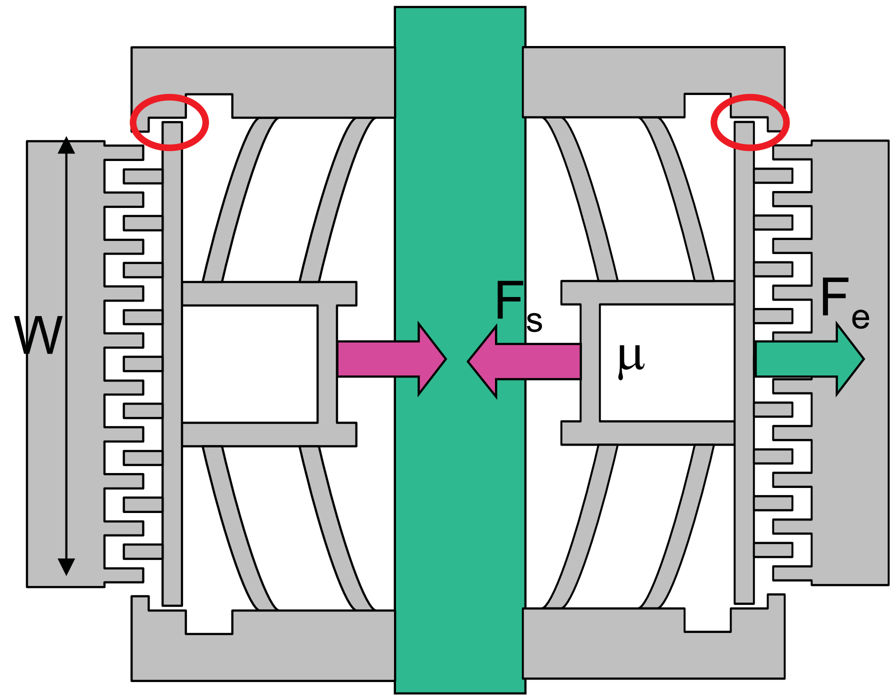

Capacitance at comb drive:

$$C = (C_{tip} + C_{side})\frac{W}{2(w+g)} = \varepsilon_0\left(\frac{w}{s-x} + \frac{l-s+x}{g}\right)\frac{hW}{w+g} \cong \varepsilon_0\frac{(l-s+x)hW}{g(w+g)}$$

Electrostatic force at comb drive F_e:

$$F_e = \frac{1}{2}\frac{\partial C}{\partial x}V^2 = \frac{1}{2}V^2\frac{\varepsilon_0 hW}{g(w+g)}$$

F_s: Tether beam restoring force
μ: friction coefficient
F_e: Electrostatic force

For unclamping, $F_e > F_s$
Maximum clamp load=μF_s

Modeling: Slider Force

Forces applied by slider

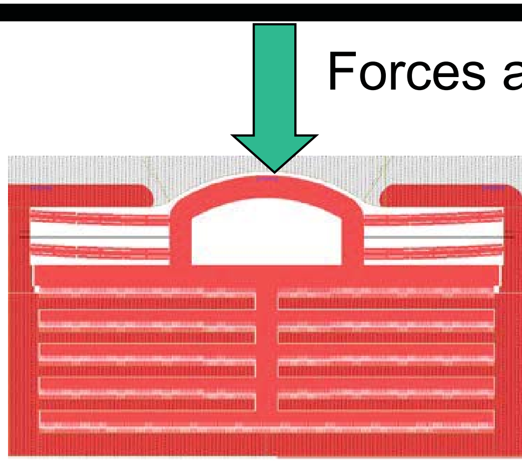

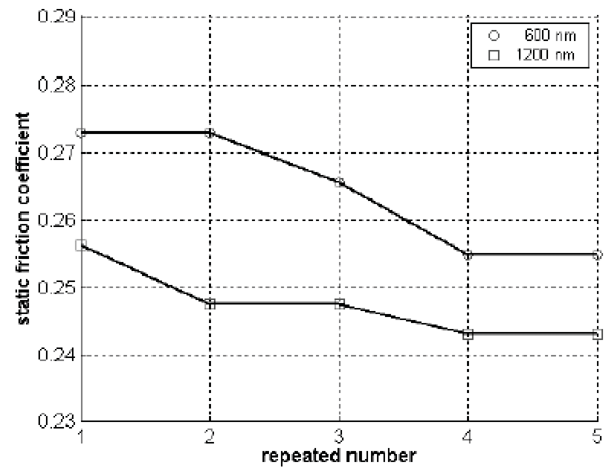

Hwang *et al*., *IEEE MEMS 06*, Istanbul, Turkey, Jan. 2006, p.210.

Assuming the static friction coefficient is 0.24, the estimated push force when actuating is approximately 24 mN. **In power-off mode, the estimated clamping force is approximately 48 mN.**

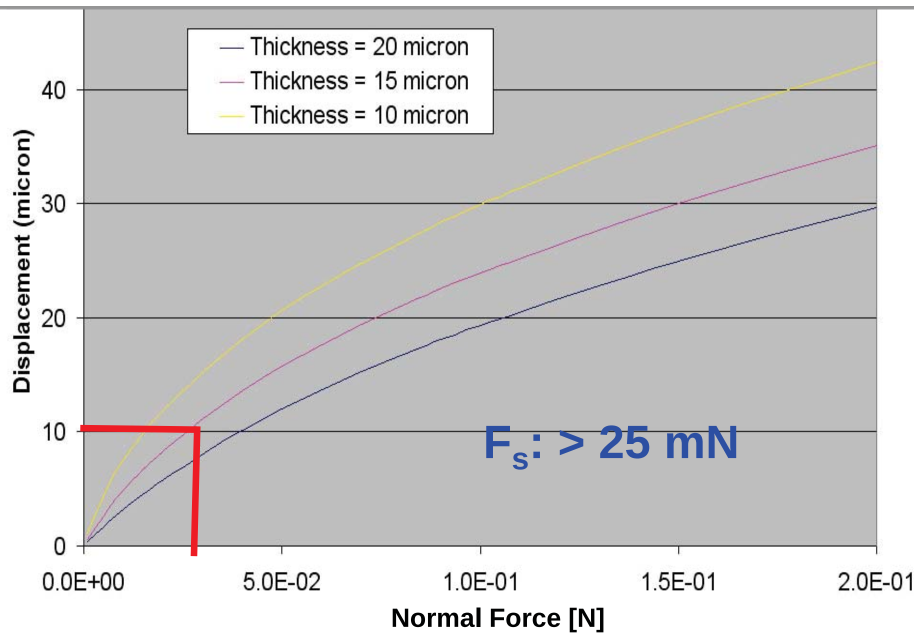

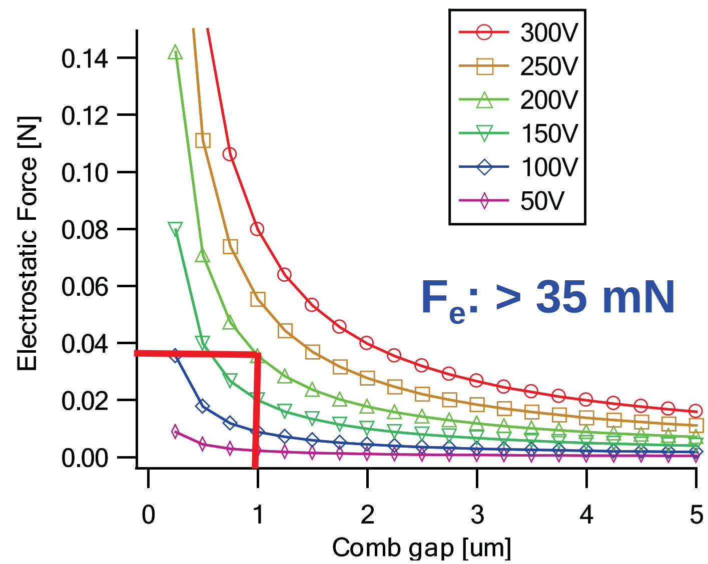

Fabrication Process Sequence

National Aeronautics and Space Administration
Jet Propulsion Laboratory
California Institute of Technology

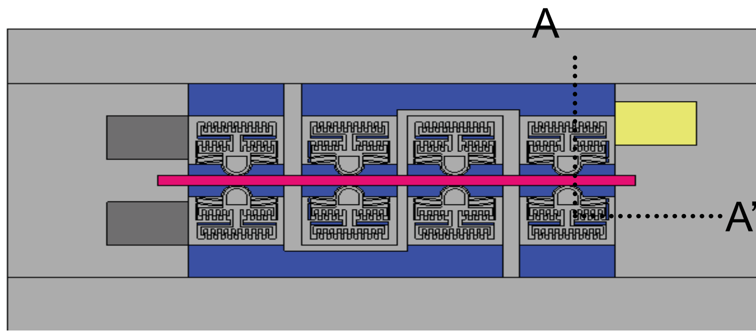

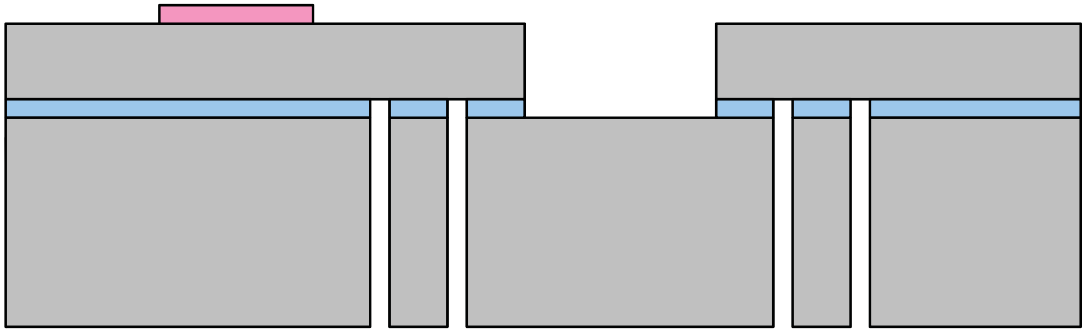

HF release

National Aeronautics and Space Administration
Jet Propulsion Laboratory
California Institute of Technology

Fabricated Silicon Components

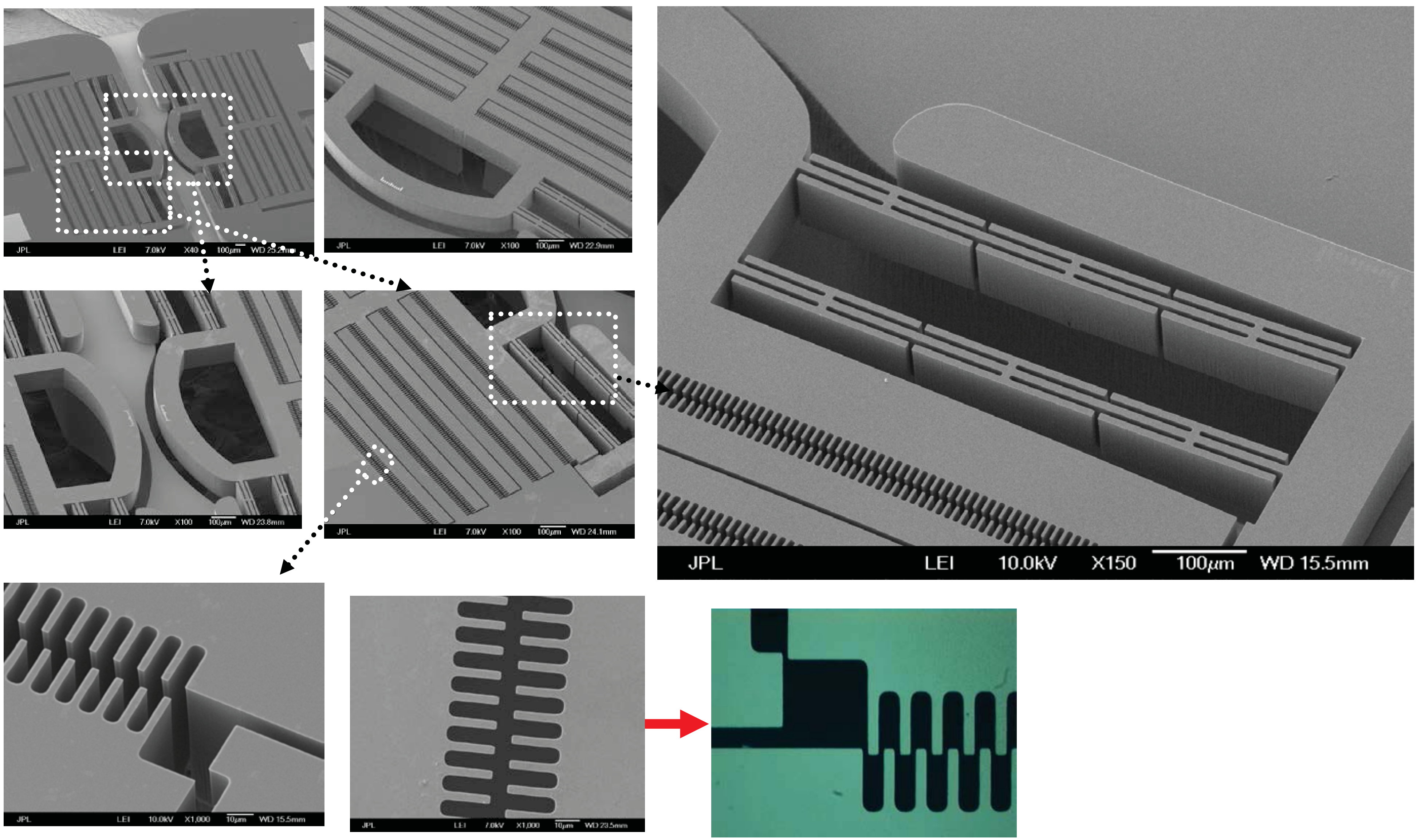

Fabricated and Assembled

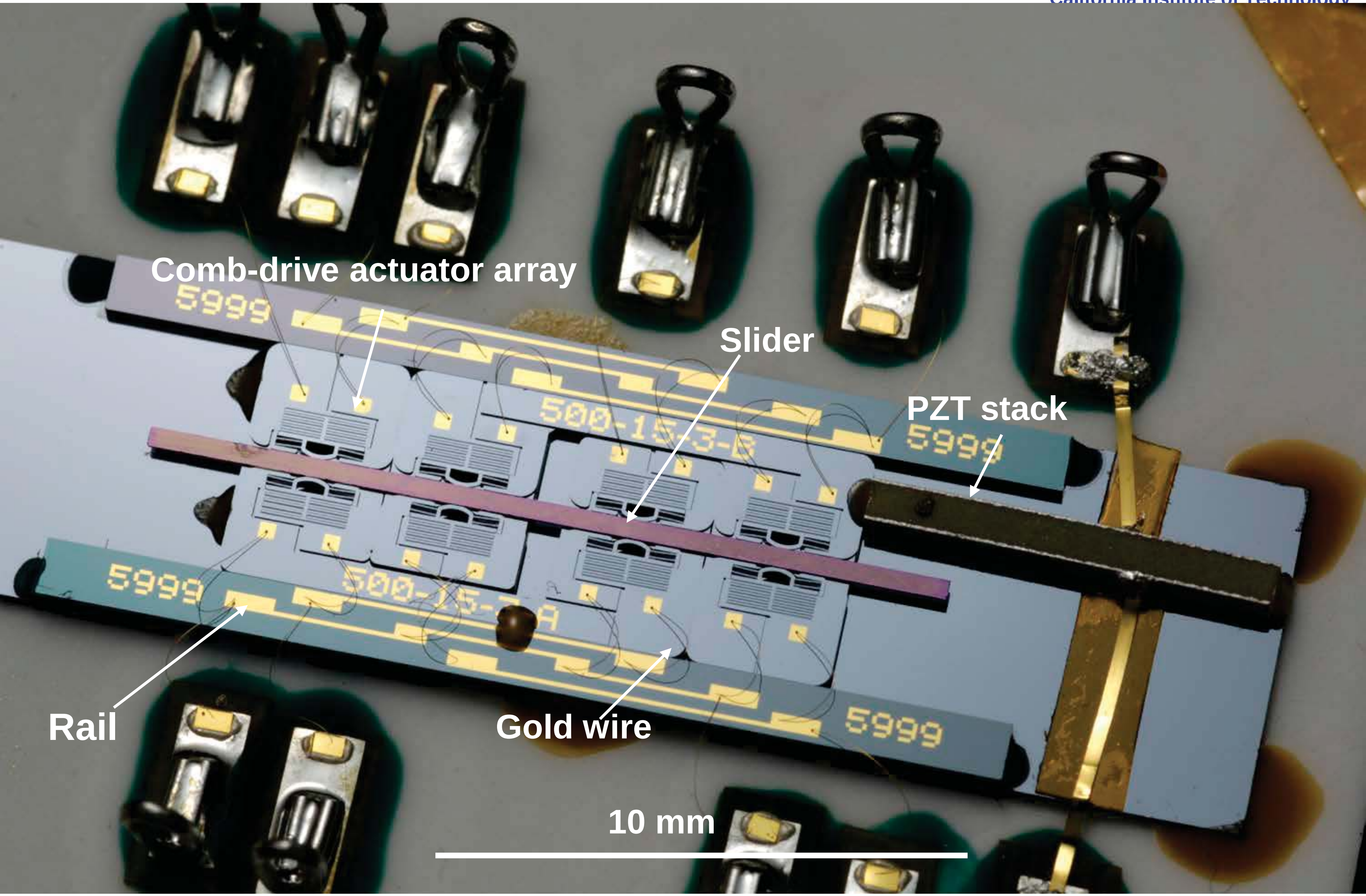

National Aeronautics and Space Administration
Jet Propulsion Laboratory
California Institute of Technology

Actuation: Measured Stroke

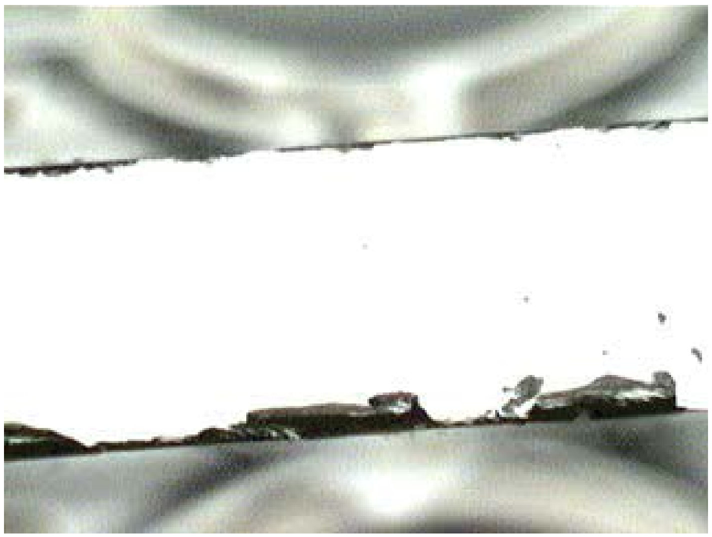

Actuation speed: 1 cycle / 2 second

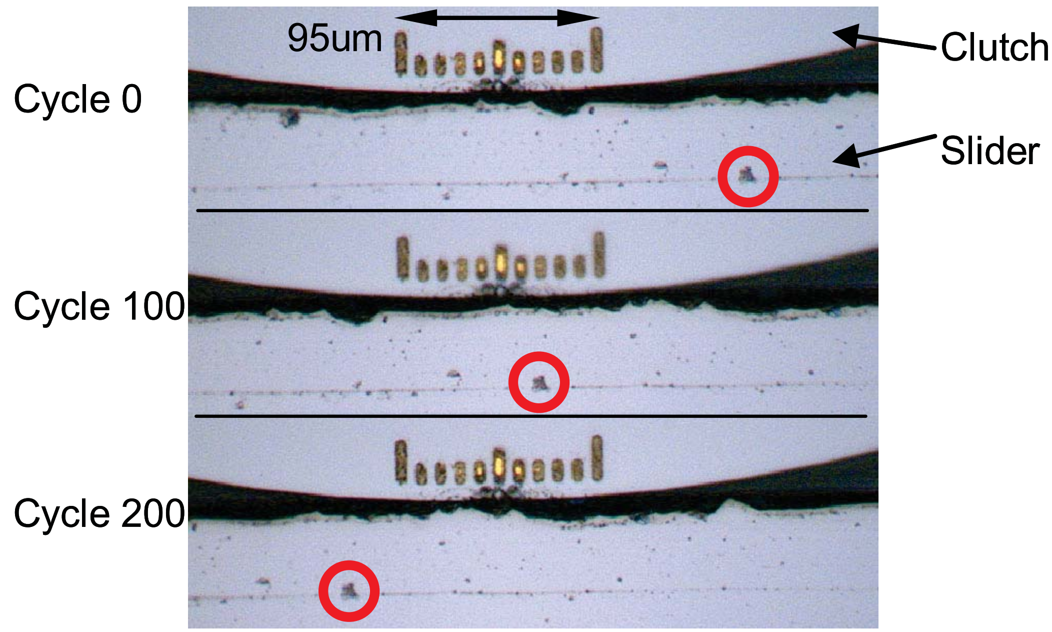

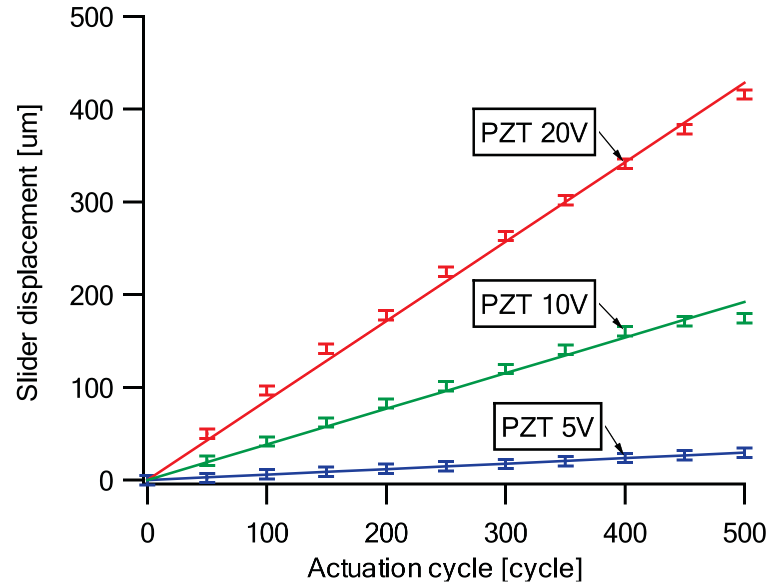

After the 500-cycle actuation, the slider was moved by approximately 450 μm. PZT voltage was 20V. **There is no conceivable limit to the maximum stroke of our actuator other than constraints imposed by length of the slider and external load.**

Slider Motion (3rd Batch Actuator)

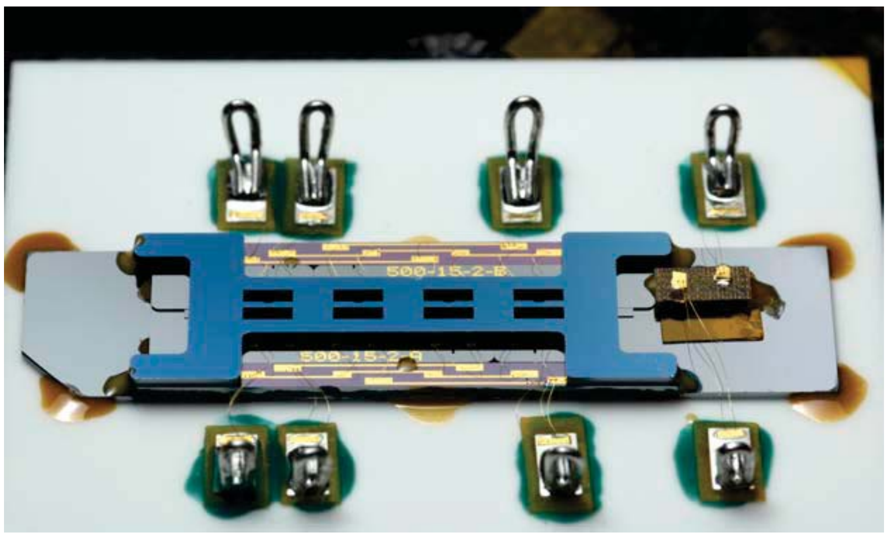

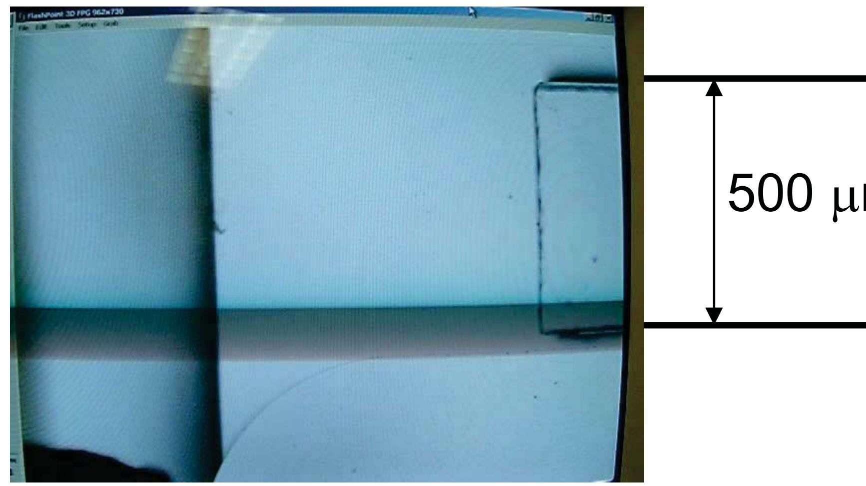

Actuated @ 20-cycle per second with 100 V to PMN-PT

Pathfinder Mirror Modeling

National Aeronautics and Space Administration
Jet Propulsion Laboratory
California Institute of Technology

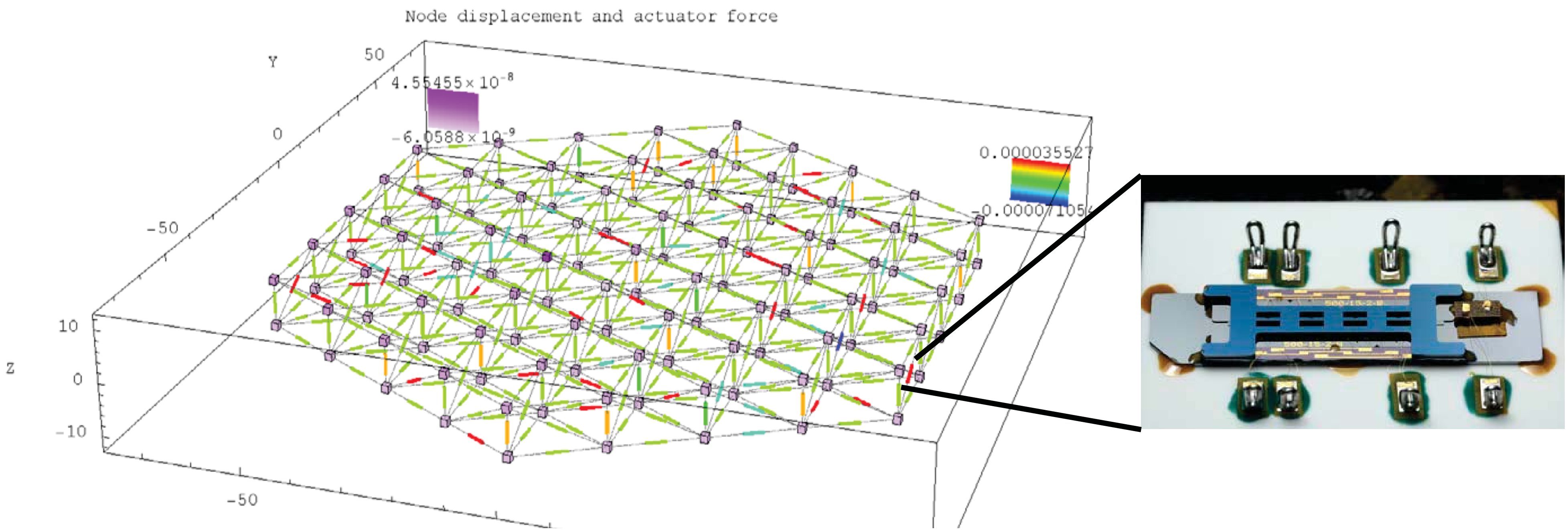

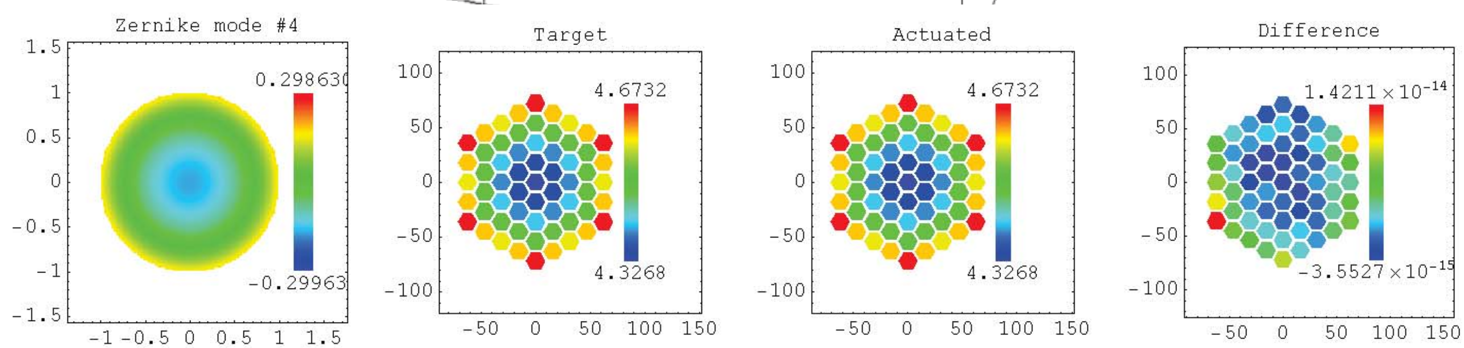

Structure control to the Zernike* mode 4. Actuator displacement commands were calculated and were subsequently applied, and the structure response to the commands was computed.

* In optics, the aberrations are often represented as a sum of special polynomials, called *Zernike polynomials*. Atmospheric random aberrations can be considered in the same way; however, the coefficients of these aberrations (defocus, astigmatism, etc.) are now random functions changing in time. A Zernike polynomial is defined in polar coordinates on a circle of unit radius .

National Aeronautics and Space Administration
Jet Propulsion Laboratory
California Institute of Technology

Current Status

- Improve the actuator design and the fabrication process.
- Address the packaging issue.
- Study integration feasibility with a membrane-mirror face-sheet.
- Model a pathfinder mirror consisting of the inchworm actuators.

	Target	**Demonstrated**	
Max. Freq.	~1 kHz	20-cycle/s	(1)
Stroke	> 1 mm	0.5 mm @ 130-cycle	(2)
Resolution	<30 nm	50 nm	(3)
Force	> 30 mN	48 mN	
Power	100 μW	0 W when latched	
Mass	~100 mg	100 mg	

(1) *The higher-speed actuation (>20Hz/cycle) could not be demonstrated due to the frequency limit of the mechanical relay used for supplying electrical AC signal to actuators.*

(2) *The stroke of our actuator is limited only by the slier length and imposed force.*

(3) *The measured resolution was limited by the image quality for image processing. Actual resolution (minimum step size) is expected to be better.*

Outline

- MEMS Deformable Mirror
- Inchworm Microactuator

For space telescopes

- **Piezoelectric Microvalve**

For microspacecrafts

Small Spacecrafts Requiring Microvalves

National Aeronautics and Space Administration
Jet Propulsion Laboratory
California Institute of Technology

Microspacecraft envelope:
1~ 10 kg mass, 10x10x10 cm^3 Volume, 1 W power

➔ Requiring microvalves capable of fast-actuation, low-leak, high-pressure and low-power operation for micropropulsion

Microvalve Requirements

- Leak Rate - 0.005 sccm He
- Inlet Pressure - ~ 1000 psi
- Actuation Speed - << 1 ms
- Power - << 1 W
- Package Weight - < 10 g
- Temperature - 0 ~ 75 °C

• Conventional microvalve technologies: mass/volume, power consumption

➔ *Moog, VACCO μ-valves: 3-8 W to operate*

• Typical MEMS-based valves: leak or narrow pressure range

➔ *Redwoods microvalve: 400 ms, 0.2 sccm (20 psi), 2 W*

Microvalve Actuation Choices

National Aeronautics and Space Administration
Jet Propulsion Laboratory
California Institute of Technology

	Thermo-pneumatic	Bi-metalic	SMA	Electrostatic (w/spring)	Piezoelectric
Governing Equations	$F = A\ P_2\ (T_1 / T_2)$ P = pressure A = area T = temperature	$F = w\ t^3\ (\Sigma E)\ d / l^3$ w = beam width t = beam thickness ΣE = sum of moduli l = beam length d = deflection	$F = K\ A\ \delta$ A = actuator area δ = strain K = constant, based on Flexinol ™ data	$F = \varepsilon_0 A V^2 / 2g^2$ g = gap, V = voltage, A = area	$F = E_P\ A\ \delta$ E_P = piezo modulus A = area, δ = strain
Geometry	Gas Capsule 10 mm diameter 5 mm high	8 2mm × 2 mm Beams 100 μm thick, (50/50 Ni, Si)	SMA disk 10 mm diameter 5 mm high	Capacitor disk 10 mm diameter w/ spring	Piezo disk 10 mm diameter 5 mm high
Force	~ 1N	~ 2 mN	~ 14 kN	~ 2 μN	~ 5 kN
Max Deflection	-	10 μm	20 μm	5 μm	5 μm
Power	high	high	high	low	low
Actuation Time	long	long	long	short	short

National Aeronautics and Space Administration
Jet Propulsion Laboratory
California Institute of Technology

Microvalve Design

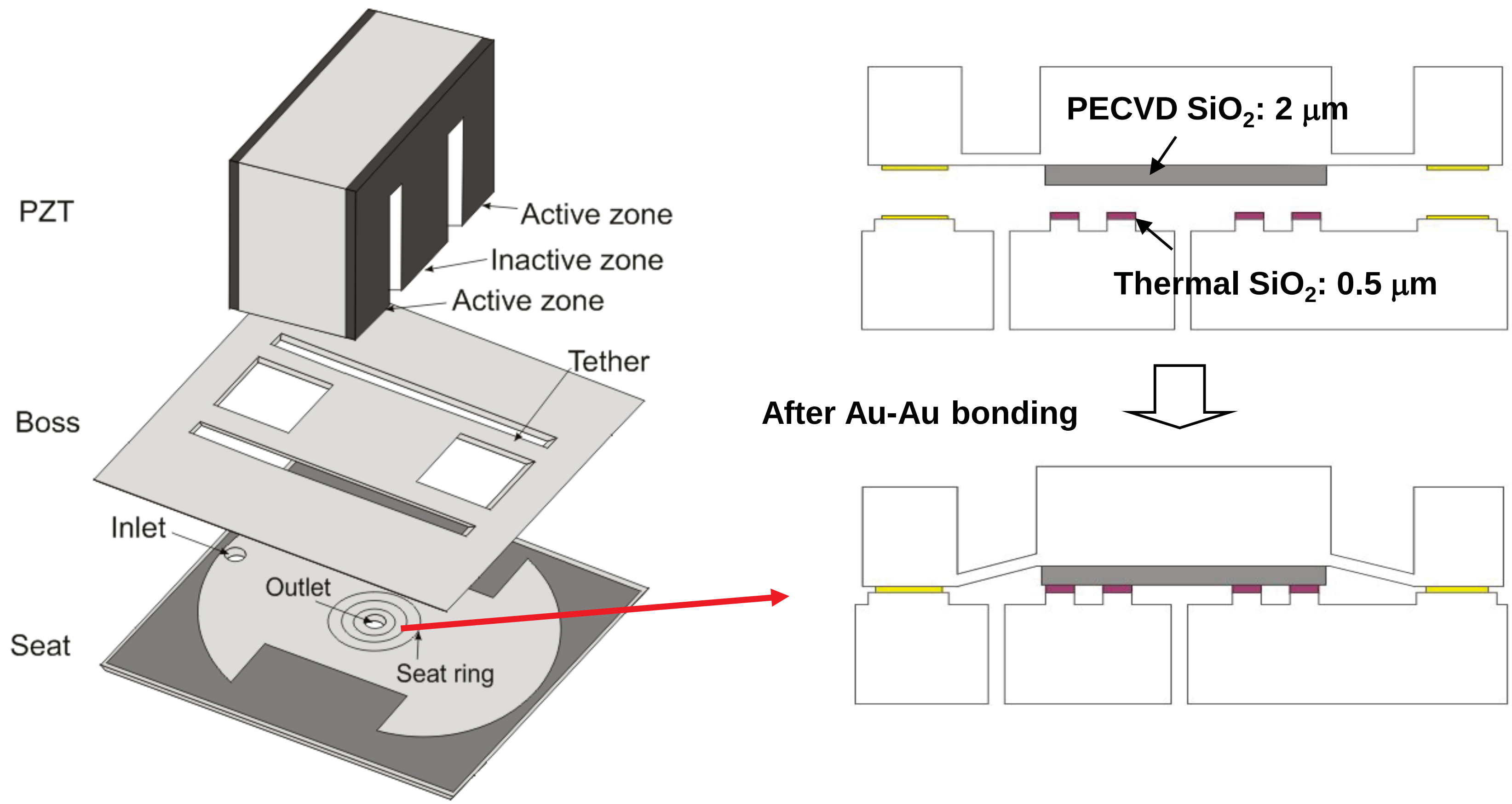

Estimated maximum stresses in the tethers (ANSYS): 80 MPa (on-state).

Seating pressure from pre-stressed PZT: 50 GPa (reducing leak rates)

Microvalve Design

National Aeronautics and Space Administration
Jet Propulsion Laboratory
California Institute of Technology

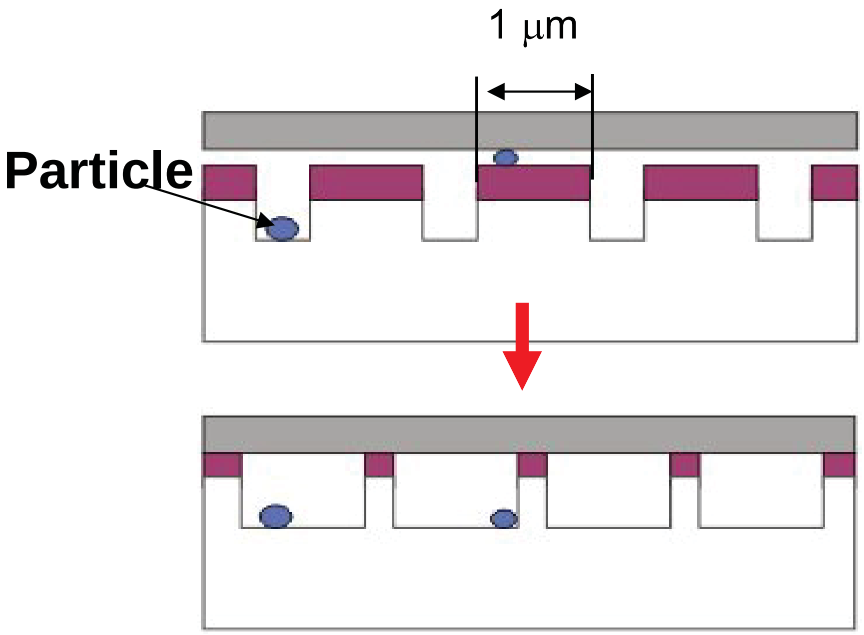

Narrow valve seat rings

a. Immune to particles

b. Enhance seating pressure

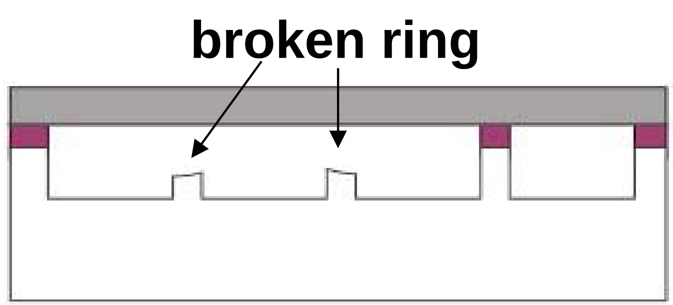

Multiple valve seat rings provide redundancy.

Custom-Designed PZT-Stack

National Aeronautics and Space Administration
Jet Propulsion Laboratory
California Institute of Technology

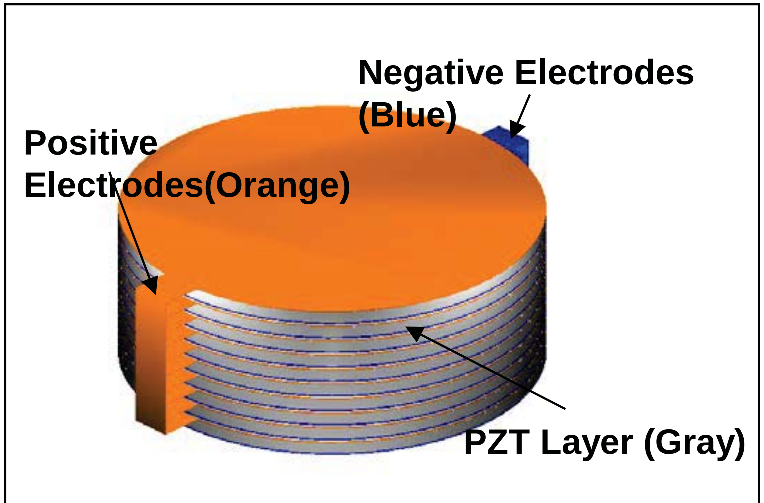

Laminated Piezoelectric Stack

- Thin layers of PZT (100 μm),
- Each layer sandwiched between +/- electrodes
- d33 mode actuation

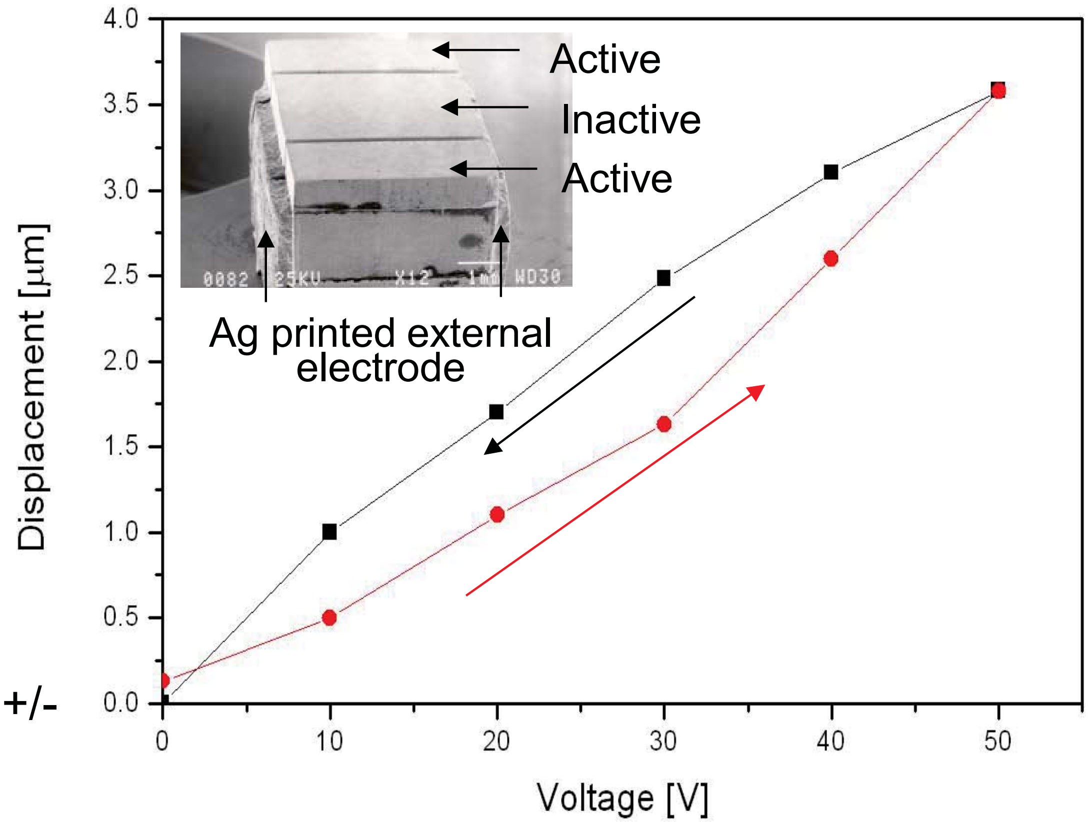

- Displacement of the PZT-stack

Microvalve Operation

National Aeronautics and Space Administration
Jet Propulsion Laboratory
California Institute of Technology

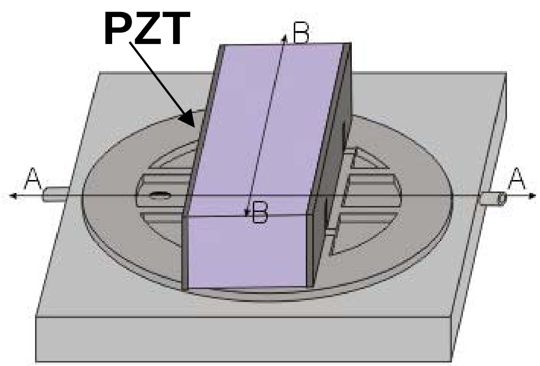

BB

AA

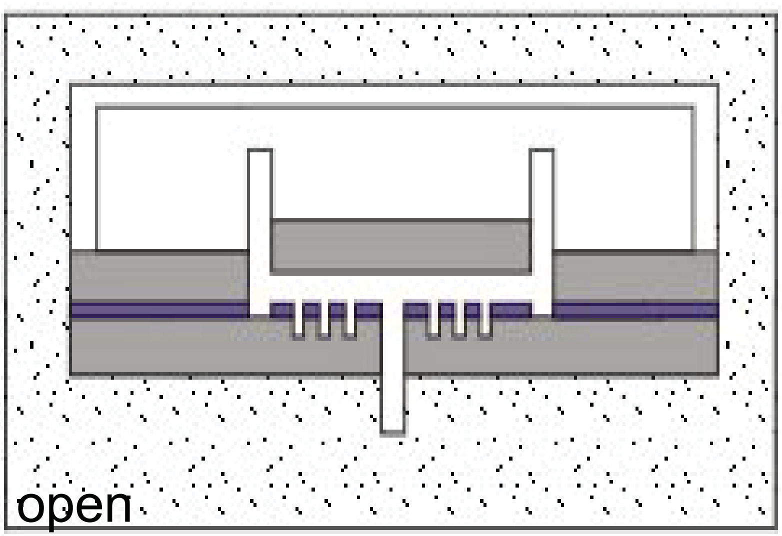

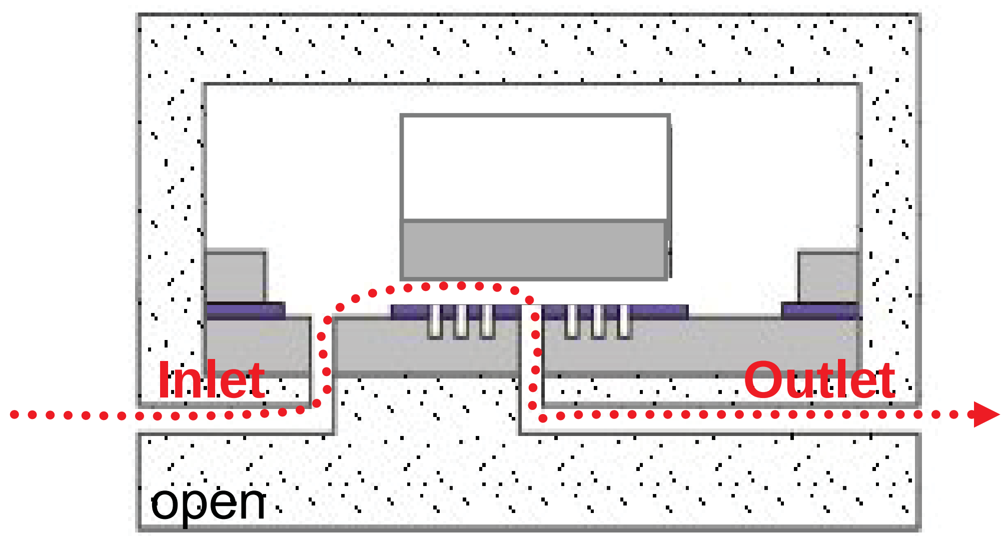

E.H. Yang, L. Wild, N. Rohatgi and D. Bame, "A Piezoelectric Microvalve under Ultra-High Upstream Pressure for Integrated Micropropulsion and Method for Operating the Same", CIT-3889, <u>US Patent Pending, 10/853,072</u>.

Fabrication Process

National Aeronautics and Space Administration
Jet Propulsion Laboratory
California Institute of Technology

- Seat process

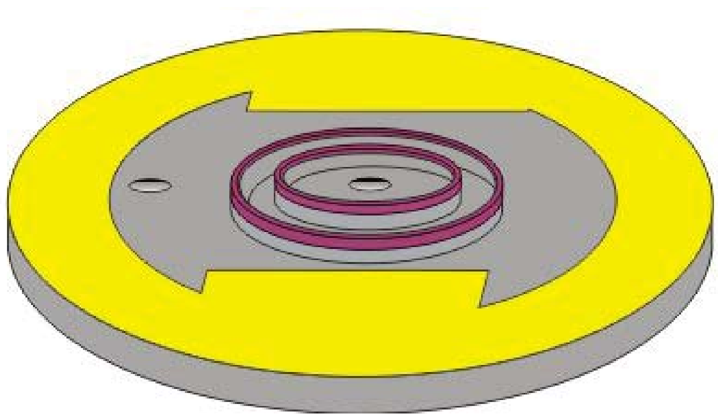

Etching: inlet & outlet holes

Fabrication Process

National Aeronautics and Space Administration
Jet Propulsion Laboratory
California Institute of Technology

- Boss process

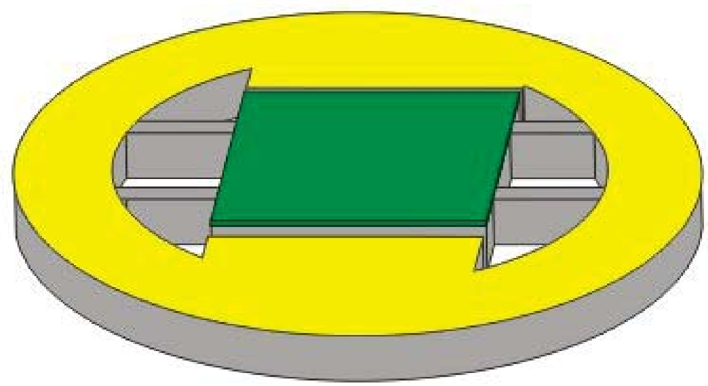

Etching: boss & tethers

National Aeronautics and Space Administration
Jet Propulsion Laboratory
California Institute of Technology

Assembly

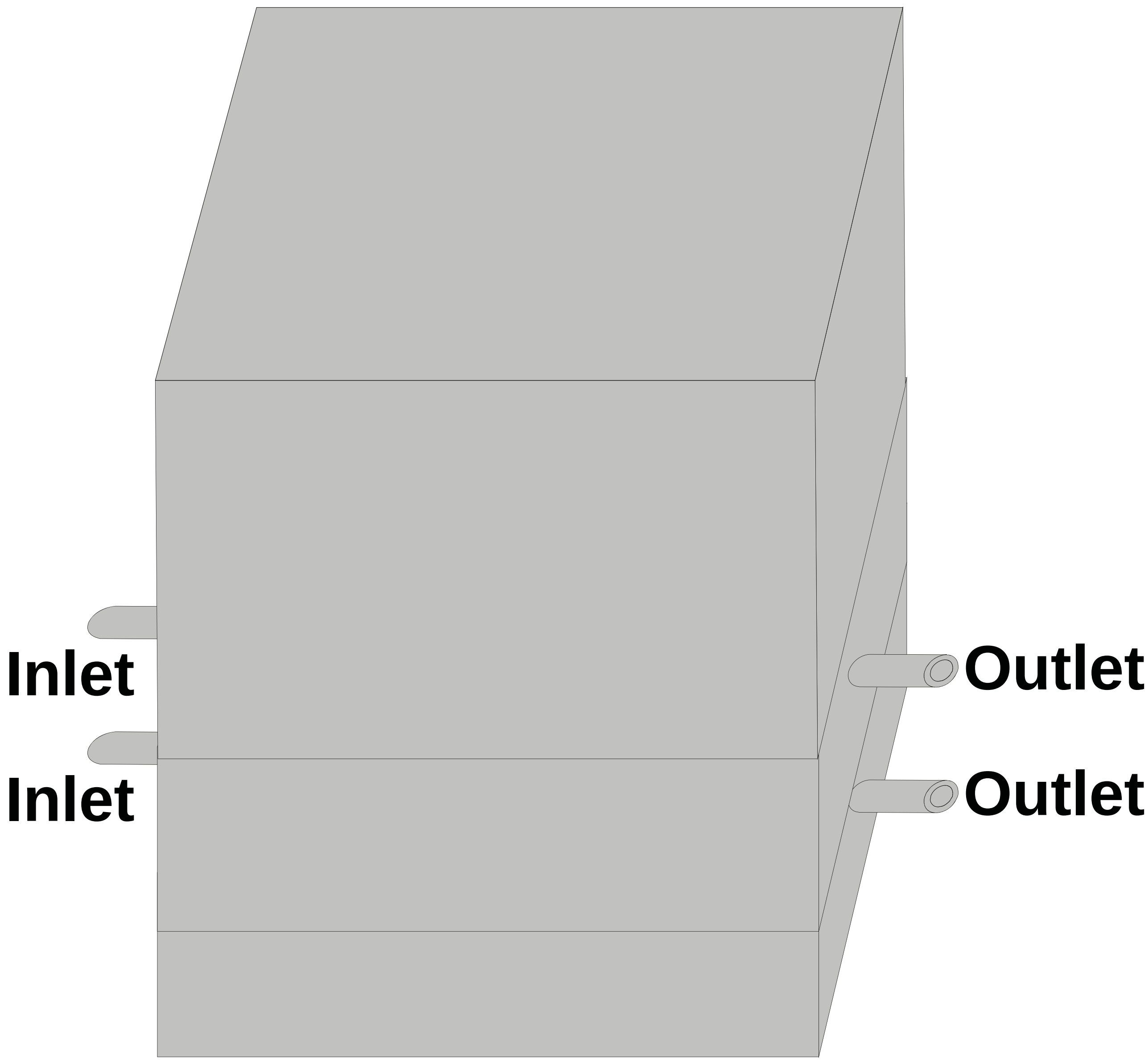

National Aeronautics and Space Administration
Jet Propulsion Laboratory
California Institute of Technology

Fabricated Microvalve

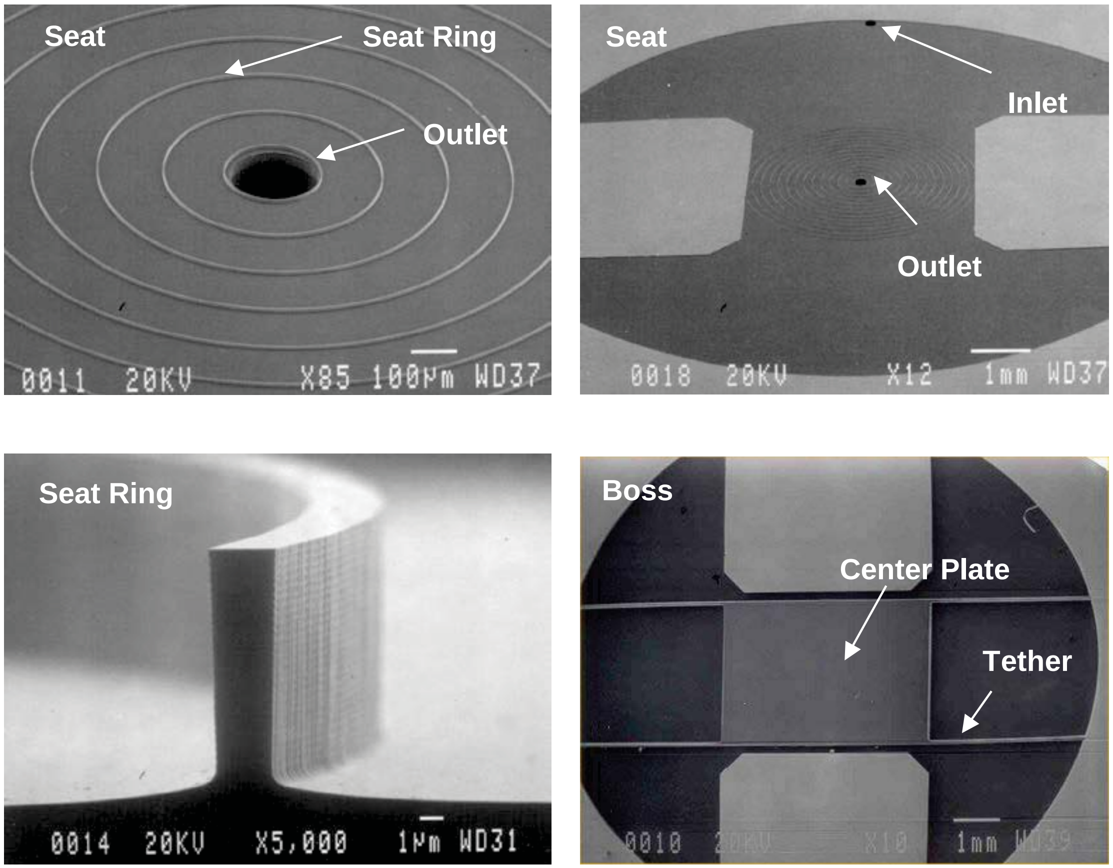

Fabricated Silicon Components

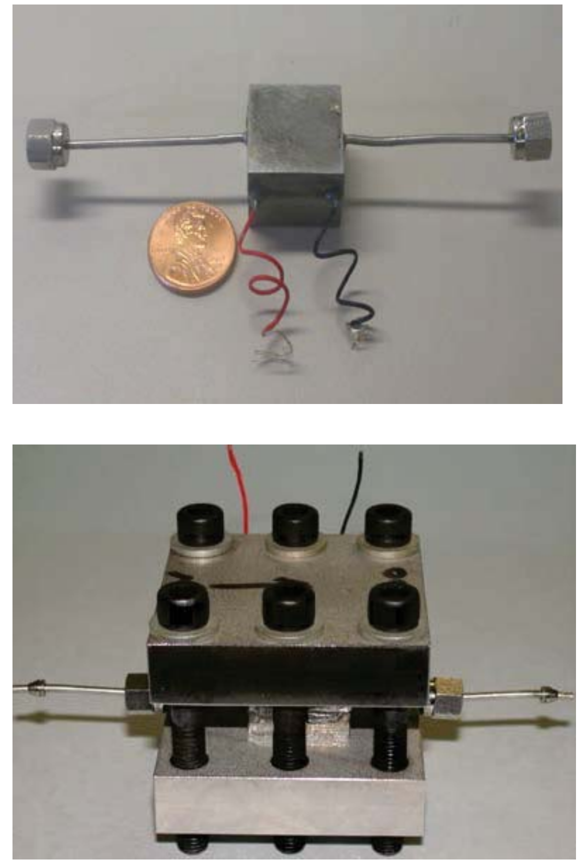

Packaged Microvalve for High-Pressure Test

E. H. Yang, C. S. Lee, J. Mueller and T. George, "Leak-Tight Piezoelectric Microvalve for High-Pressure Gas Micropropulsion," *IEEE/ASME Journal of Microelectromechanical Systems, Vol. 13, No. 5,* pp. 799-807, Oct. 2004.

Leak Performance

National Aeronautics and Space Administration
Jet Propulsion Laboratory
California Institute of Technology

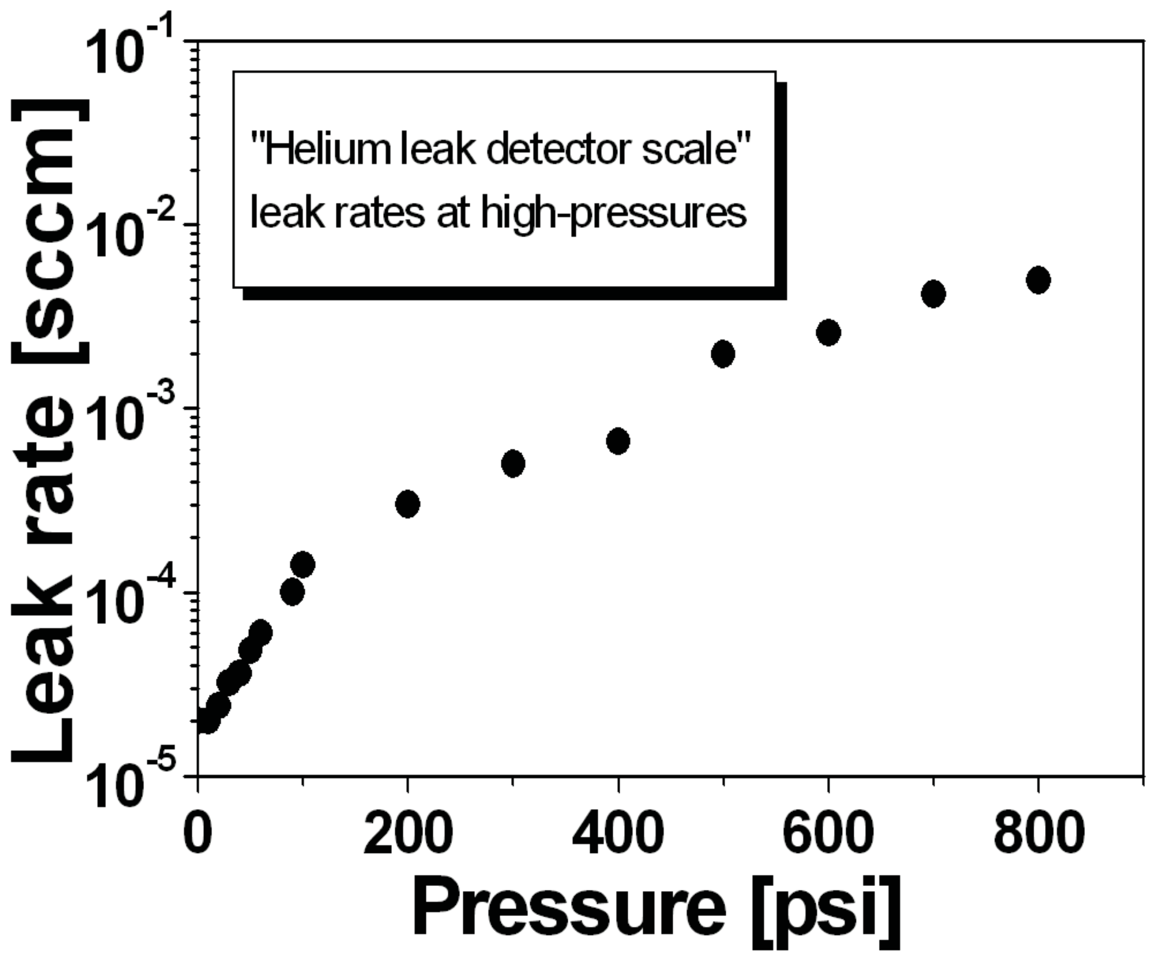

National Aeronautics and Space Administration
Jet Propulsion Laboratory
California Institute of Technology

Flow Performances

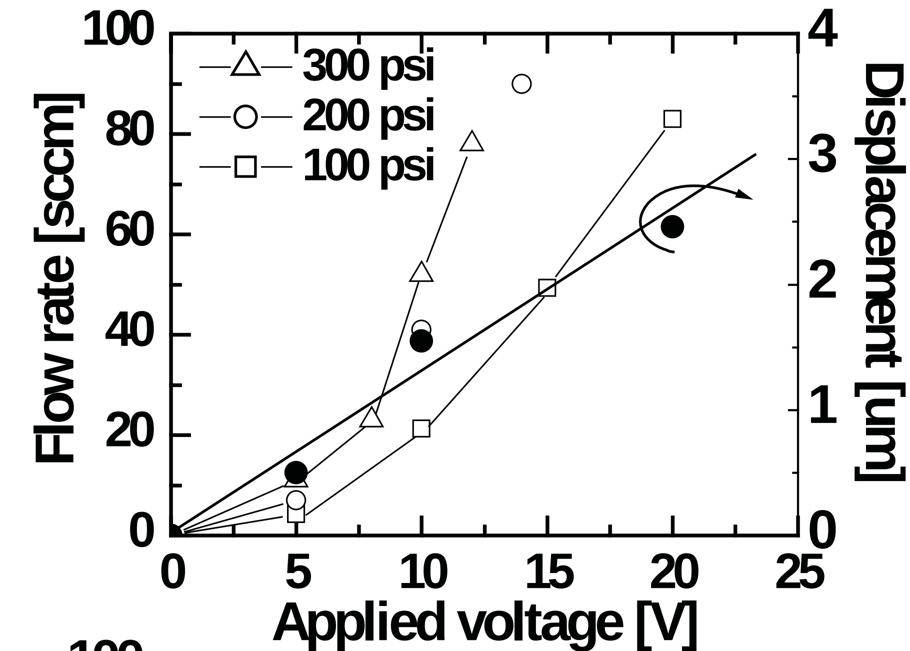

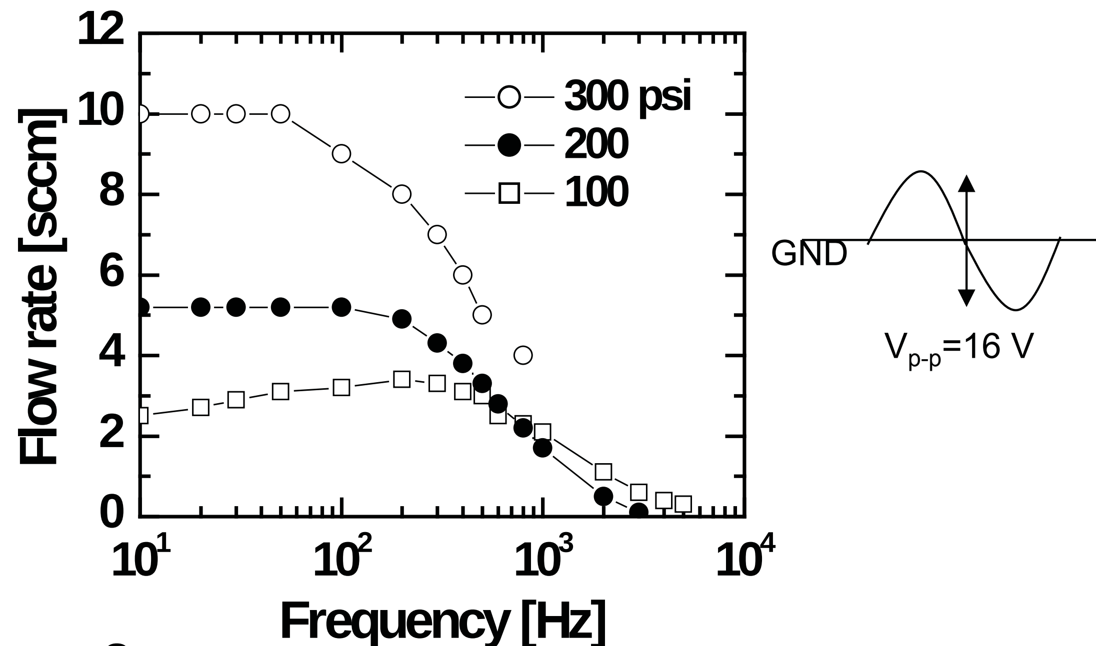

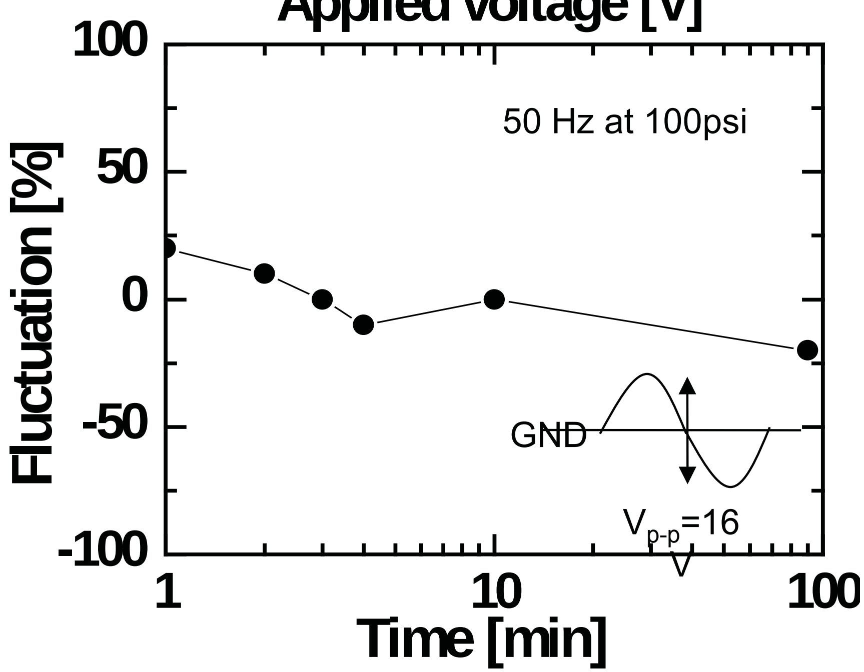

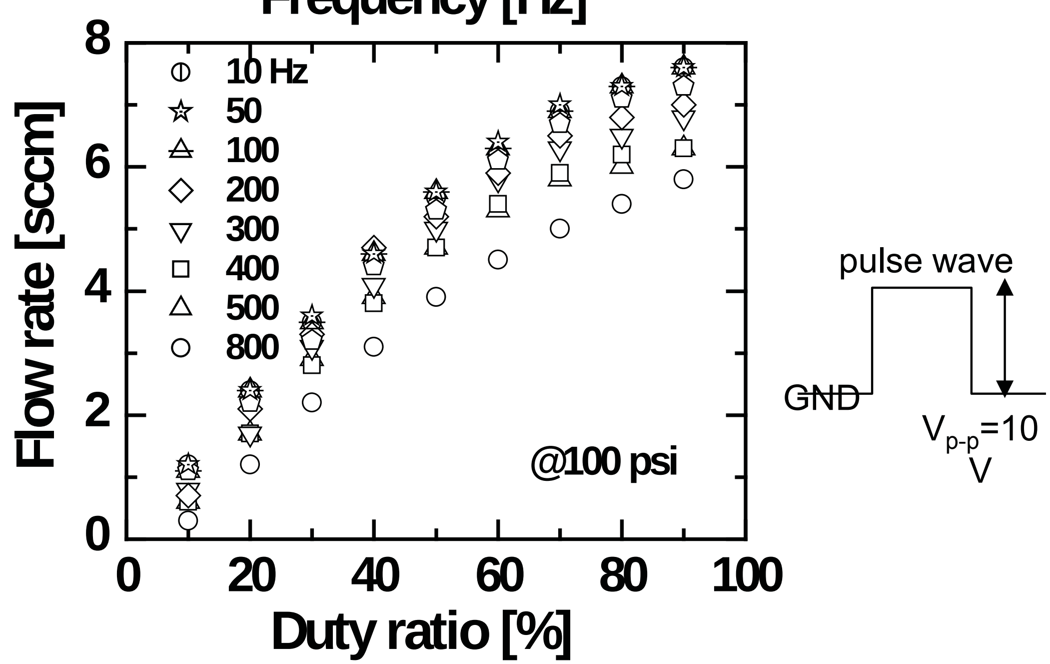

Microvalve for Liquid Flow Control

National Aeronautics and Space Administration
Jet Propulsion Laboratory
California Institute of Technology

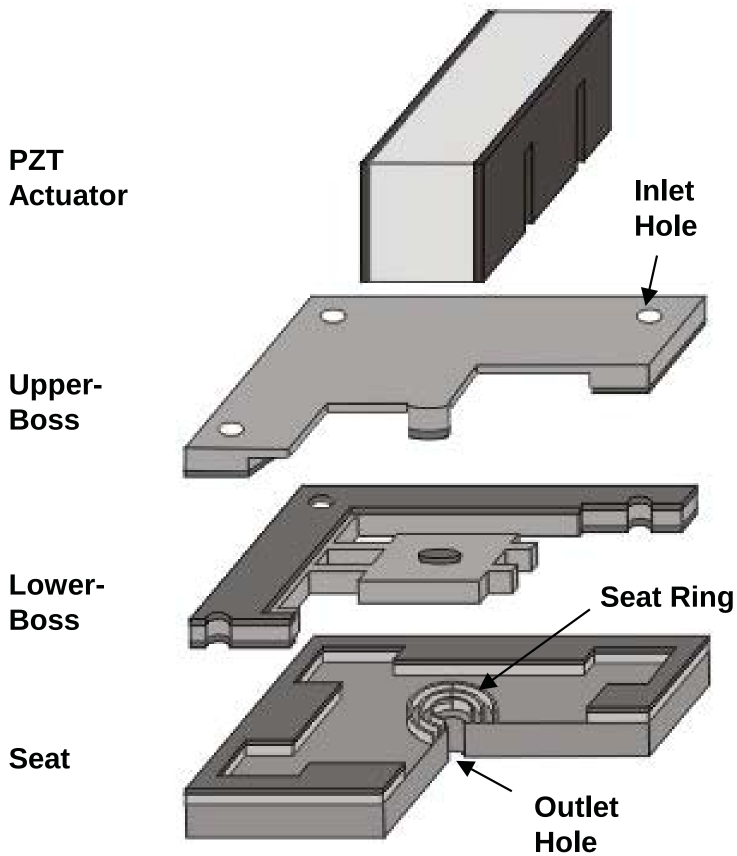

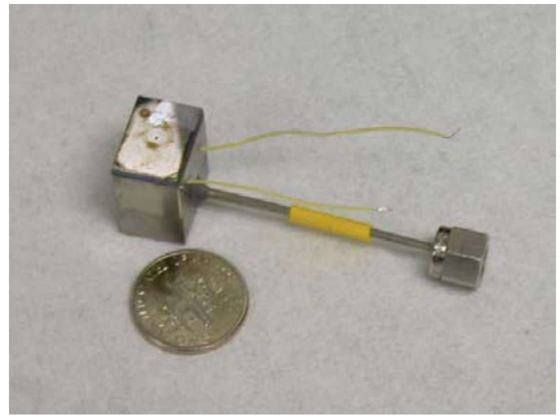

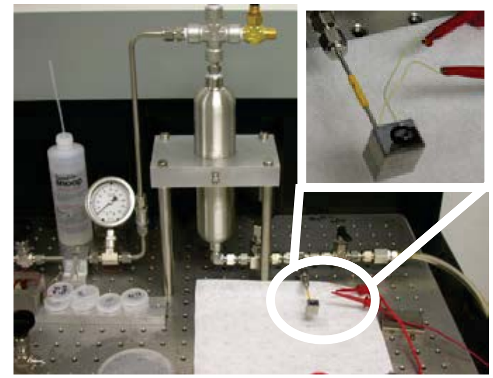

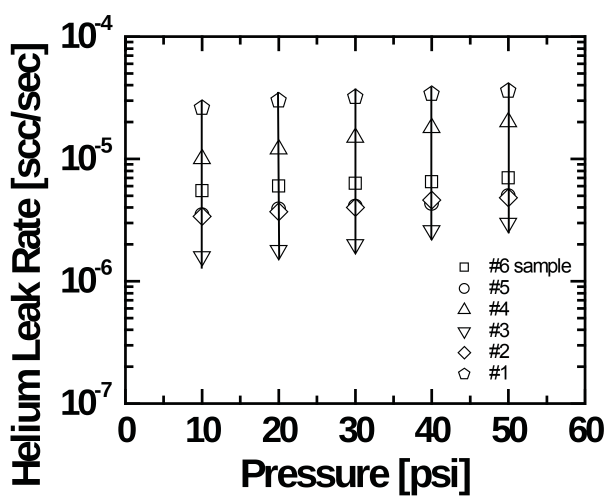

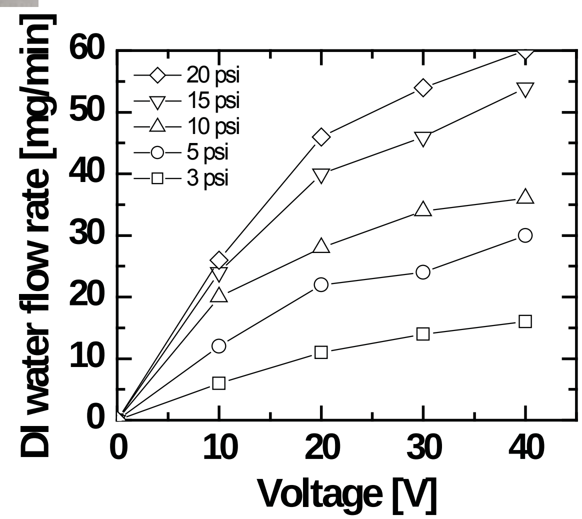

C. Lee, **E. H. Yang**, S. M. Saeidi and J. Khodadadi, "Fabrication, Characterization and Computational Modeling of a Piezoelectrically Actuated Microvalve for Liquid Flow Control," *IEEE/ASME Journal of Microelectromechanical Systems, Vol. 15, No. 3, June 2006.*

Performance Summary

National Aeronautics and Space Administration
Jet Propulsion Laboratory
California Institute of Technology

	Generic Micro-propulsion requirements	Commercially available MEMS valves		Miniaturized Solenoid valve	JPL Piezoelectric Microvalve (Demonstrated)
		Redwood (NC-1500 Fluistor™ Microvalve)	Lee (High Pressure Shuttle, .187" Spring Biased)	Moog MMV	
Leak Rate	< $5\mathrm{x}10^{-3}$ sccm He	50 $\mu l/min$ @ 100 psi, 30 ^oC	5 drops/hr	$6\mathrm{x}10^{-3}$ sccm N_2 (after 1 M cycles)	$5\mathrm{x}10^{-3}$ sccm/He @ 800 psi (after 1 M cycles)
Inlet Pressure Tolerance	~ 1000 psi	100 psi max	-	1000 psi max	0 ~ 1000 psi
Actuation Speed	< 1 ms	1 s	-	2 ms	30 μs (calculation)
Power (on-state)	<< 1 W	1.5 W	-	4 W to open	3 mW @ DC
Life Time	> 10^6 cycles	-	-	10^6 cycles (Test terminated voluntarily)	10^6 cycles (Test terminated voluntarily)

Summary

Microactuator technologies for future space missions.

(1) MEMS deformable mirror technology using PZT unimorph actuator arrays. The design can be tailored to meet several different requirements.

(2) Inchworm microactuator technology for dynamic surface figure correction of future large apertures.

(3) Leak-tight piezoelectric microvalve technology, capable of fast actuation and low power operation at extremely high-pressures for future microspacecrafts.

List of Projects and Acknowledgments

Micro Actuator TRL 2
Sponsor: JPL RTD05,06, NRO, NASA Gossamer S/T NRA, NRO-DII05
Team member: R. Toda (MEMS lead), T. Hatake (Assembly), K. Shcheglov, Zensheu Chang (modeling)
JPL Collaboration: D. Redding (phasing), P. Karlmann (cryo-test)
External Collaboration: TRS Technologies, Inc.

MEMS Microvalve TRL 3
Sponsor: NASA Code R Micro/Nano Sciencecraft
Team member: C.Lee (MEMS lead), D. Bame (Assembly and Test), T. Hatake (PZT bonding)
JPL Collaboration: J. Mueller, D. Collins
External Collaboration: Auburn University, LaRC

Nanowire Sensor Arrays TRL 2
Sponsor: JPL mDRDF05
Team member: D. Choi (process), K. Shcheglov (modeling)
JPL Collaboration: P. Conrad (astrobiology)
External Collaboration: UC Riverside

Adaptive Optics TRL 3
Sponsor: JPL DRDF02,03,04, Reimbursable, NRO-DII06 (pending)
Team member: Y. Hishinuma (MEMS lead), Xiaoqui Bao (modeling)
JPL Collaboration: E. Bloemhof (PI of the DRDF 03 and 04 projects), B. M. Levine (program manager), M. Troy, S. Rao, C. Shelton
External Collaboration: Penn State Univ.

Large Deployable Aperture TRL 2
Sponsor: NRO-DII04
Team member: R. Morgan (Optics), G. Agnes, Z. Chang (Modeling)
JPL Collaboration: Y. Bar-Cohen
External Collaboration: NASA LaRC

Nanochannel TRL 2
Team member: C. Lee, D. Choi K.
External Collaboration: Auburn University

Backup Slides

UCR
University of California, Riverside

National Aeronautics and Space Administration
Jet Propulsion Laboratory
California Institute of Technology

Towards Nano-manufacturing: Magnetic Assembly of Nanowires

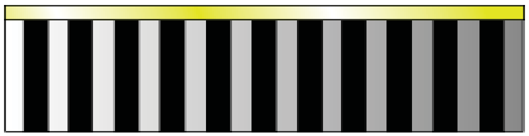

1) Sputter seed layer on Alumina Nanotemplate

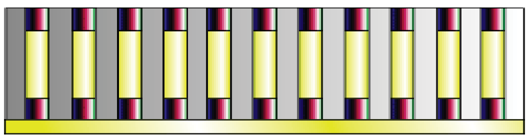

3) Nanowire / electrodeposit soft magnetic material

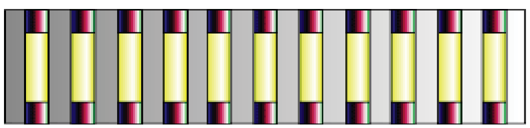

4) Removal of seed layer

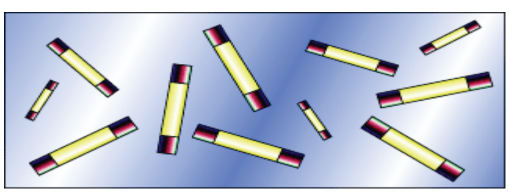

5) Removal of Alumina Template

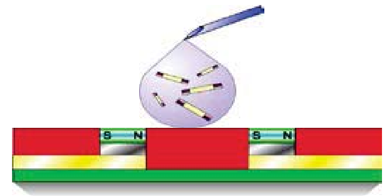

1) Dispense nanowire

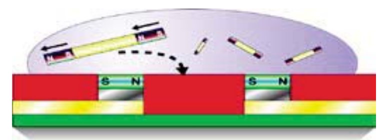

2) Magnetic attraction of nanowire

3) Nanowire align with magnetic pairs of electrodes

4) Create solid electrical contact

UCR
University of California, Riverside

Towards Nano-manufacturing: Magnetic Assembly of Nanowires

National Aeronautics and Space Administration
Jet Propulsion Laboratory
California Institute of Technology

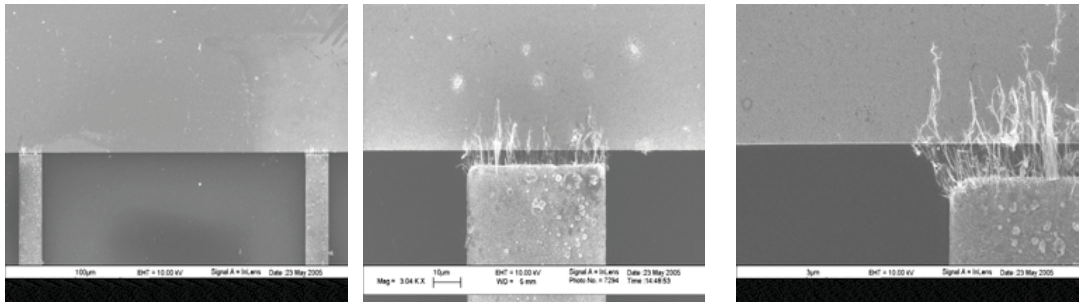

SEM images of magnetically aligned nickel nanowires on ferromagnetic electrodes.

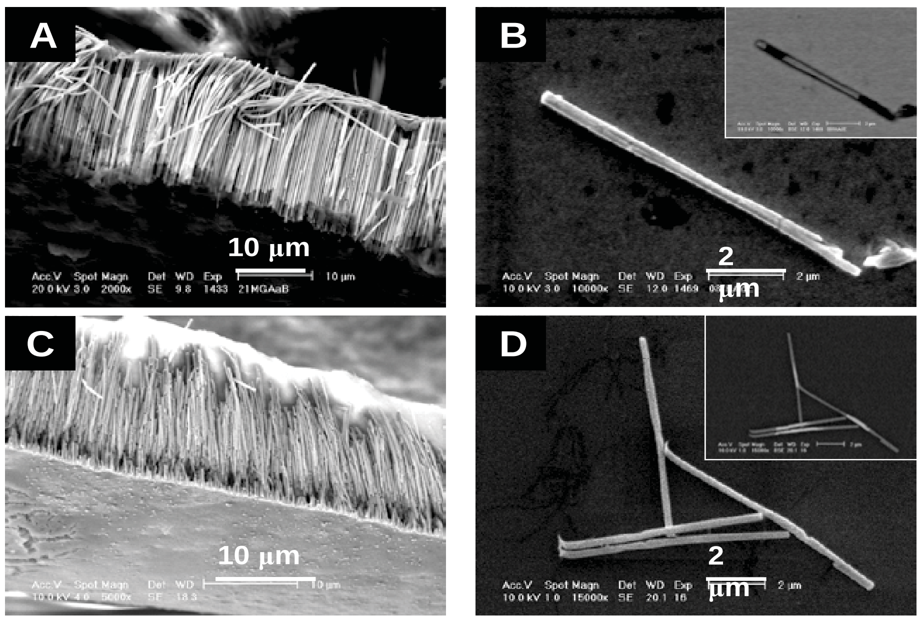

(A) Manganese oxide nanowires, (B) Ni/Au/Ni nanowires, (C) Ni/Bi/Ni nanowires and (D) Ni/Au/Polypyrrole/Au nanowires

UCR
University of California, Riverside

Towards Nano-manufacturing: Magnetic Assembly of Nanowires

National Aeronautics and Space Administration
Jet Propulsion Laboratory
California Institute of Technology

- Fabricate biofunctionalized nanowires in single steps without post functionalization, and magnetically assemble them.

- Demonstrate gas-sensing functionality by measuring conductance change of nanowires. *For instance, detection of NH3 using polyaniline, NO2 using polypyrrole, and VOC (Volatile Organic Compounds) using metal oxides are possible.*

- Calculated dynamic range (carbon) is approximately 17. Estimated detection limit (ZnO) is 1×10^{-20} grams.

An Example of Applications: High Density Nano-'Nose'

University of California, Riverside

National Aeronautics and Space Administration
Jet Propulsion Laboratory
California Institute of Technology

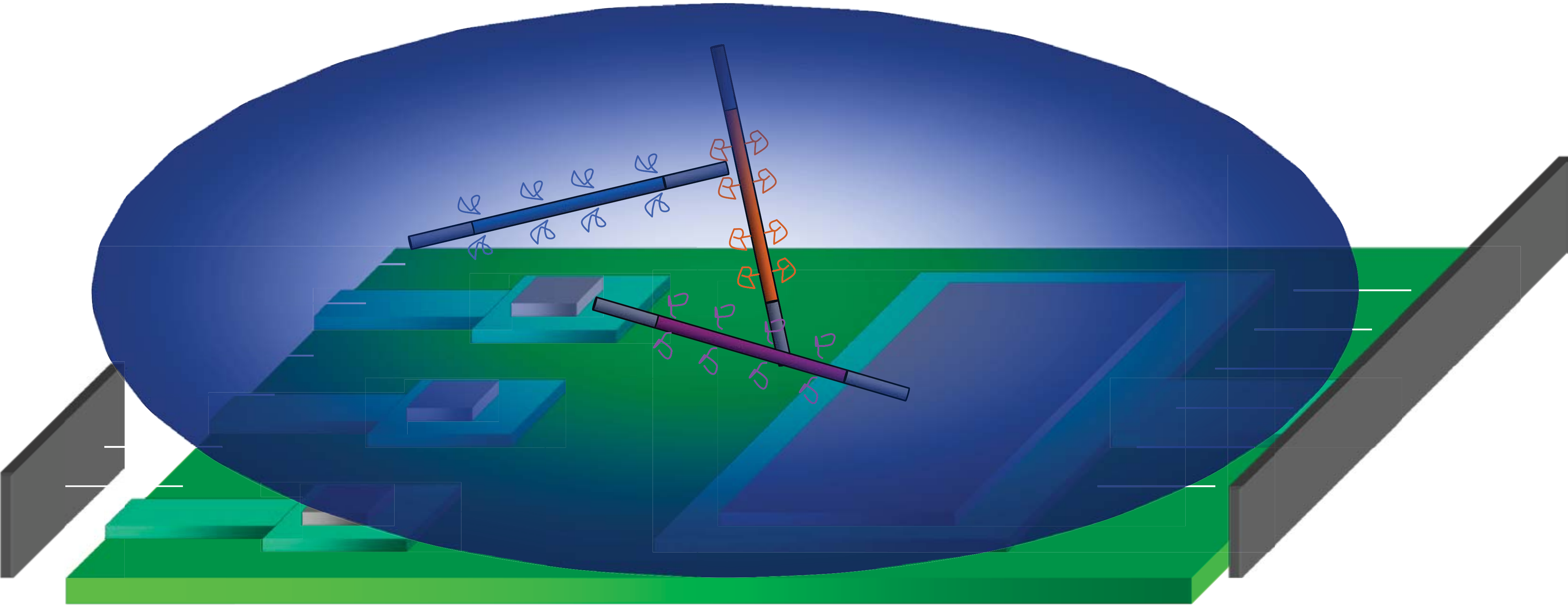

Courtesy: UC Riverside

UCR
University of California, Riverside

Benefits over Current SOAs

National Aeronautics and Space Administration
Jet Propulsion Laboratory
California Institute of Technology

	CNT	Si NWs	Proposed Nanowires
Materials	Carbon	Silicon	II-VI and III-V semiconductor, Metal oxides, Conducting polymers
Deposition Techniques	*Arc-discharge Methods *Laser *CVD (catalytic decomposition)	*Laser assisted *Supercritical fluid solution method	*Electrochemical method
Manufacturability	Difficult	Difficult	Easy
Surface Modification	Limited	Well-known	Well-known
Functionality	Limited	Limited	Ability to functionalize individual nanowires
	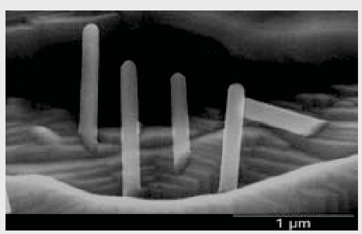	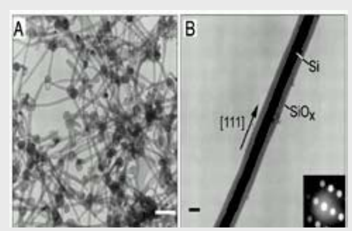	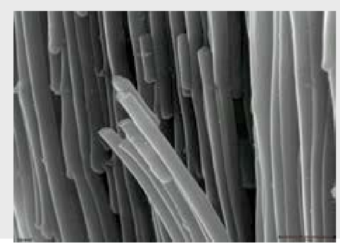

Fabrication of Nanochannels

National Aeronautics and Space Administration
Jet Propulsion Laboratory
California Institute of Technology

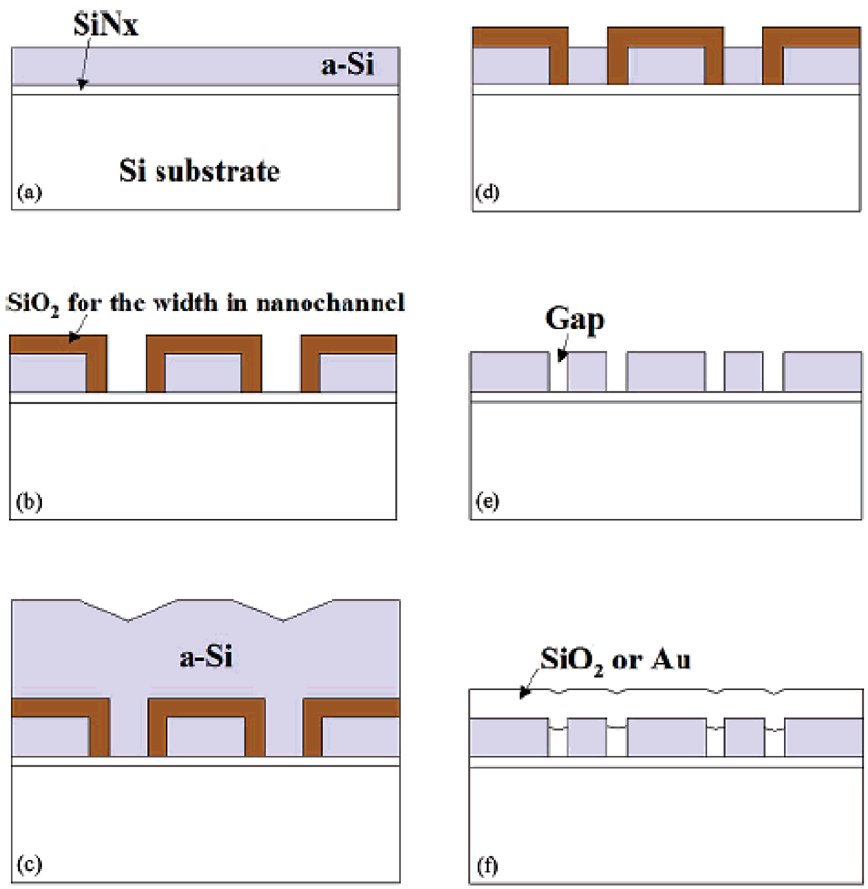

Figure 1. Fabrication procedures. (a) SiN_x and first amorphous Si deposition; (b) RIE and dry O_2 oxidation for the nanometer gap; (c) second amorphous Si deposition; (d) CMP until the gap oxide is exposed. (e) The oxide in the nanometer gap is etched. (f) The Au or oxide layer is used for sealing.

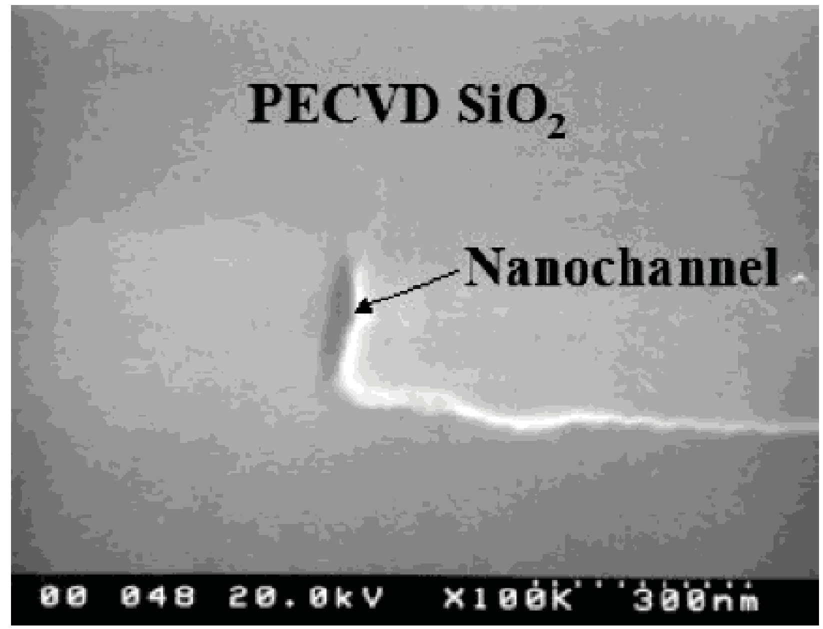

Figure 3. SEM micrograph of nanochannel with PECVD oxide sealing: The width is approximately 25 nm.

C. Lee, E. H. Yang, N.V. Myung, and T. George, "A Nanochannel Fabrication Technology without Nanolithography," *NanoLetters, Vol. 3, No. 10*, pp. 1339-1340, Oct. 2003.

Advantages and Disadvantages of Micro and Nano Technologies

- **Benefits**
  - *Powerful "medium" to create new devices, components and systems*
  - *Low mass, power and size*
  - *Large scale replication and hence lower costs*
  - *Integration with electronics is possible*
  - *Manual assembly can be eliminated*
  - *Chemical Sensor/Reactor applications*
    - *Low processing volumes*
    - *Massively parallel ("digital") scale-up is possible*

- **Downside**
  - *Low TRL. Very few system/sub-systems*
  - *Relative tolerances are low*
  - *Not all devices are amenable to miniaturization*
  - *Lower sensitivity than macroscopic devices*
  - *Packaging is difficult*

Microfabrication

National Aeronautics and Space Administration
Jet Propulsion Laboratory
California Institute of Technology

Anisotropic Bulk Micromachining

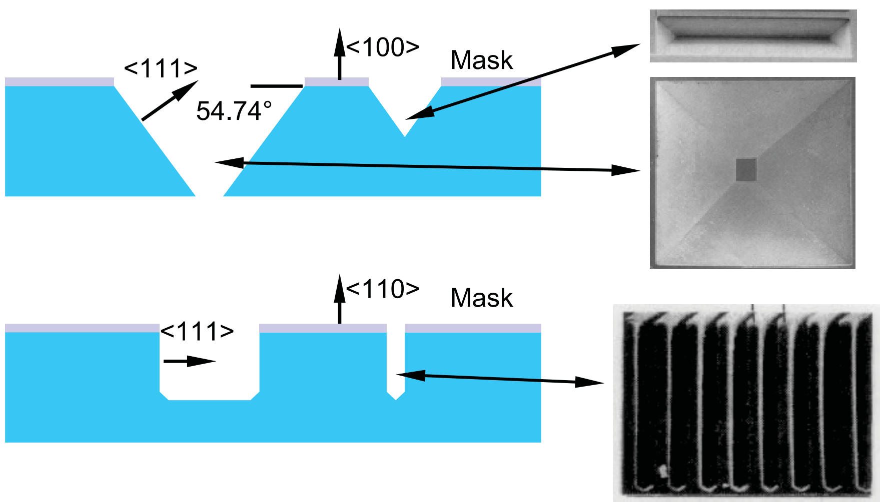

LiGA

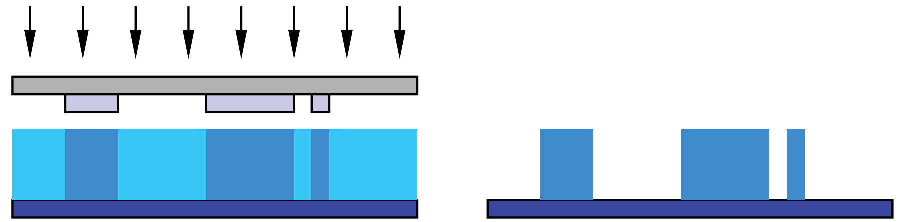

Polysilicon Surface Micromachining

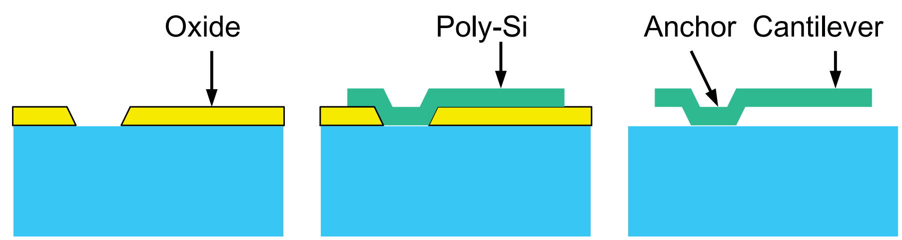

Deep Reactive-Ion Etching of Si

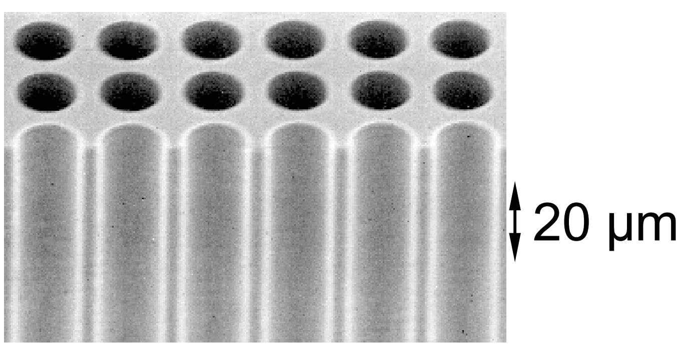

Anodic Wafer Bonding

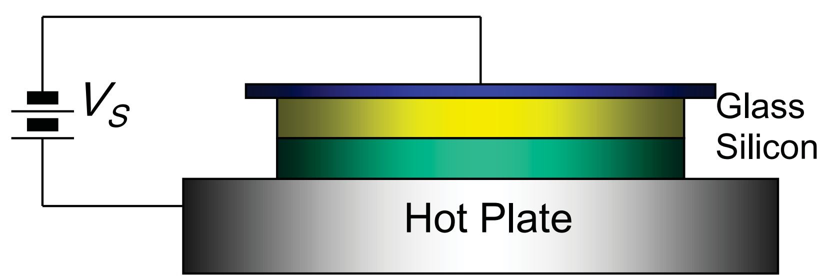

The Keck Telescope

National Aeronautics and Space Administration
Jet Propulsion Laboratory
California Institute of Technology

Adaptive optics lives here

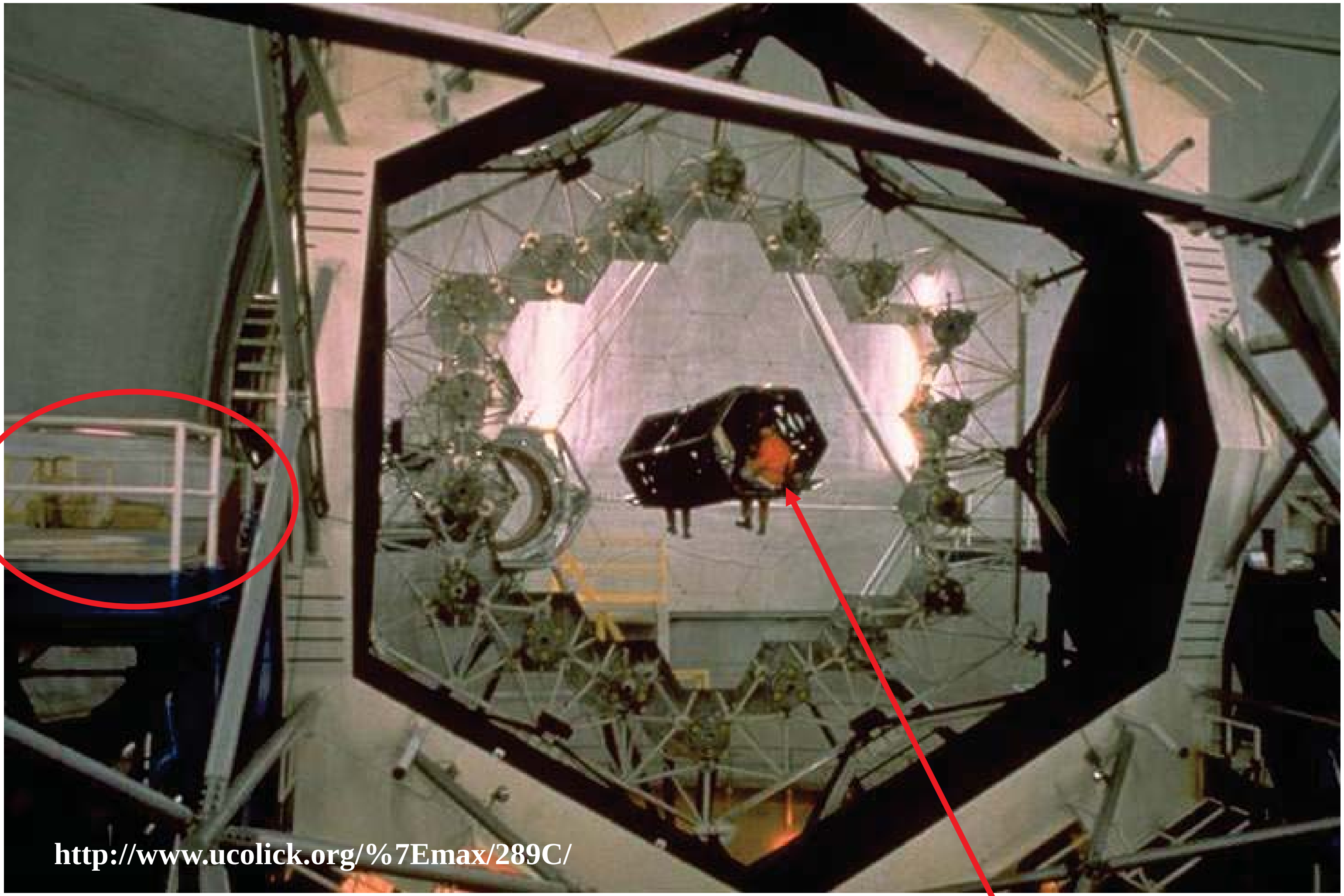

Person!

Future Ultra-Large Telescopes

National Aeronautics and Space Administration
Jet Propulsion Laboratory
California Institute of Technology

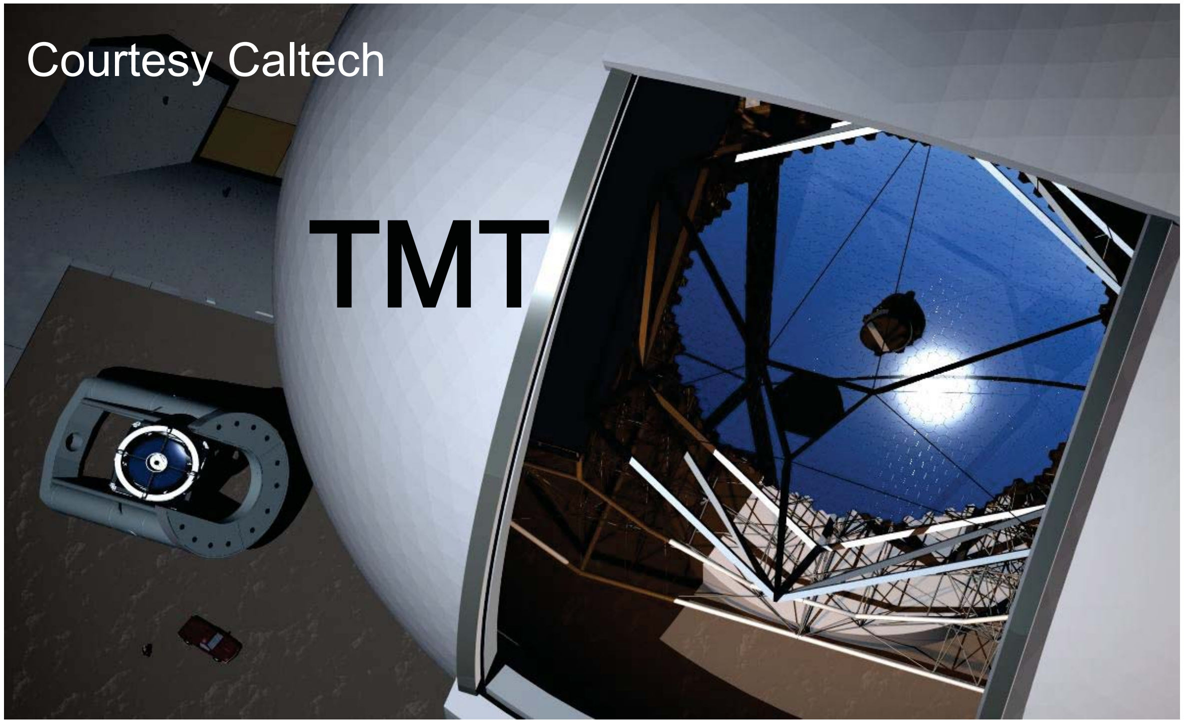

Under ideal circumstances, the resolution of an optical system is limited by the diffraction of light waves. The "diffraction limit“ is generally described by the following angle (in radians) calculated using the light's wavelength and optical system's pupil diameter:

$$\alpha = 1.22\frac{\lambda}{D}$$

where the angle is given in radians.

State of the Art Deformable Mirrors

National Aeronautics and Space Administration
Jet Propulsion Laboratory
California Institute of Technology

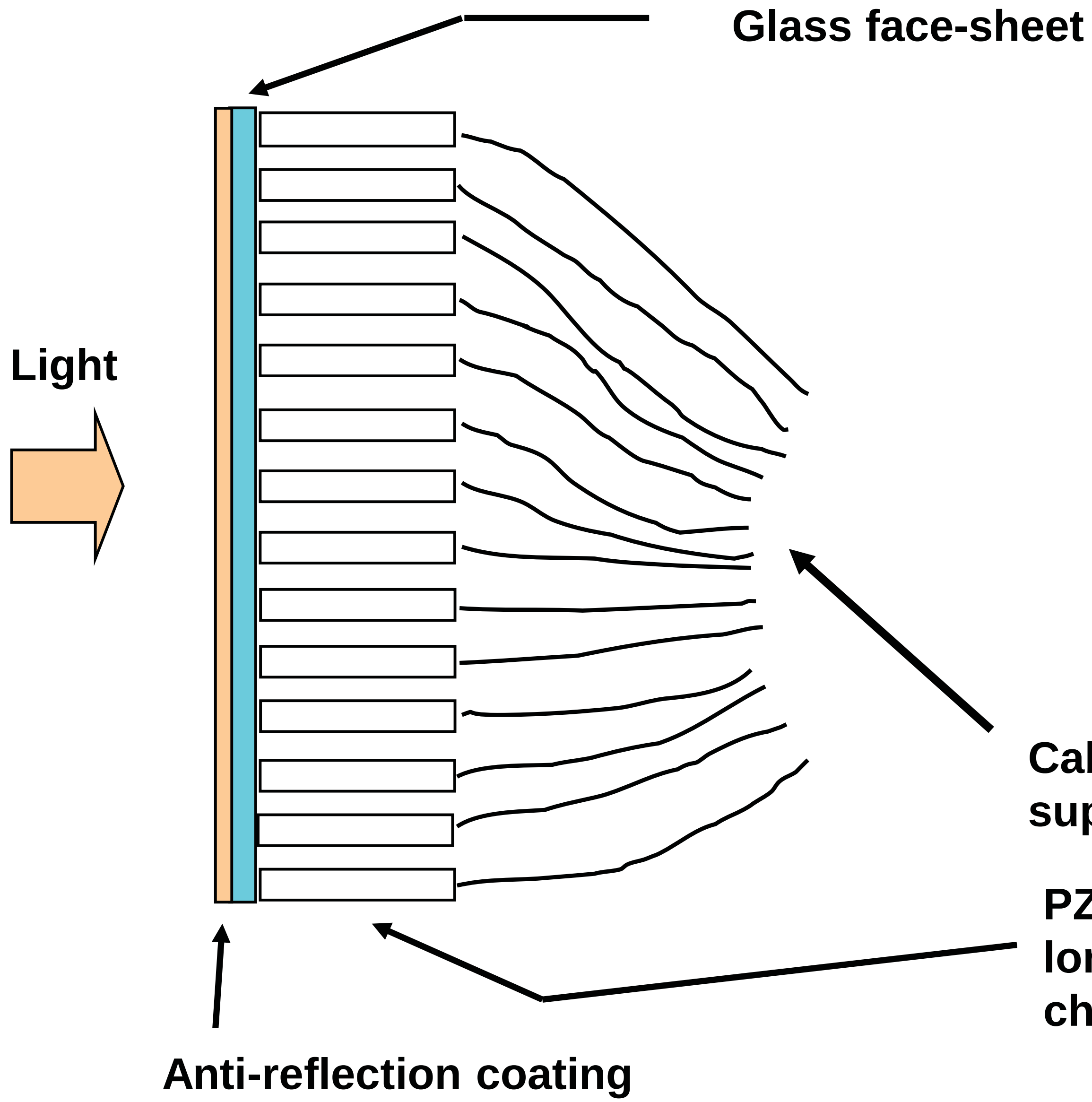

Most deformable mirrors today have thin glass face-sheets.

Xinetics photonics module
Cost: ~$800K (64x64)
Stroke 0.1~0.2 μm
Interconnection and wiring problem

Measuring Turbulent Distortions

National Aeronautics and Space Administration
Jet Propulsion Laboratory
California Institute of Technology

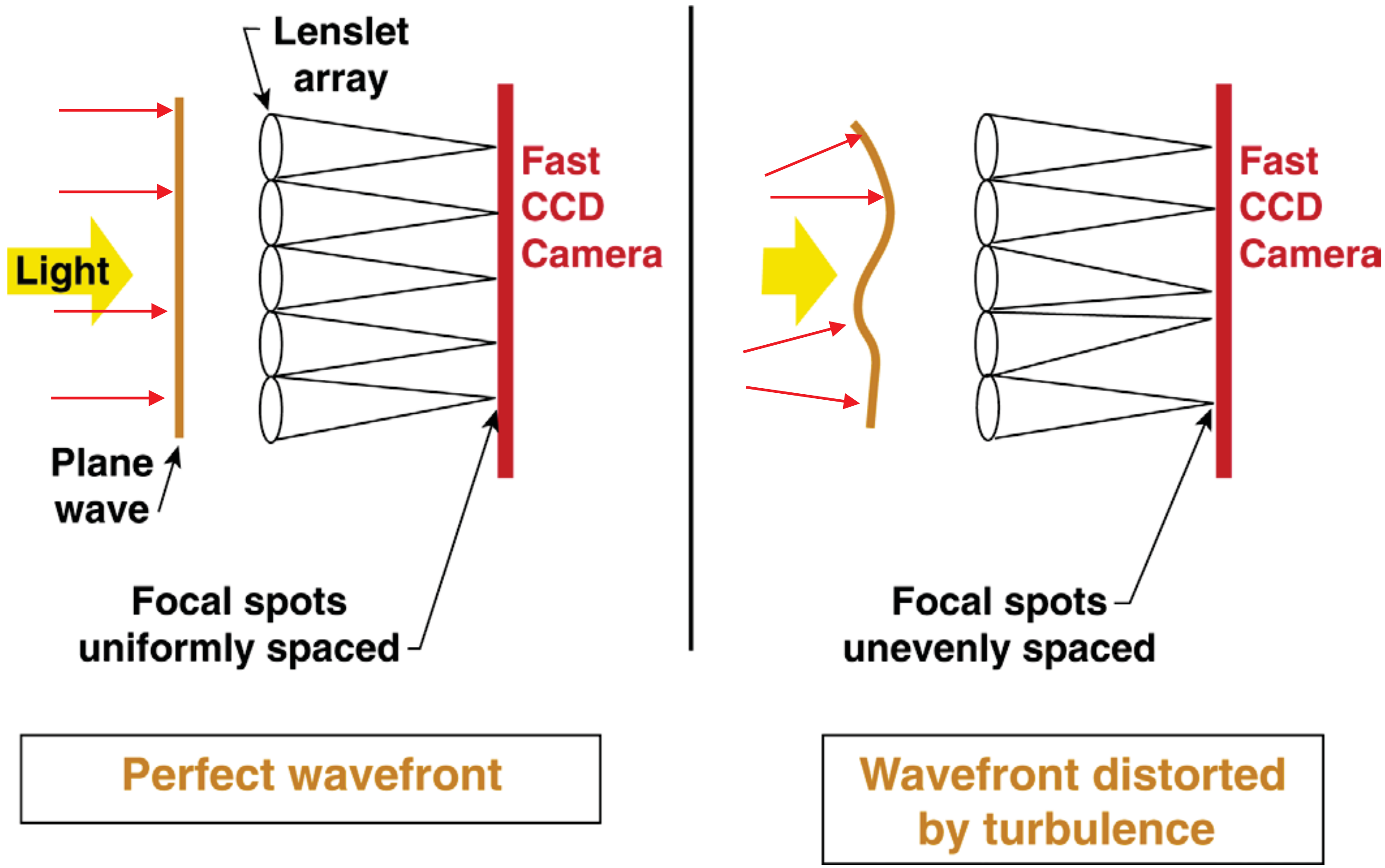

Shack-Hartmann wavefront sensor (one method among many)

National Aeronautics and Space Administration
Jet Propulsion Laboratory
California Institute of Technology

Unimorph Actuator Modeling

Modeling

1) Thin plate theory
2) Energy minimization

Find deflection profile using Thin Plate Theory

$\times \lambda$

Find total energy of membrane under deflection

$$U_{tot} = U_{el} + U_s + U_M$$

Apply energy minimization condition $\dfrac{\partial U_{tot}}{\partial \lambda} = 0$

Find deflection at the center

Change parameters

Repeat

Unimorph Actuator Modeling

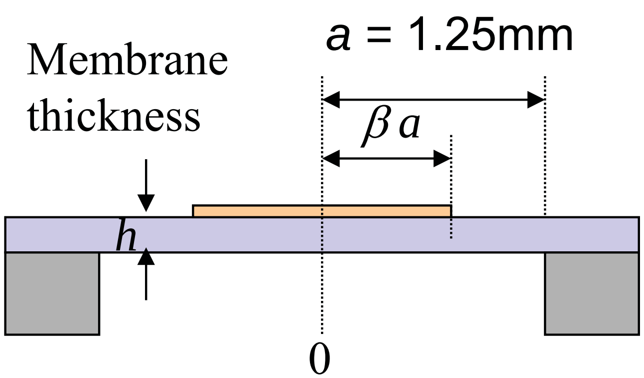

Y = 107 GPa : Young's Modulus of Silicon

ν= 0.22 : Poisson's ratio

e_{31} = -6 C/m^2

$\sigma_{Ti,\ Pt}$= 300 MPa

σ_{PZT}= 260 MPA

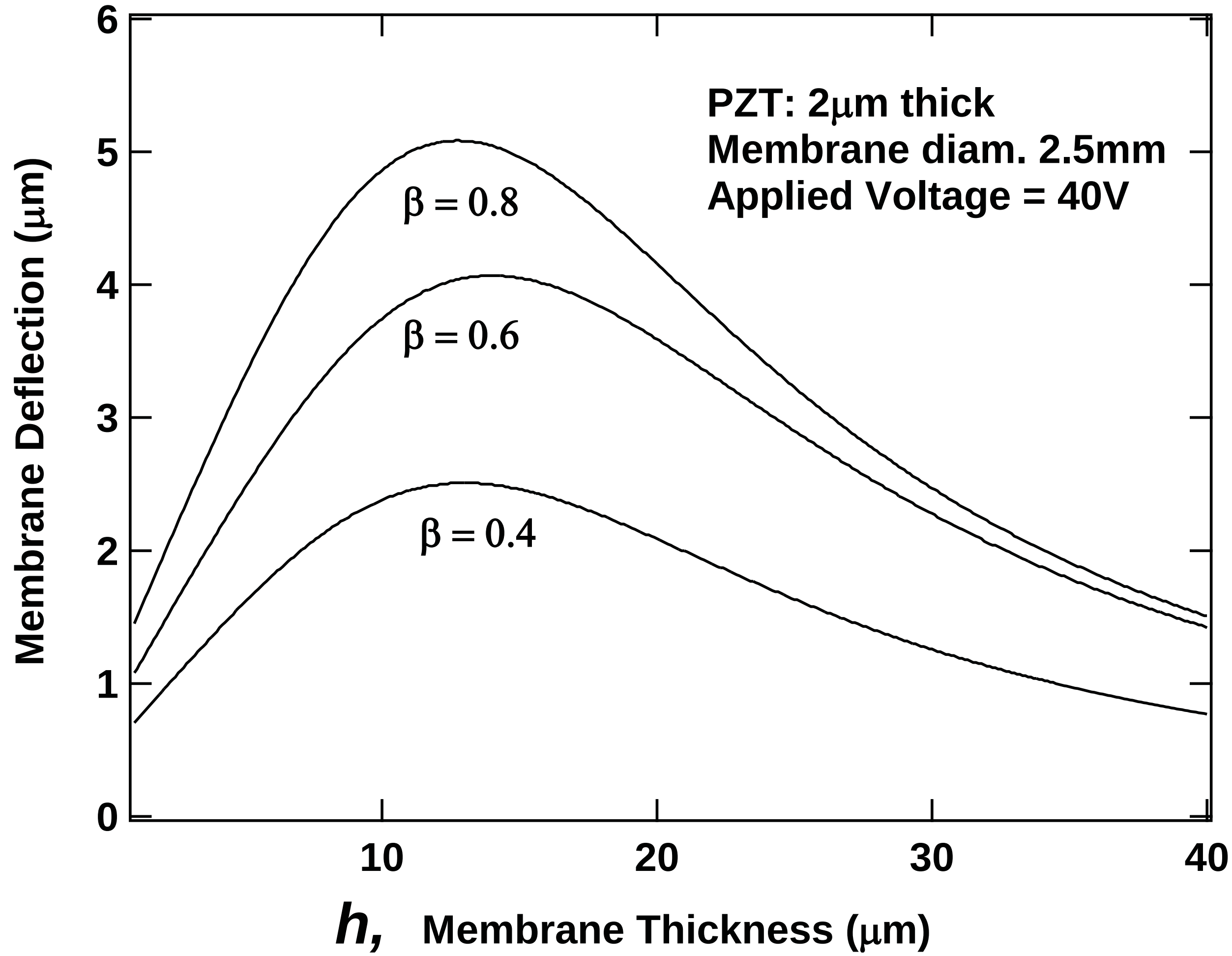

Maximum deflection occurs at intermediate membrane thickness

National Aeronautics and Space Administration
Jet Propulsion Laboratory
California Institute of Technology

Unimorph Actuator Patterns

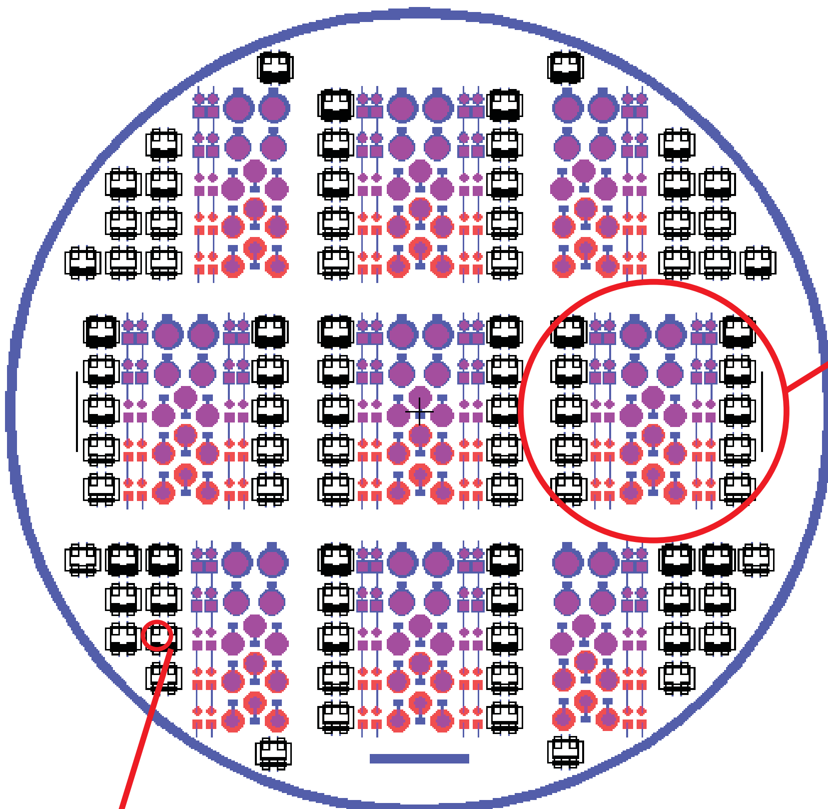

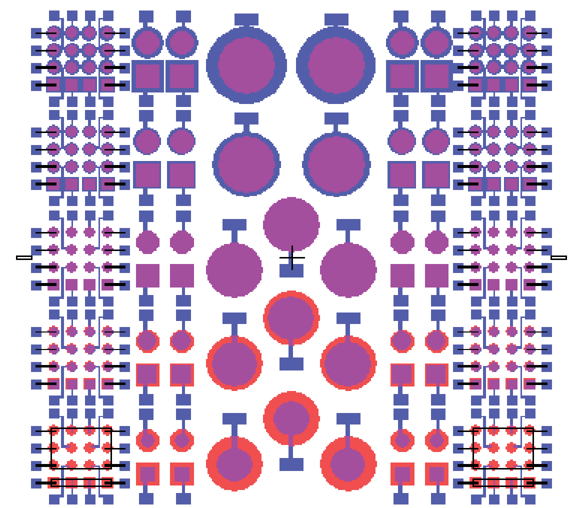

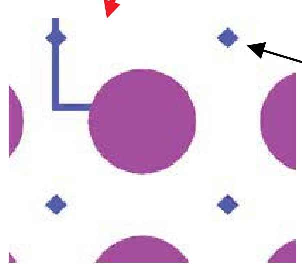

Reference points for Wyko measurement

Mem. Size
Elect/mem ratio

0.5mm 140%	1mm 140%	2.5mm 140%	1mm 140%	0.5mm 140%
0.5mm 120%	1mm 120%	2.5mm 120%	1mm 120%	0.5mm 120%
0.5mm 100%	1mm 100%	2.5mm 100%	1mm 100%	0.5mm 100%
0.5mm 80%	1mm 80%	2.5mm 80%	1mm 80%	0.5mm 80%
0.5mm 60%	1mm 60%	2.5mm 60%	1mm 60%	0.5mm 60%

Piezoelectric Unimorph Actuator: Optimization for Actuation

Optimizing actuator design

2 Regimes of unimorph membrane actuators

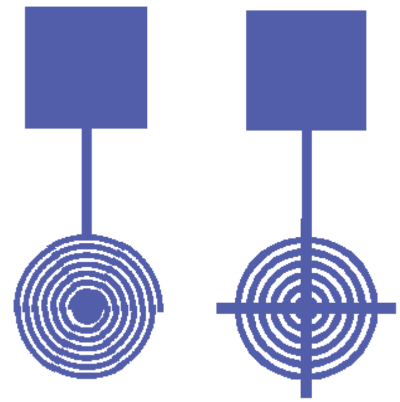

A. Thin silicon membrane (≈ PZT film thickness)

- Dominated by membrane stress
- Larger deflection with spiral and concentric ring electrodes

B. Thick silicon membrane (>> PZT film thickness)

- Membrane stress no longer dominates dynamics
- Larger deflection with full circle electrodes

We decided to work only with thick-silicon unimorph design.

PZT Film: Preparation

National Aeronautics and Space Administration
Jet Propulsion Laboratory
California Institute of Technology

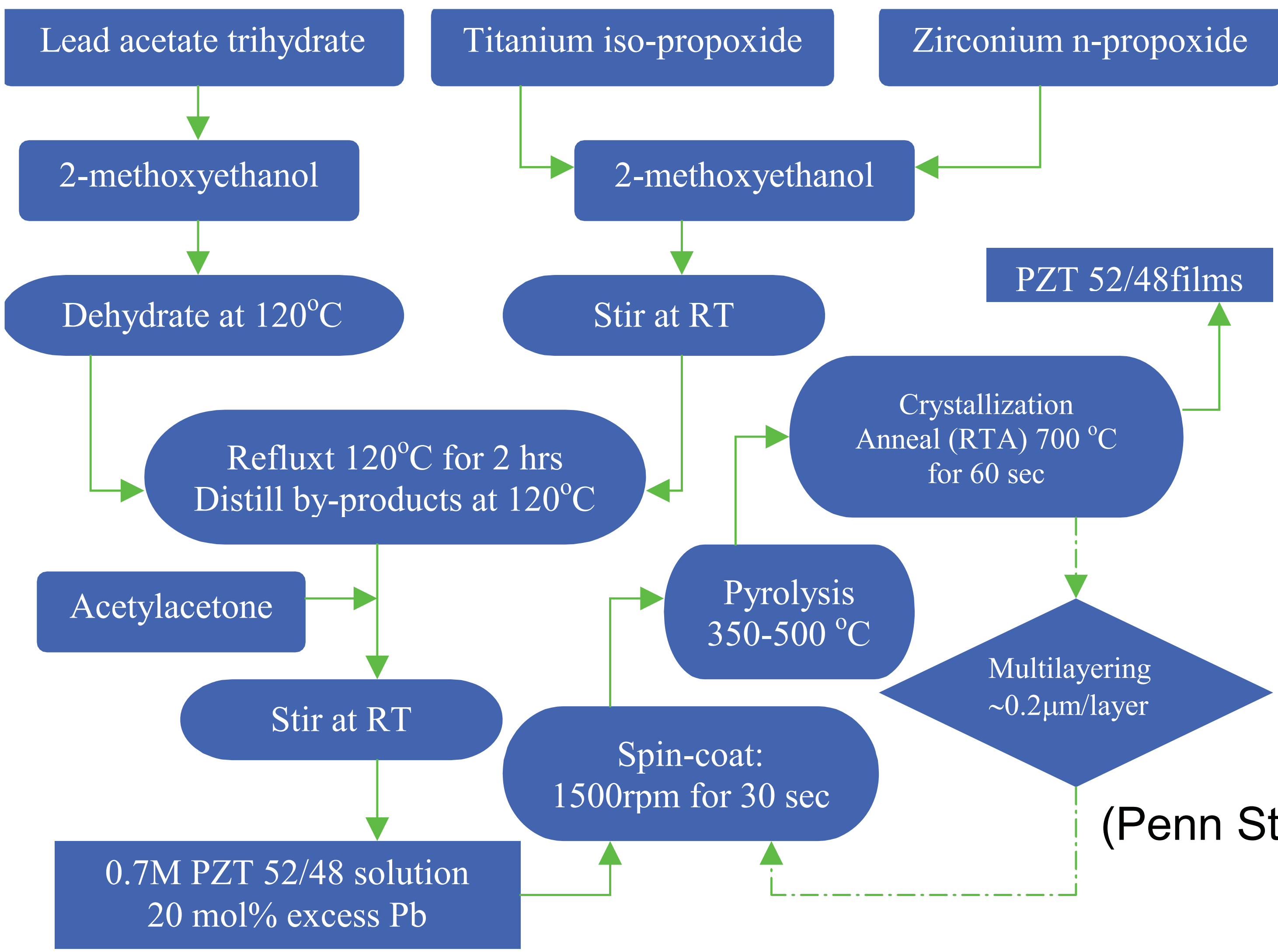

(Penn State process)

PZT Film preparation performed at Penn State University

Large-Area DM Fabrication

National Aeronautics and Space Administration
Jet Propulsion Laboratory
California Institute of Technology

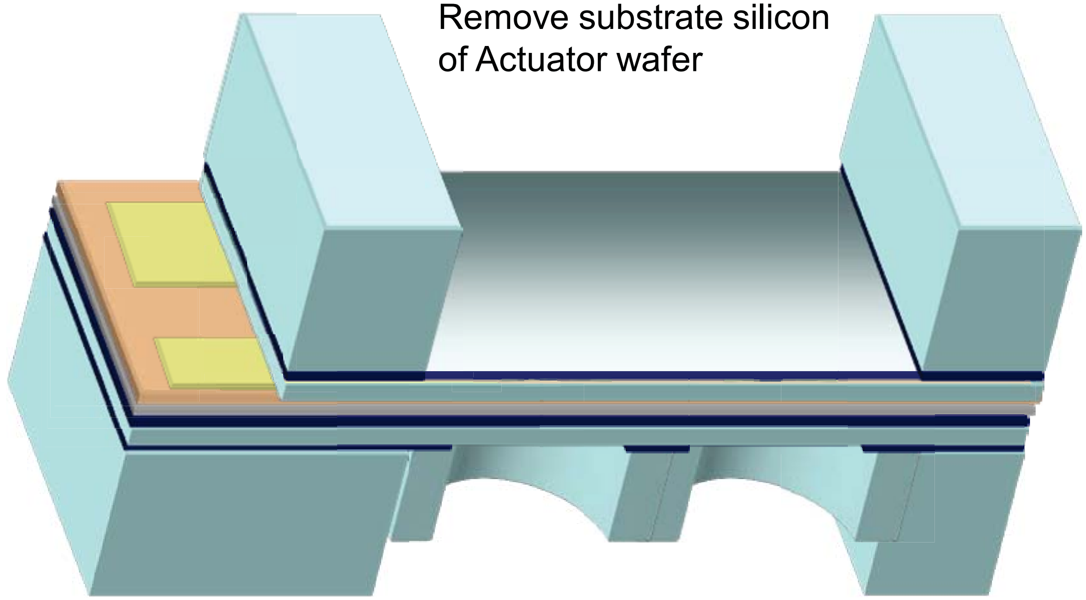

National Aeronautics and Space Administration
Jet Propulsion Laboratory
California Institute of Technology

Fabricated Unimorph Actuators

Actuator arrays

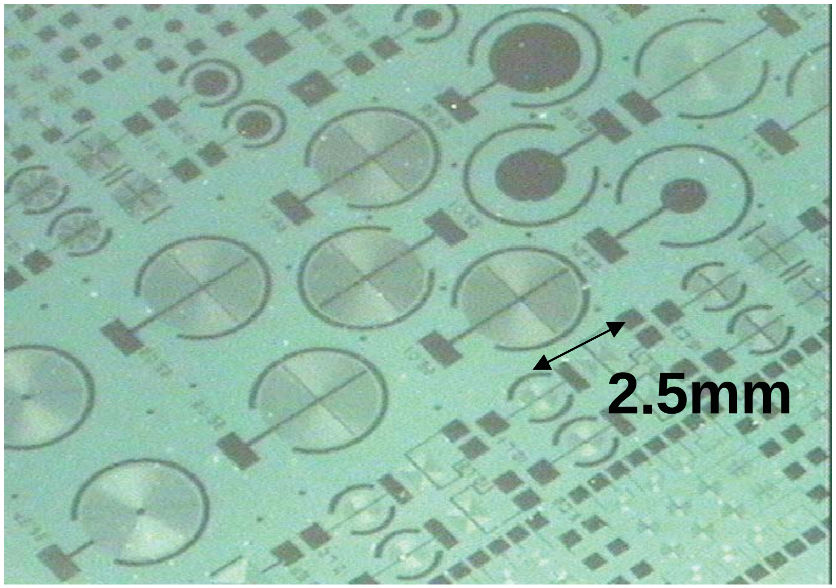

WYKO optical interferometer

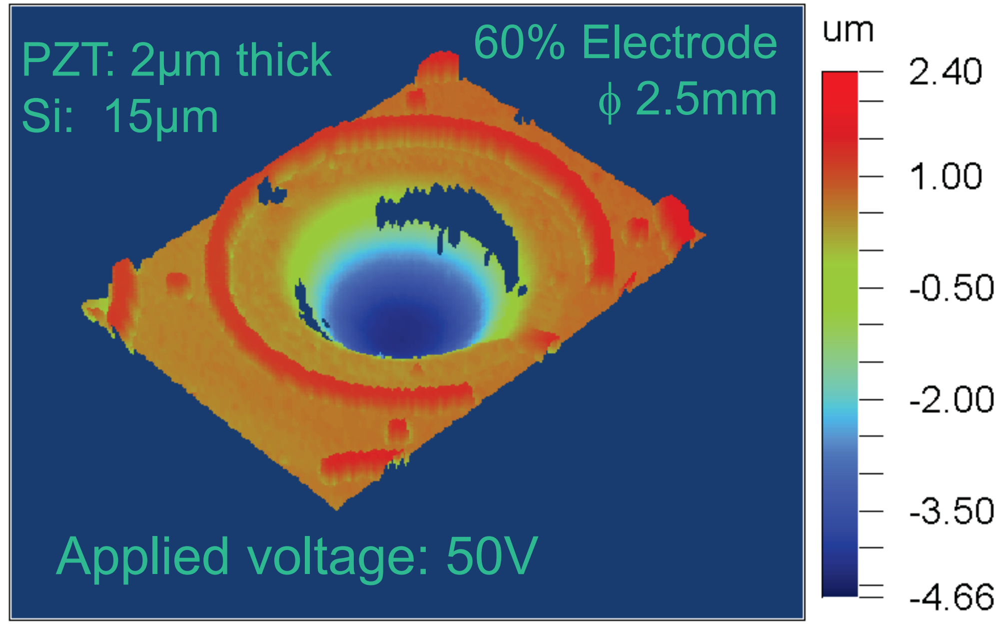

1) Place actuator wafer on the WYKO stage
2) Turn on WYKO monitor and white LED lamp
3) Apply probe needle to top & bottom electrodes
4) Find interference fringes on WYKO
5) Make sure voltage on the power supply is zero.
6) Turn on the power supply
7) Take a profile measurement
8) Get a cross-section of the profile. Place one cursor at a reference, another cursor at the center of the membrane.
9) Find the height difference between a reference point and the center of the membrane. Record.
10) Raise the voltage, repeat 7)~10).

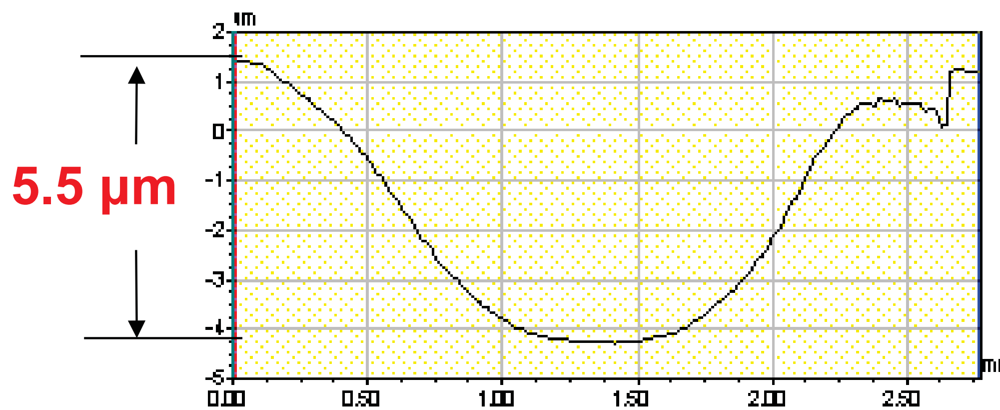

WYKO interferometer image of a PZT unimorph actuator under actuation.

National Aeronautics and Space Administration
Jet Propulsion Laboratory
California Institute of Technology

Preliminary DM: Testing

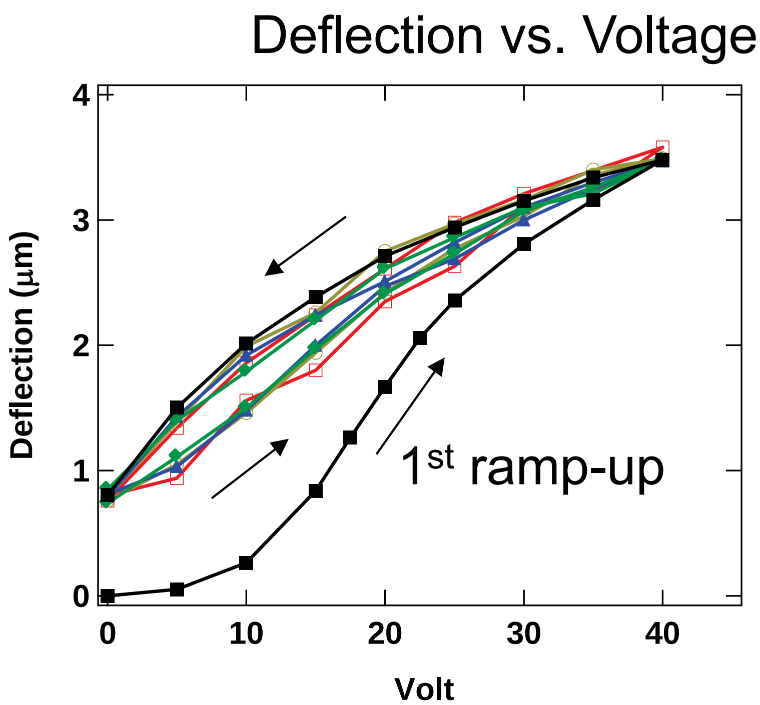

PZT: 2-µm-thick
Si membrane: 1-µm-thick
Electrode diam. 60%
Diaphragm diam. 2.5mm

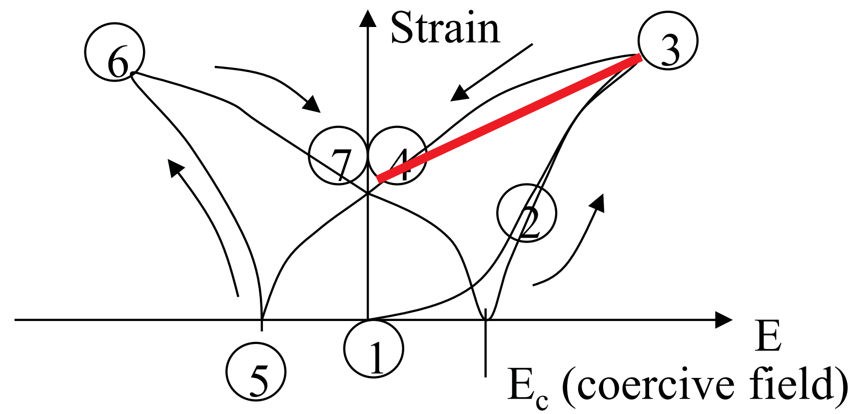

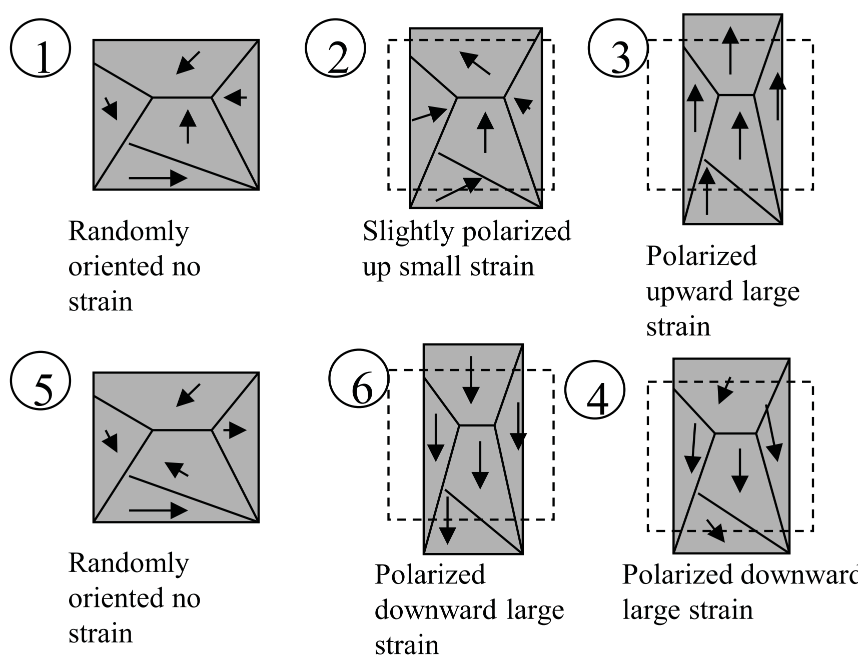

Reference: Kenji Uchino *"Piezoelectric Actuators and Ultrasonic Motors"*, 1997

National Aeronautics and Space Administration
Jet Propulsion Laboratory
California Institute of Technology

Wafer-Scale Membrane Transfer

[Bonding and etching process]

Thermo-compression bonding

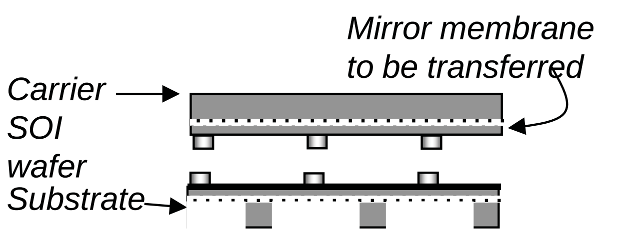

(c)

Backside silicon etch

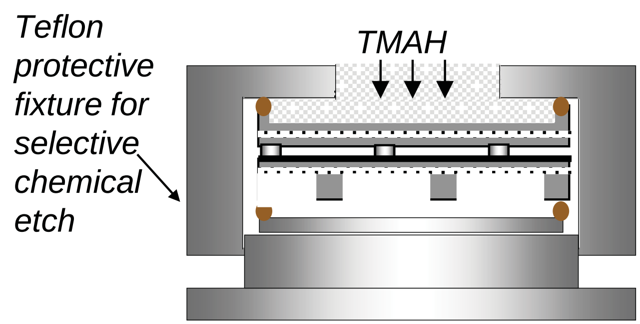

(d)

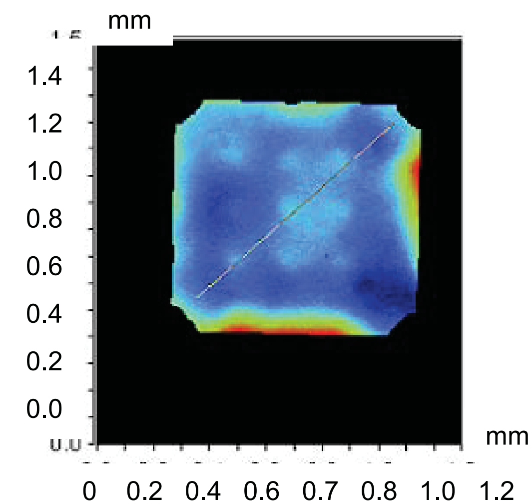

Timed droplet etch of buried oxide

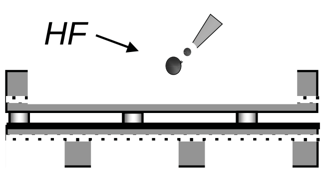

(e)

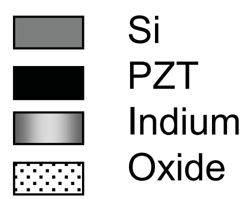

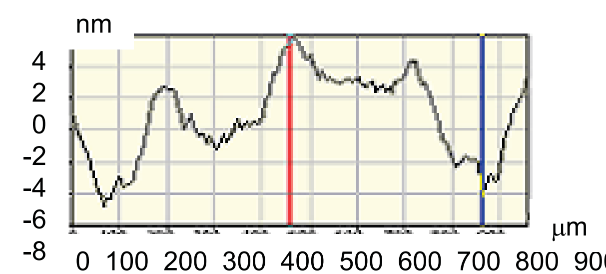

E. H. Yang et al. "A Wafer-Scale Membrane Transfer Process for the Fabrication of Optical Quality, Large Continuous Membranes," *IEEE/ASME Journal of Microelectromechanical Systems, Vol. 12, No. 6*, Dec. 2003.

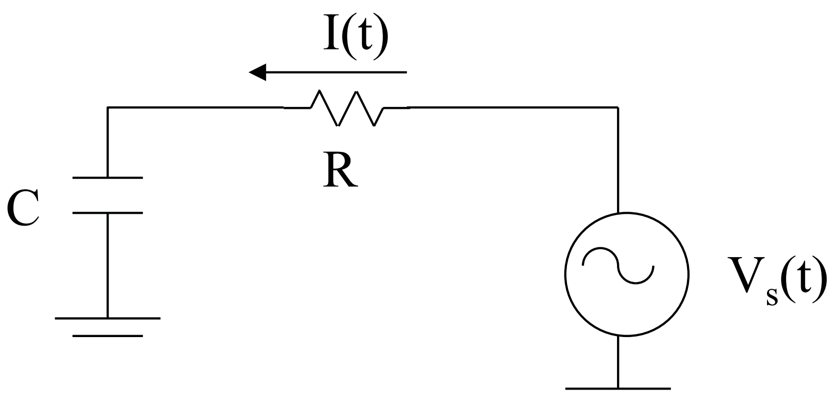

$$V_s(t) = I(t)\cdot R + I(t)\cdot\frac{1}{j\omega C}$$

$$I(t) = \frac{1}{R+\frac{1}{j\omega C}}V_s(t) = \frac{1}{\sqrt{R^2+\frac{1}{\omega^2 C^2}}}e^{j\theta}\cdot V_s(t)$$

$$\theta = \tan^{-1}\left(\frac{1}{\omega RC}\right)$$

$$V_s(t) = V_s\sin(\omega t)$$

Frequency = 800 kHz
Δt = 290 ns
R=5.3 Ohm
C=4.3 nF

Stiffness of PZT Unimorph Actuator

$$k = \frac{64\pi}{12}\frac{Et^3}{r^2} = \frac{64\pi}{12}\frac{1.9\times10^{11}\cdot\left(15\times10^{-6}\right)^3}{\left(1.25\times10^{-3}\right)^2} = 6876\,{N}/{m}$$

$$f = \frac{10.2}{2\pi}\cdot\frac{t}{r^2}\sqrt{\frac{E}{12\cdot w}}$$

t = thickness
r = radius of disk
E = Young's modulus
w = density

f = 41 kHz with t=15µm, r=1.25mm

Force of PZT Unimorph Actuator
1µm displacement: ~ 7 mN

PZT Film: Characterization

National Aeronautics and Space Administration
Jet Propulsion Laboratory
California Institute of Technology

After deposition of a single layer, the film is pyrolyzed to remove organics and heat-treated (typically at 700 °C) to crystallize the film.

Dielectric constant: ~1000
Loss tangents of about: 2-3%
Remanent polarizations: >20μC/cm^2
Effective transverse piezoelectric coefficients: $e_{31,f}$ ~ –5 to –7 C/m^2

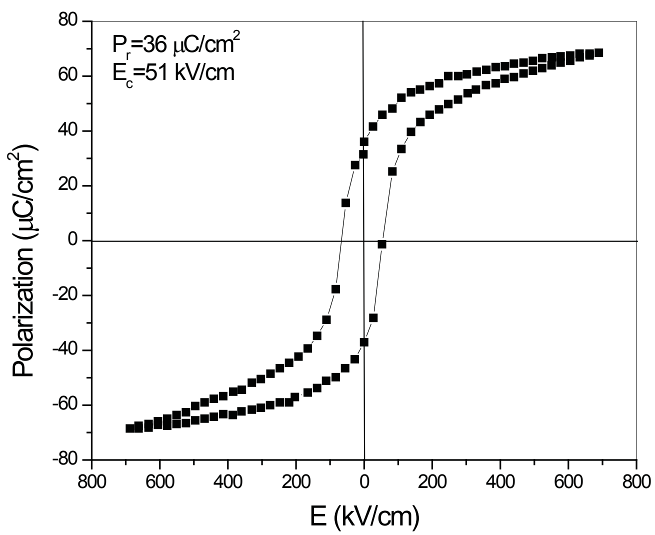

Polarization hysteresis loop

PZT Film preparation & characterization performed at Penn State University

Flipping Polarization Direction

National Aeronautics and Space Administration
Jet Propulsion Laboratory
California Institute of Technology

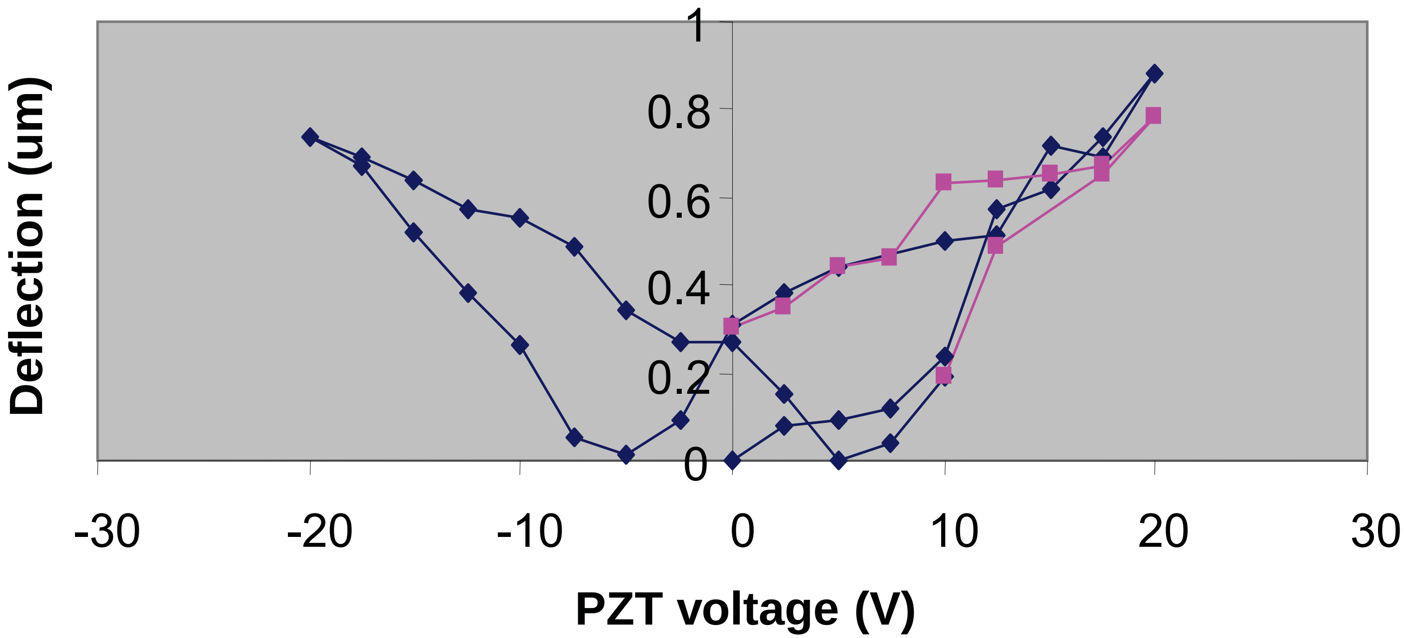

-Membranes deflecting downward for both +/- PZT voltage

Meeting Requirements of Several Applications

DMs	AOptics (PZT bimorph)	BMC (MEMS Electrostatic)	Xinetics (PMN Electrostrictive)	JPL (Projected near term performance)	JPL (projected ultimate performance)	How to get to the projected performance?
Stroke (μm)	16	2	0.2	6	6~16	Optimizing unimorph structure
Operating temperature	Data N/A	Data N/A	RT only. (Cryo version does not work at RT.)	-55°C ~ 50°C	-140°C ~ 100°C	Optimizing PZT film by tailoring the transition temperature (data available).
Bandwidth (KHz)	12	3	2	30	20~100	Tailoring the actuator design
Voltage (V)	400	200	100	50	28~50	Thin film PZT
DOF	35	1024	4096	400	400~10,000	Photomask-based microfabrication
Active mirror area (mm)	20 (diameter)	20 × 20	70 × 70	50 × 50	250 × 250	Membrane transfer technique in conjunction with large-format arrays
Mirror material (before coating)	Polished PZT	Poly-Silicon	Glass	Silicon	Nanolaminate or other optical materials	Membrane transfer technique
Mass production	No	Yes	No	Yes	Yes	Microfabrication
Production cost when fully developed ($K)	Data N/A	50	800	50	50~100	Microfabrication

Inchworm Actuator: Objectives

National Aeronautics and Space Administration
Jet Propulsion Laboratory
California Institute of Technology

- Objective: Develop self-latched inchworm microactuators capable of large-stroke, high-precision actuation for ultra-large, ultra-lightweight space telescope mirrors.

Requirements (performance goal)

• Max. Freq.	~1 kHz
• Stroke	> 1 mm
• Resolution	<30 nm
• Force	> 30 mN
• Power	100 μW
• Mass	~ 100 mg

National Aeronautics and Space Administration
Jet Propulsion Laboratory
California Institute of Technology

Conventional Inchworm Actuator

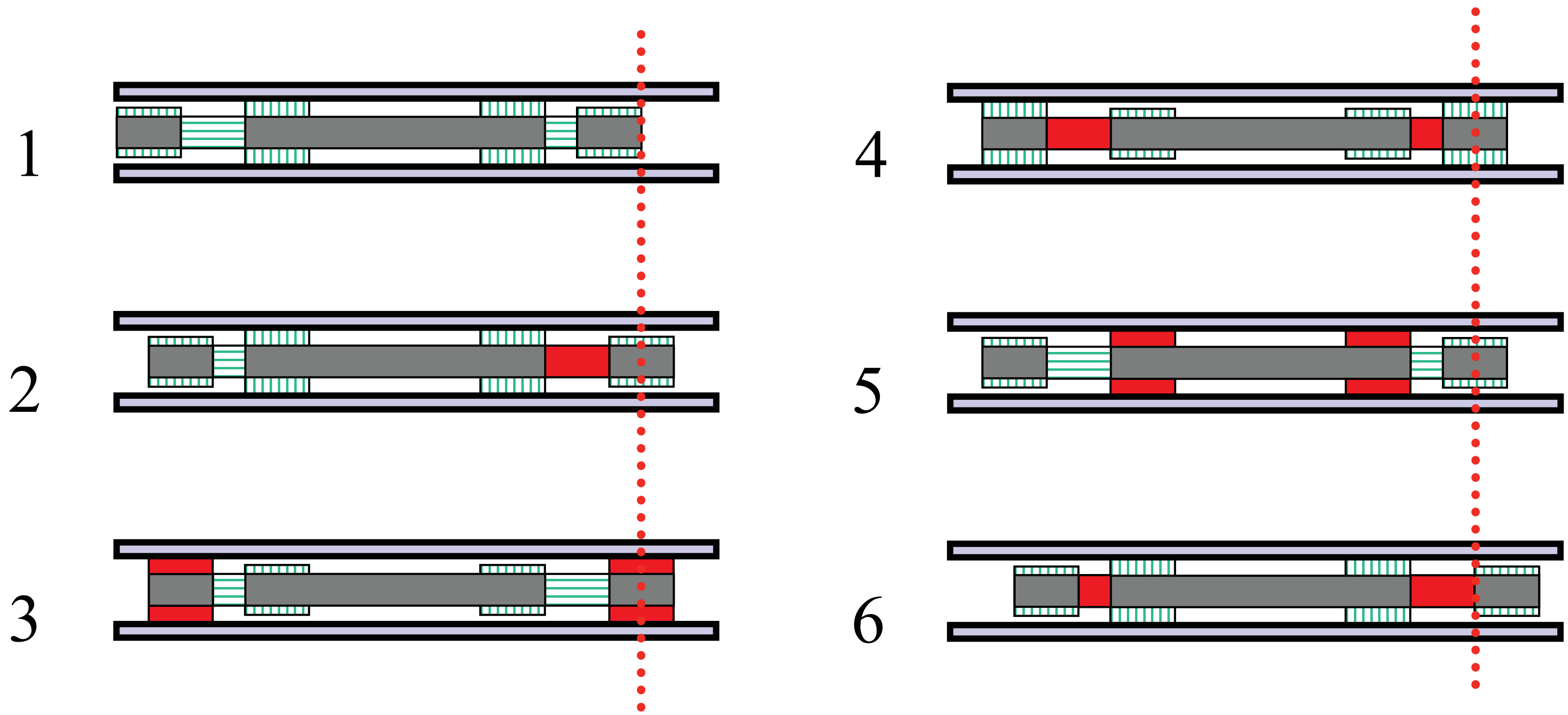

Typical inchworm actuation sequence

•Conventional inchworm actuator [1]: 100g (mass)

[1] Q. Chen, D. J. Yao, C. J. Kim, G. P. Carman, "Mesoscale Actuator Device with Micro Interlocking Mechanism", MEMS 98, Heidelberg, Germany, pp. 384-389, 1998.

1st Generation Microactuator

National Aeronautics and Space Administration
Jet Propulsion Laboratory
California Institute of Technology

- Slider is clutched with holder and driver by electrostatic force
  - This version is not of self-latching.
- Driver is pushed by external PZT for vertical movement

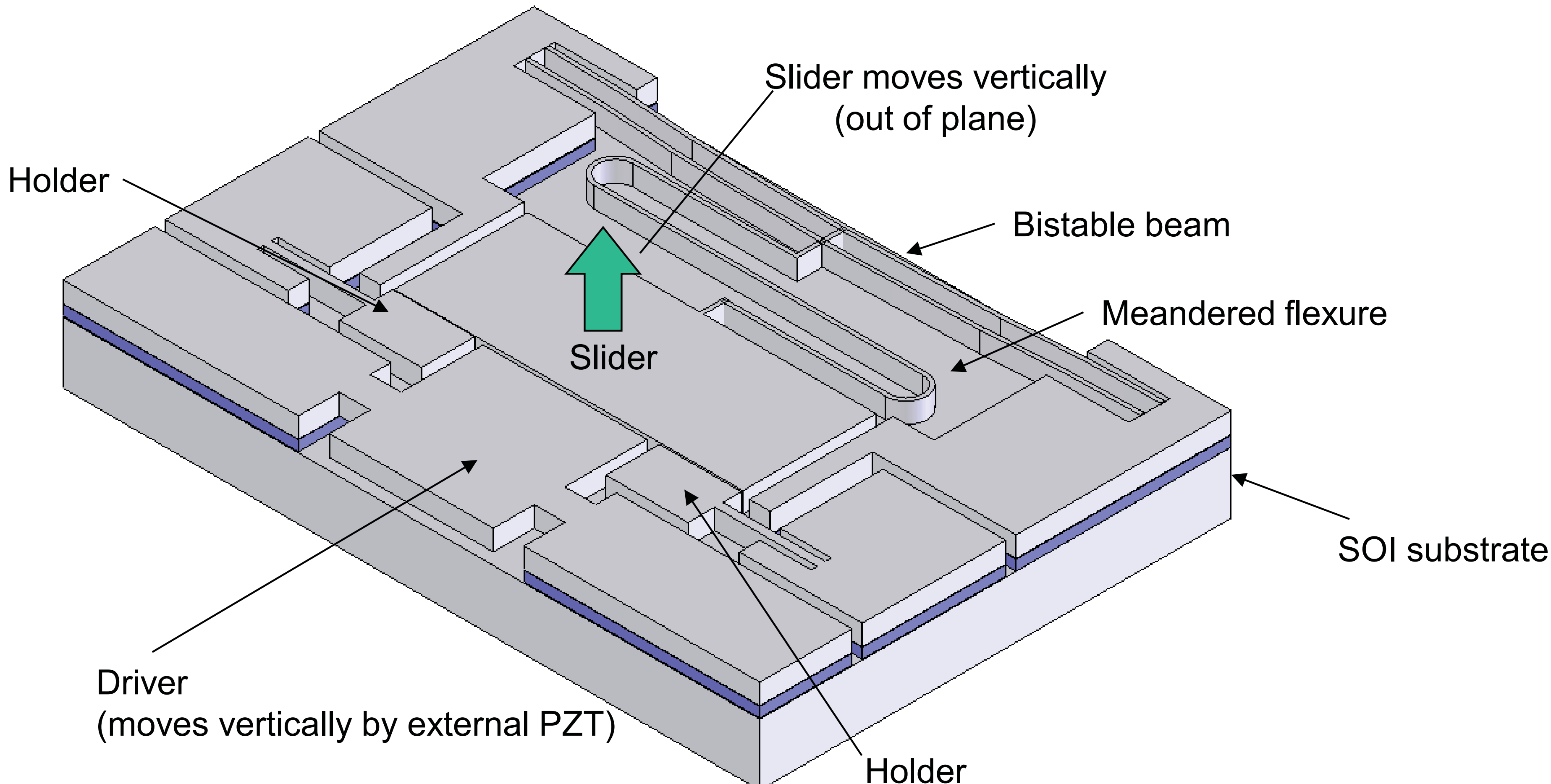

Footprint 2mmx4mm

Actuation Sequence

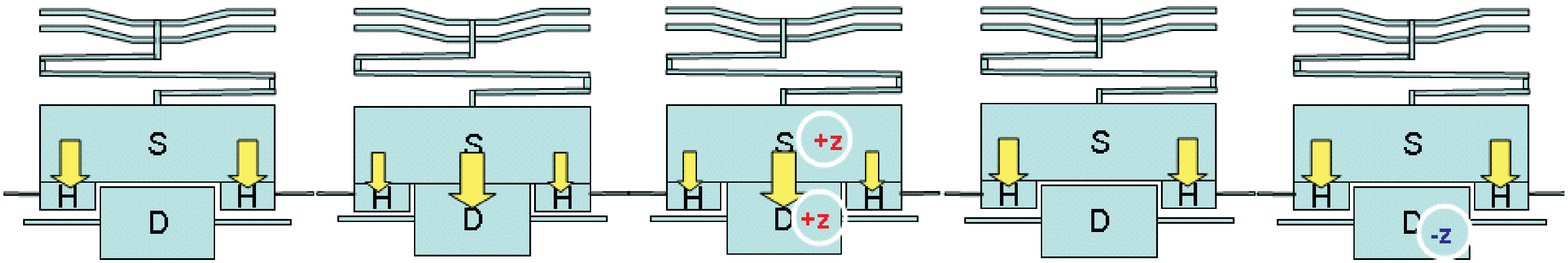

Step 0. Initial position

Step 1. Slider clamped to driver

Step 2. Driver moves up one step (+z)

Step 3. Slider is clamped to holder

Step 4. Driver moves back one step (-z)

4. Driver moves back

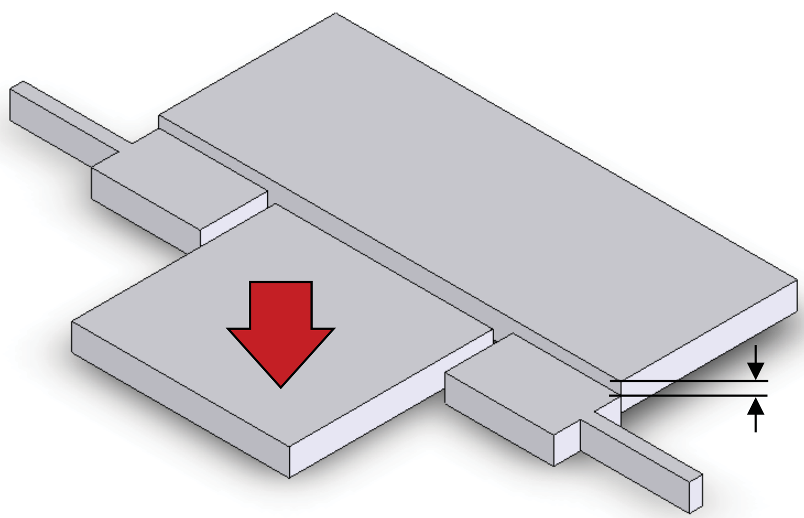

Actuator Test Setup

Wafer

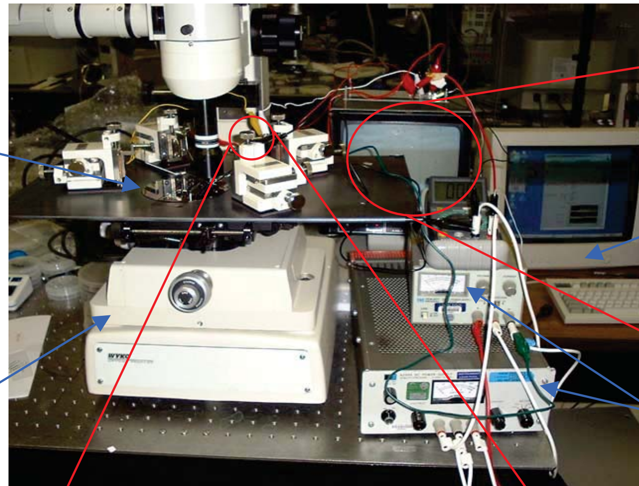

WYKO

LabVIEW PC

Power supply

Test setup

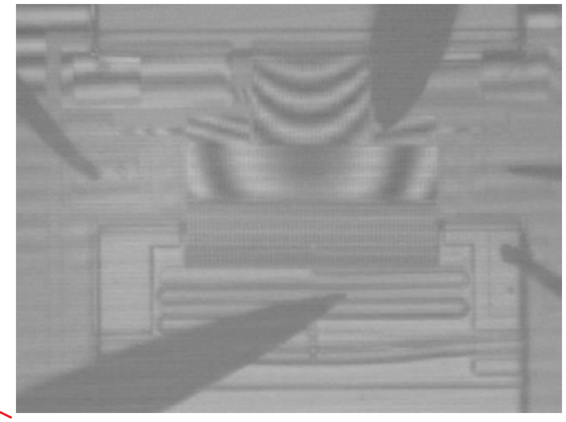

WYKO screen image

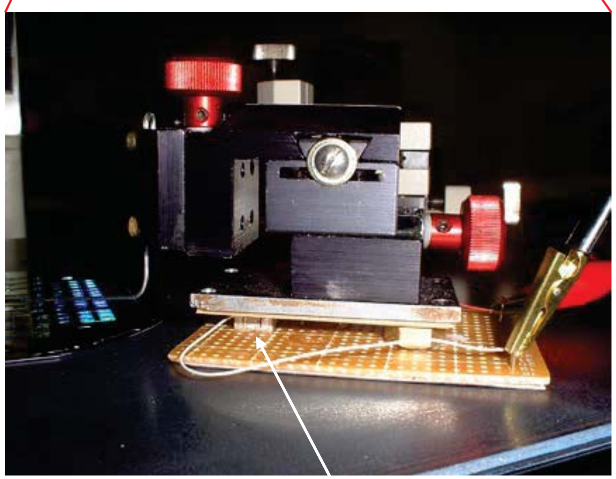

PZT actuator under prober

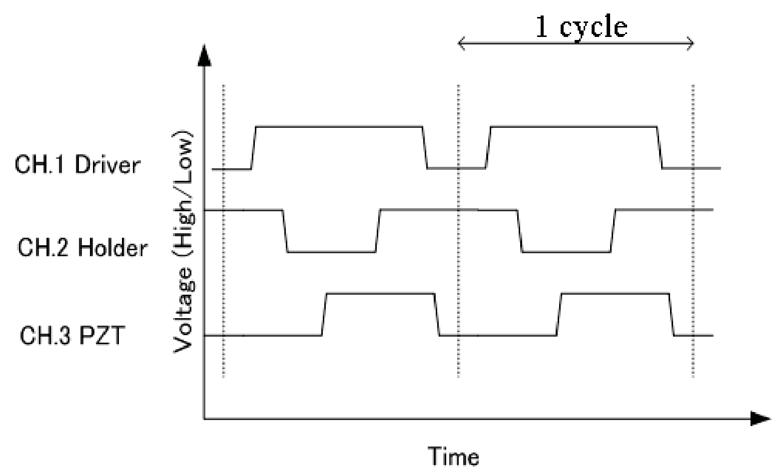

Actuation Results

National Aeronautics and Space Administration
Jet Propulsion Laboratory
California Institute of Technology

- Step-by-step measurement of actuation showed pull-back behavior.
- Step height change was not repeatable.
- Electrostatic clutching force appeared to be weaker than estimation.

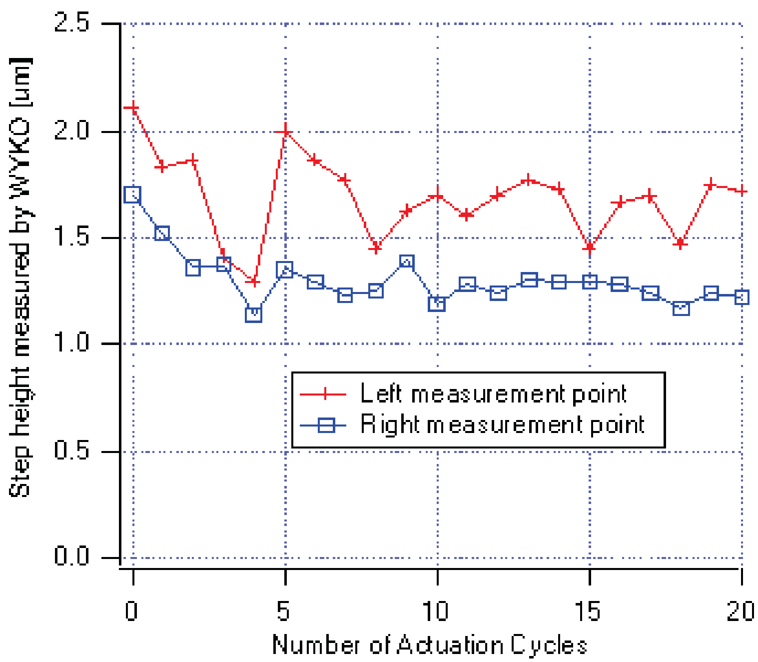

Actuation trend

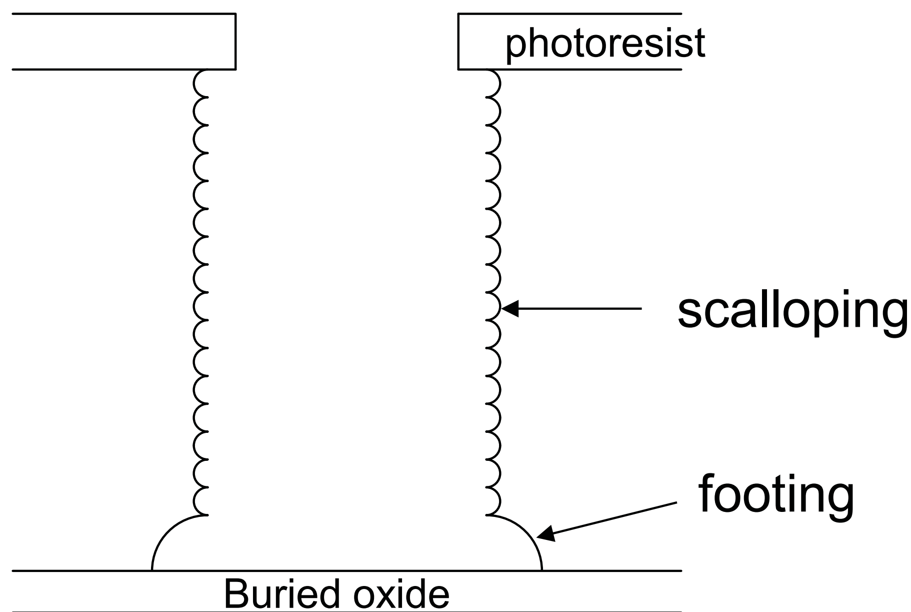

Typical surface profile of DRIE sidewall

→Weaker electrostatic force

→Friction at scallop notch

Bi-Stable Beam Mechanism

National Aeronautics and Space Administration
Jet Propulsion Laboratory
California Institute of Technology

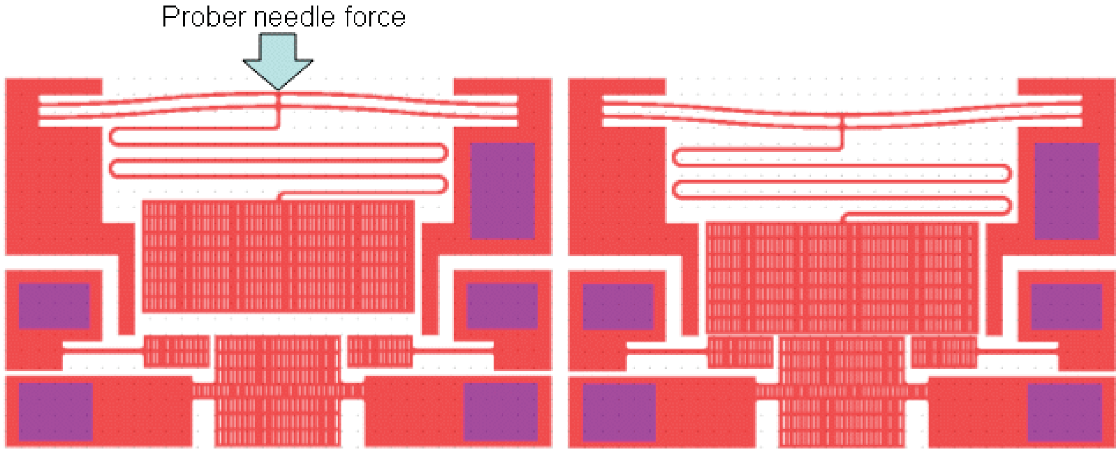

(a) First stable position

(b) Second stable position.
Electrode gap narrowed.

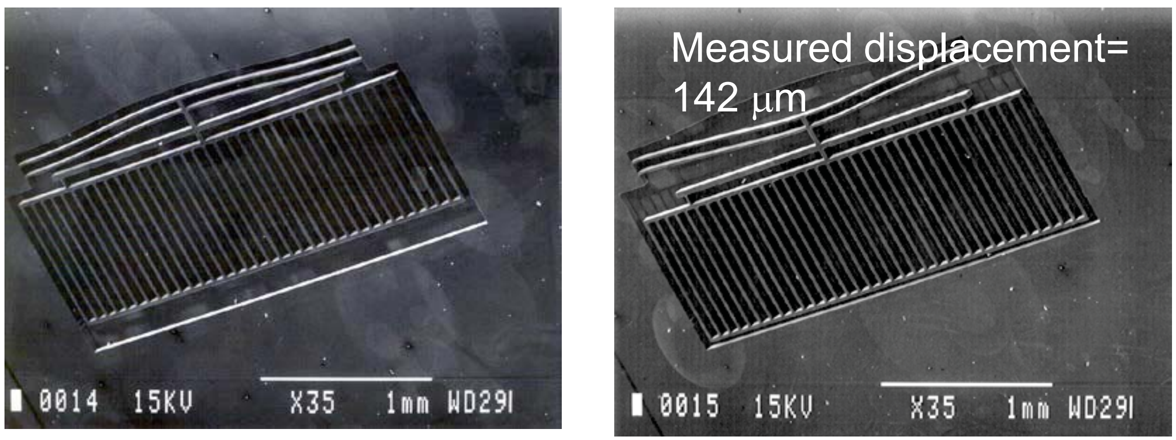

Bistable beam test structure

- Bistable beam is buckled to its 2nd stable position; electrode gap narrows from 143 μm to approximately 1 μm.

- Electrostatic force enables pull-in clutching.

Pull-in Force

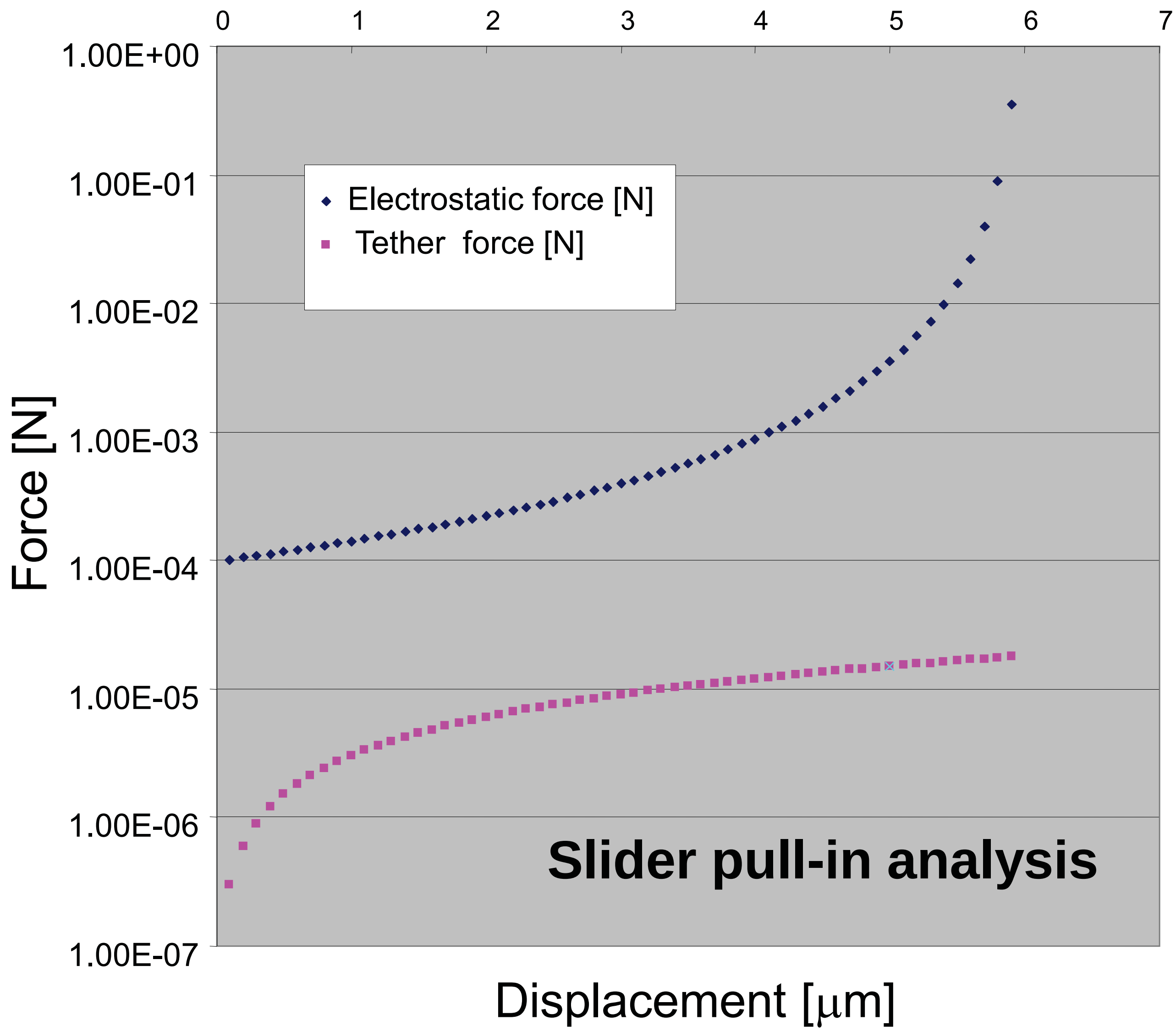

$$F = e_0 AV^2 / 2g^2$$

g = gap,

V = voltage

A = area

$$d = Fl^3/(3EI)$$

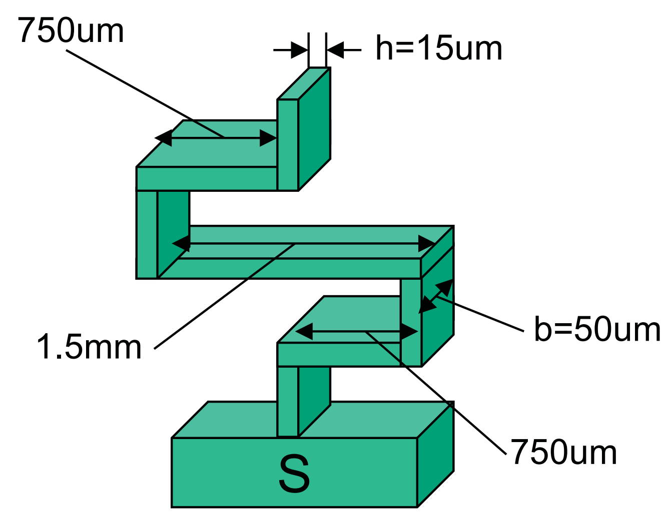

Microfabrication

National Aeronautics and Space Administration
Jet Propulsion Laboratory
California Institute of Technology

•DRIE→HF Release→Oxidation→Stenciled RIE

•Reduce oxide stress by oxide etch at bistable beam.

•Electrode sidewall oxide not etched.

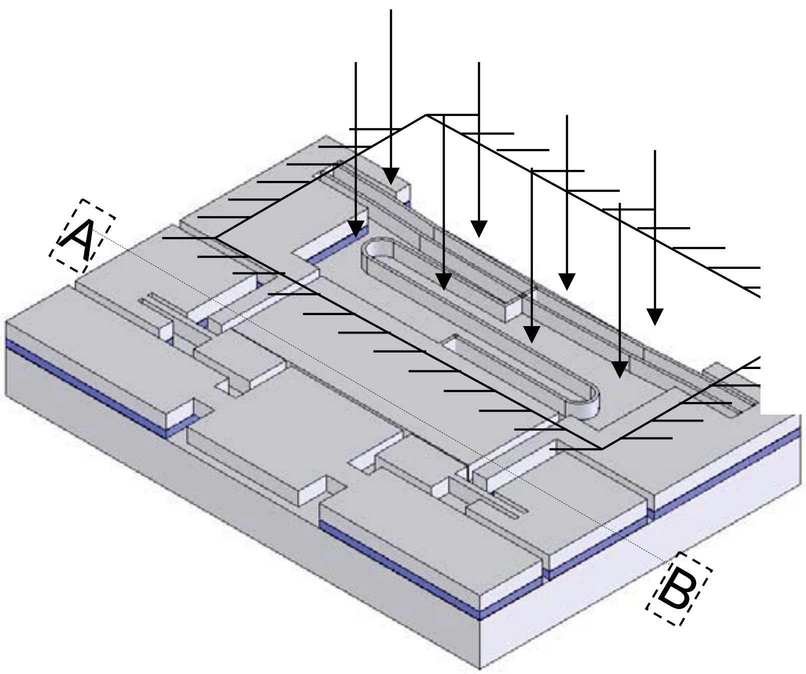

Oxide etch (RIE) with stencil

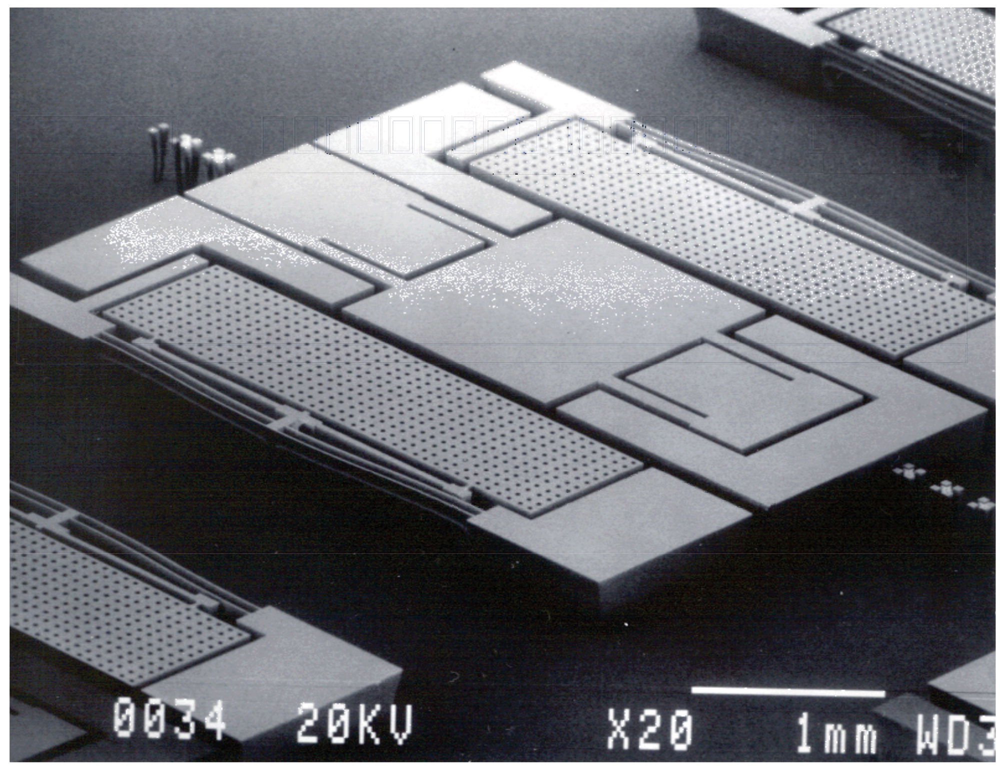

National Aeronautics and Space Administration
Jet Propulsion Laboratory
California Institute of Technology

Characterization Setup-LabVIEW

•LabVIEW-controlled power relays provide square-wave at arbitrary timing.
•Applied DC voltage 100~300V (for electrostatic pull-in), ~50V (for PZT actuator).

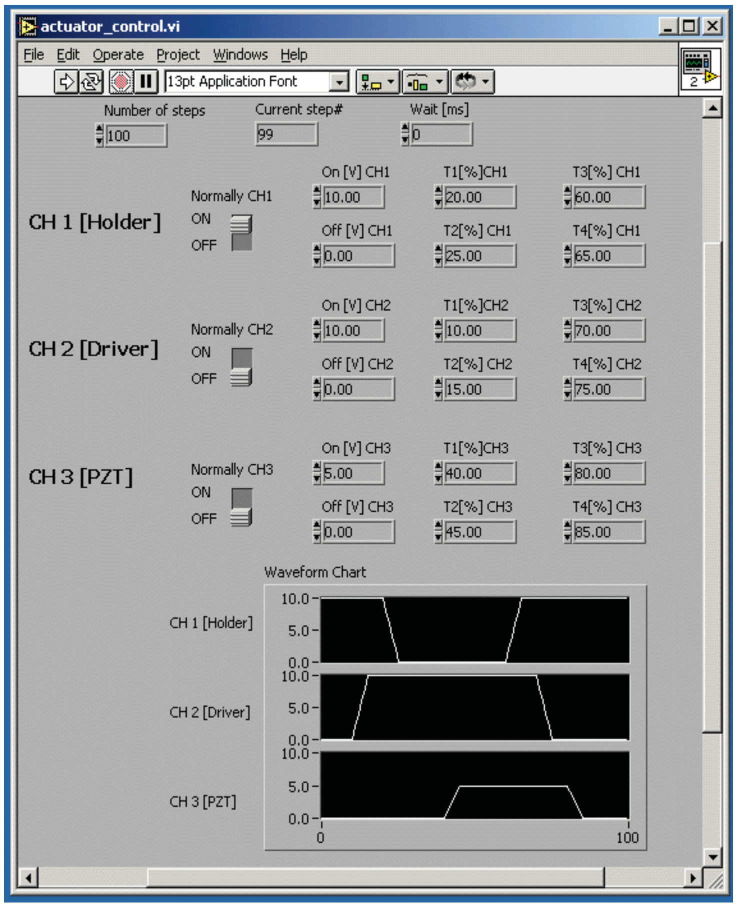

LabVIEW VI

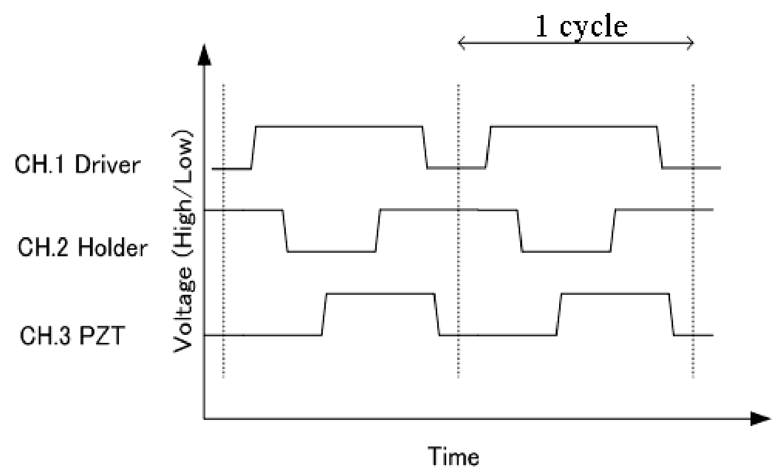

Timing chart

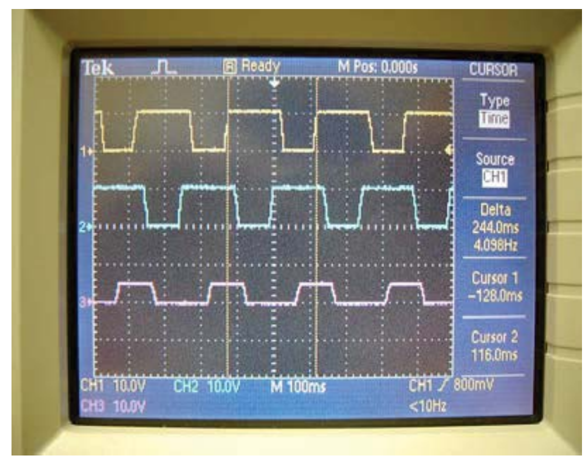

2nd Generation Microactuator

National Aeronautics and Space Administration
Jet Propulsion Laboratory
California Institute of Technology

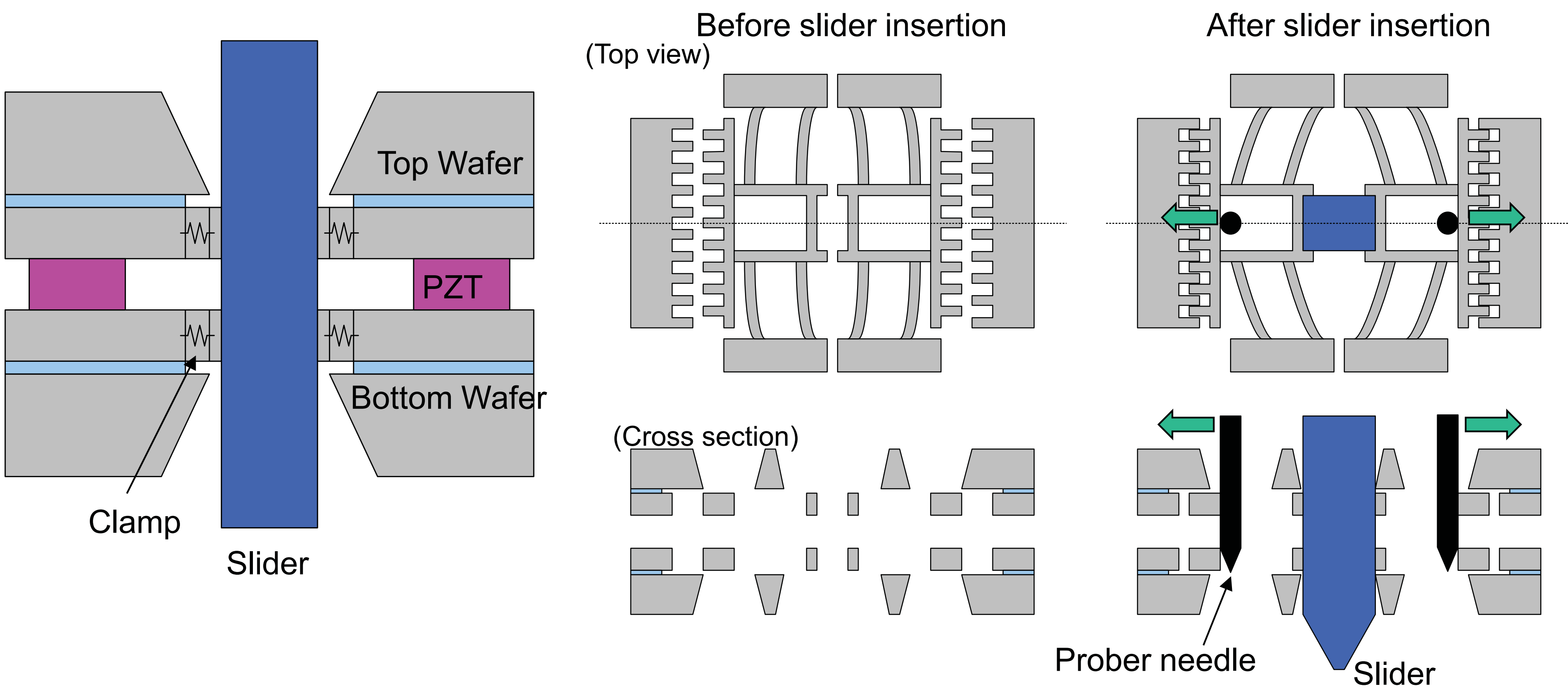

Advantages

•Latching: using tether restoring force. Zero power latching.

•Travel distance not limited by meander suspension beam.

National Aeronautics and Space Administration
Jet Propulsion Laboratory
California Institute of Technology

Working Principle

0. Power-off steady state

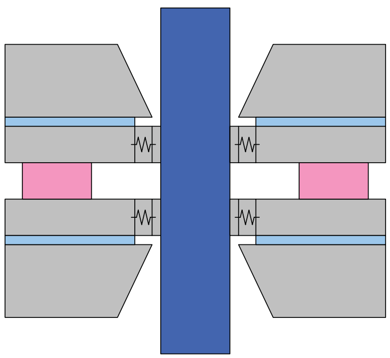

1. Top clamps released

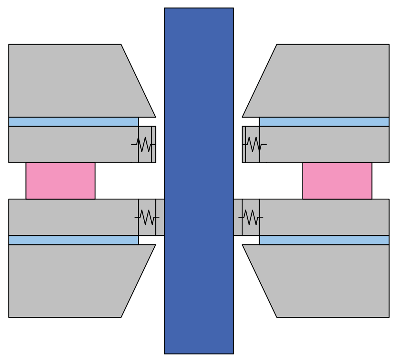

2. PZT expands

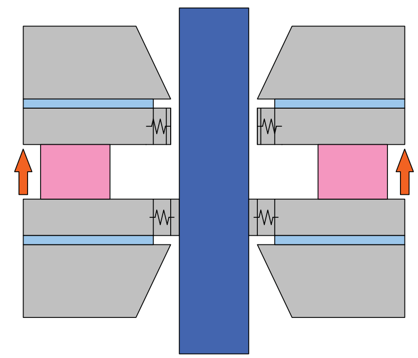

3. Top clamps closed

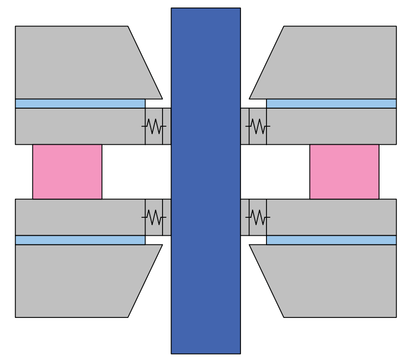

4. Bottom clamps released

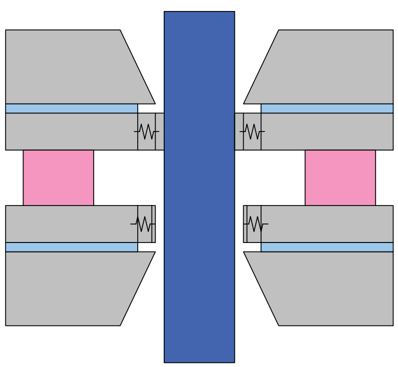

5. Slider moved down one step as PZT contracts

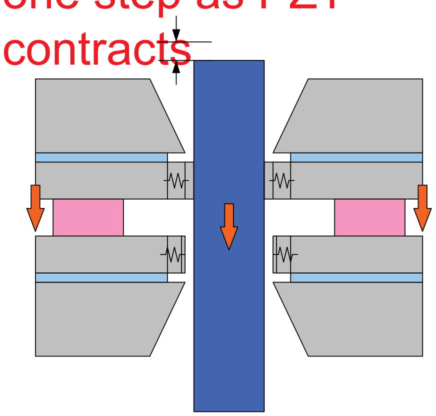

6. Bottom clamps closed (Power off)

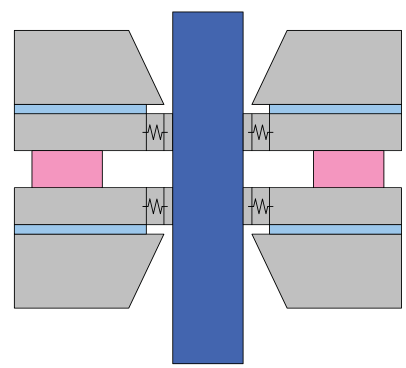

Fabricated Structures

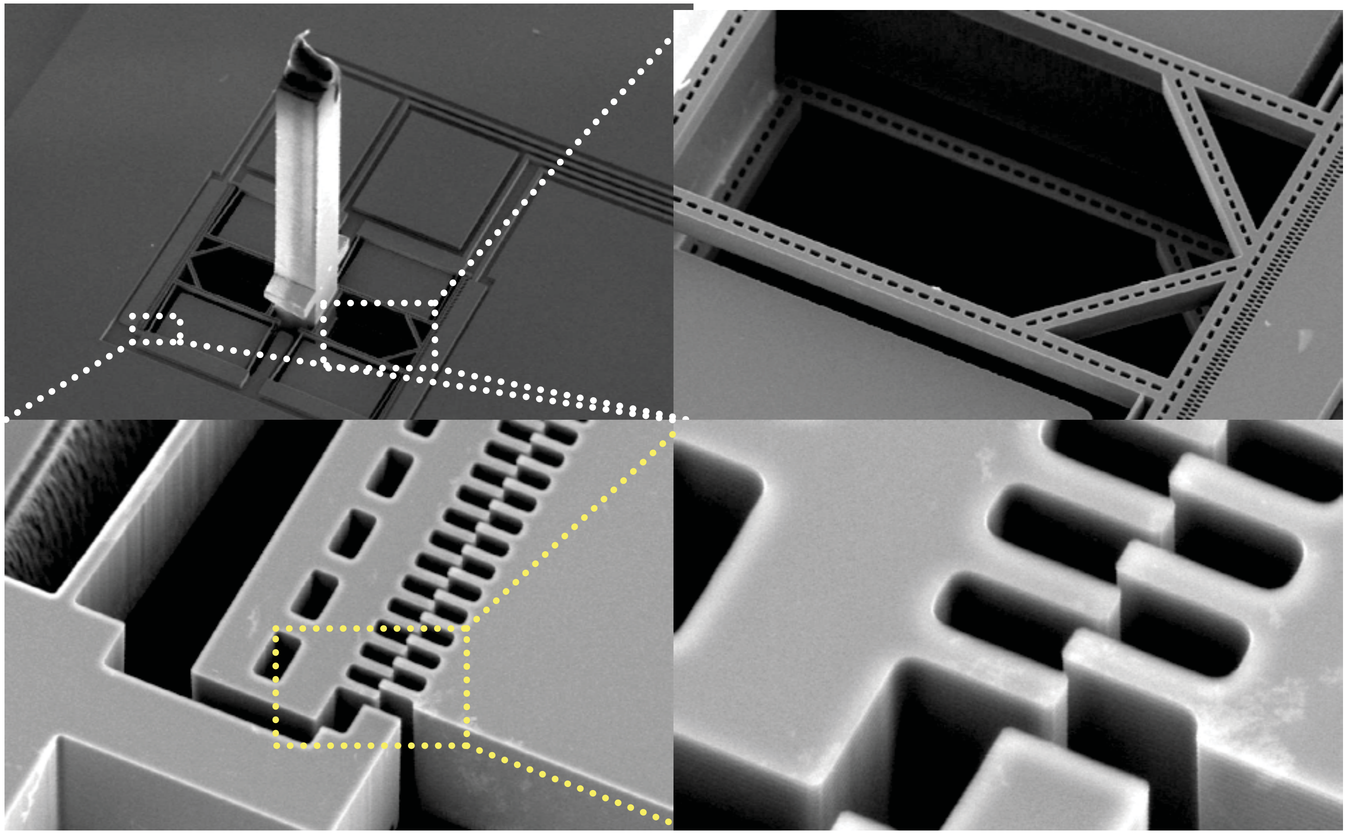

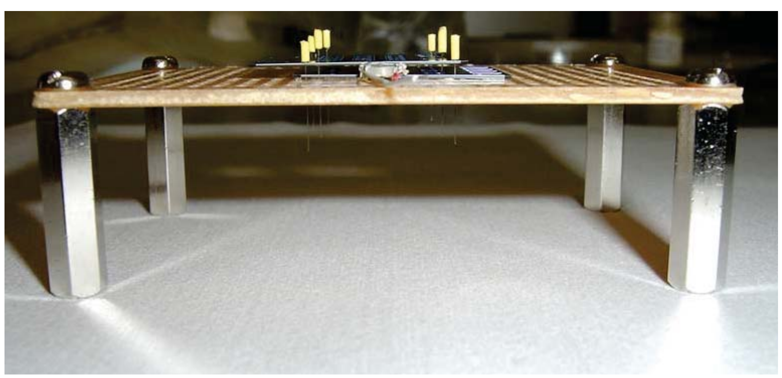

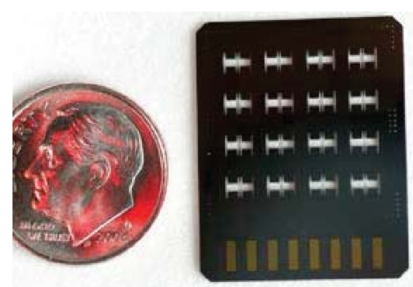

Comb Drive Fabrication Issue

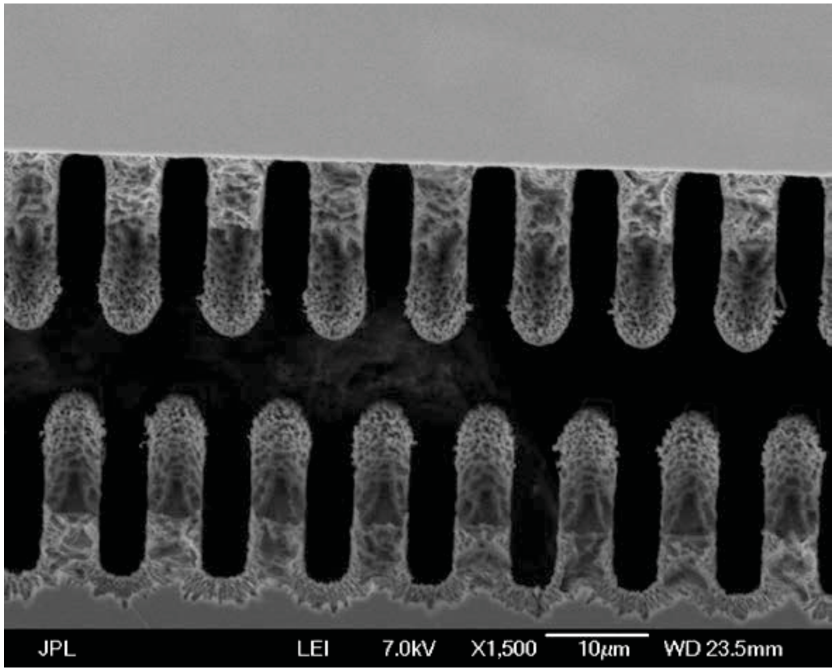

The bottom of the comb is too wide because of insufficient etching.

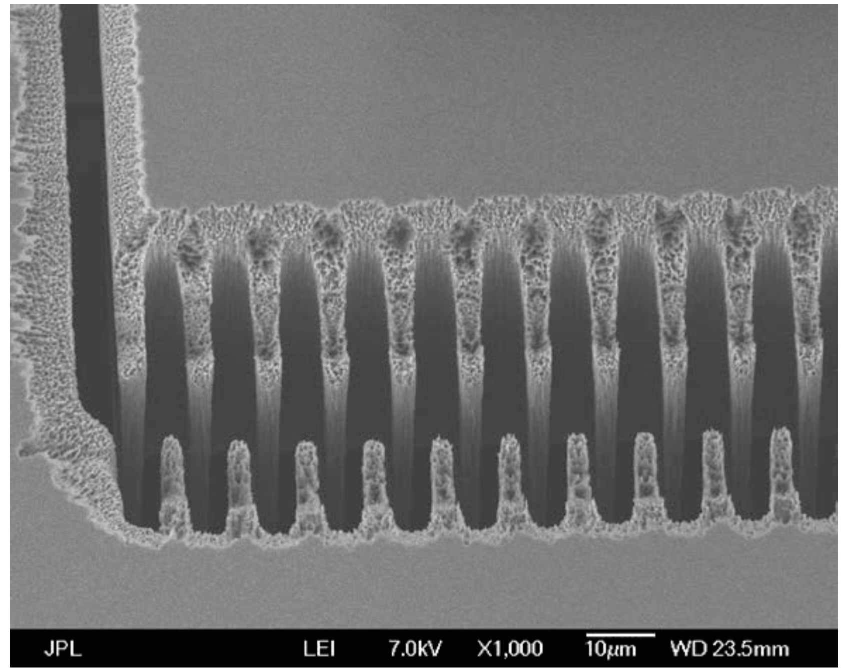

The bottom of the comb is over-etched.

Sticking Issue

- Sticking behavior: The successfully demonstrated slider did not move when the device was tested two weeks after initial successful actuation.
  - A Si-O-Si chemical bond was formed in the silicon interface (between the slider and the driver plate)
  - The slider coated with thermal silicon dioxide to avoid the sticking.
  - The problem solved.

Actuator Test Setup

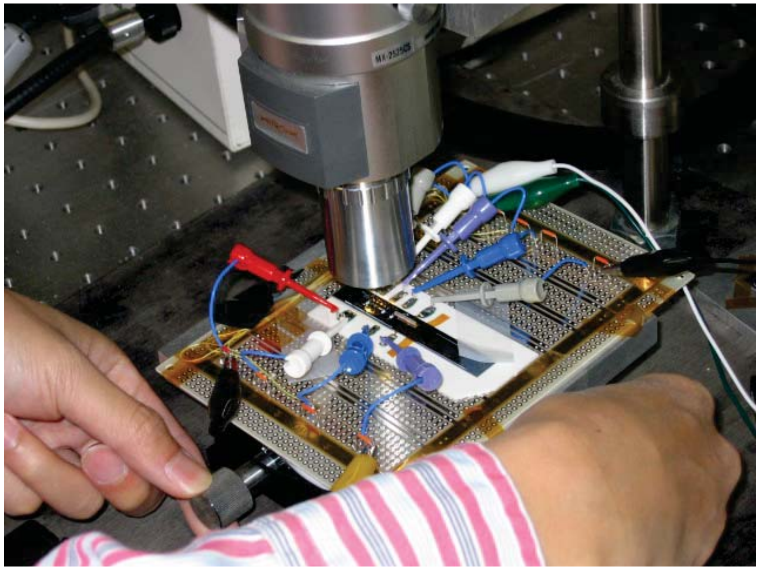

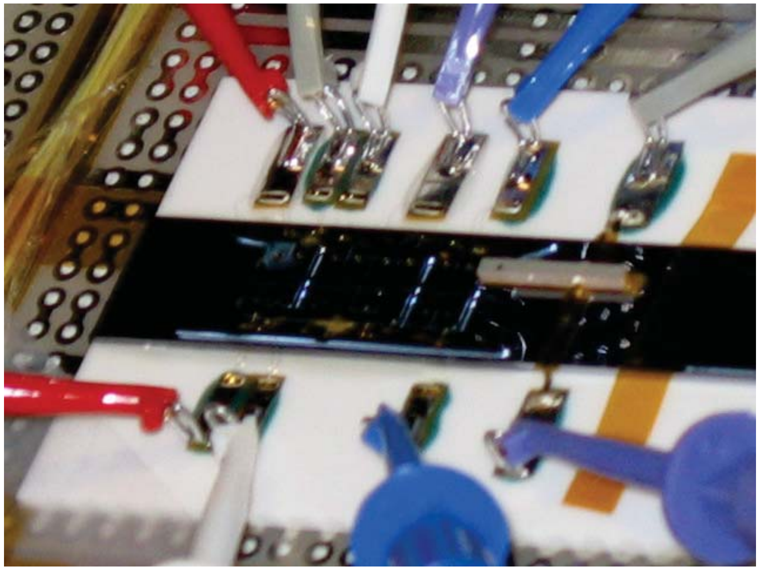

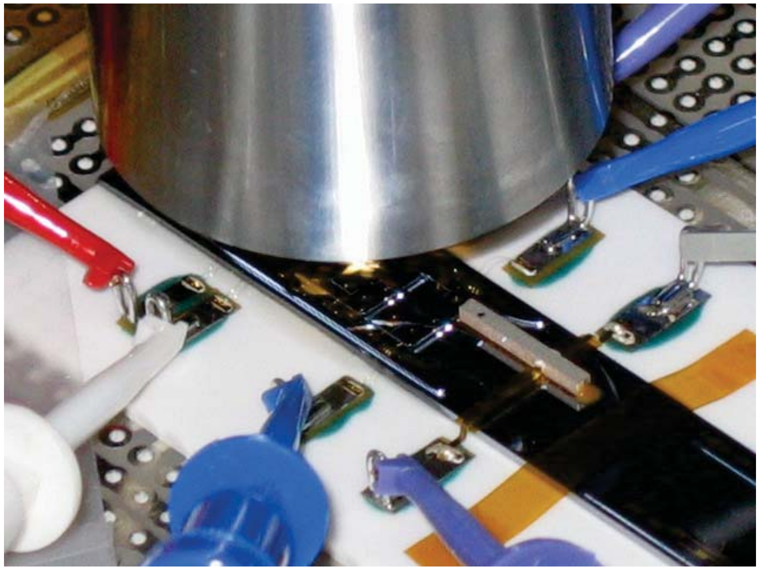

Image Processing Using Matlab

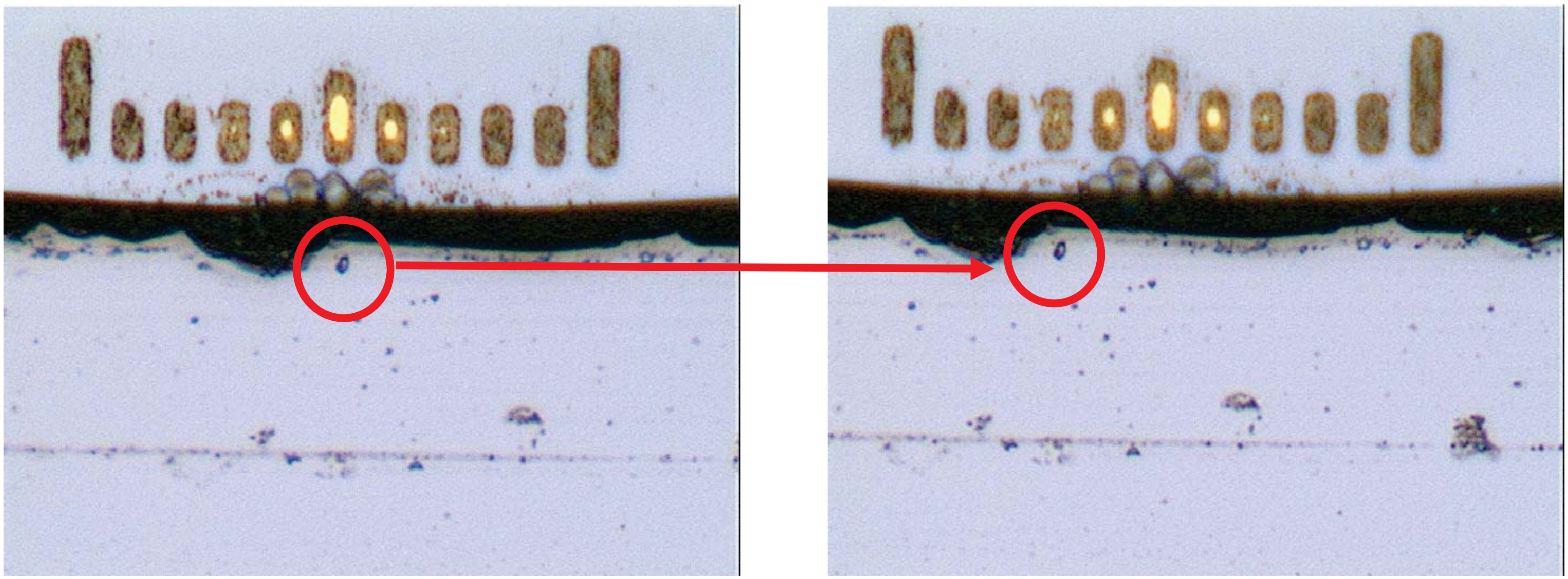

Actuator images taken before and after 100-cycle actuation:

Image processing was performed to accurately calculate the slider movement, by comparing two different images taken before and after the actuation. The resolution from the calculation is approximately 50 nm.

Modeling: Lateral Forces Applied on Clutch

National Aeronautics and Space Administration
Jet Propulsion Laboratory
California Institute of Technology

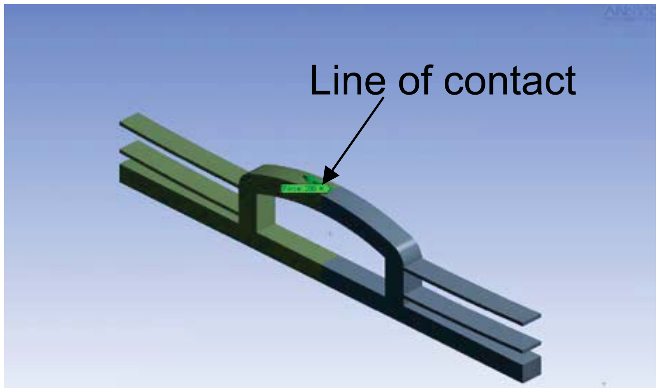

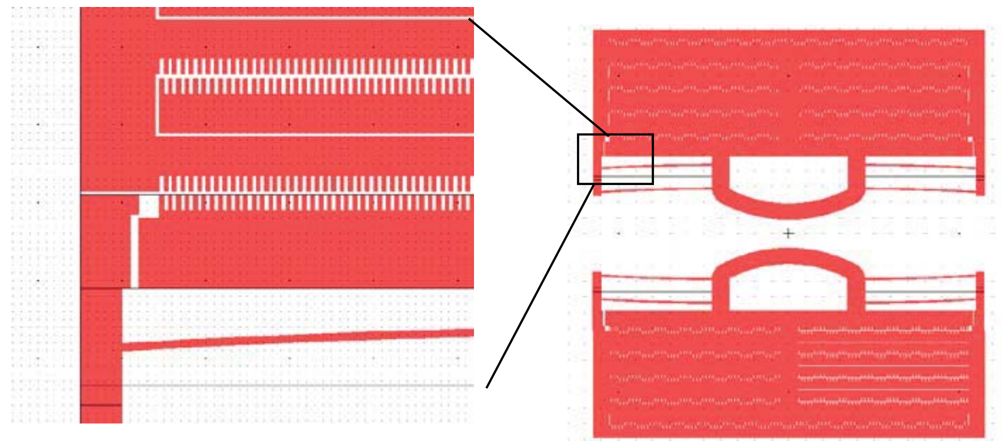

Fixed normal displacement: 10 μm at the line of contact

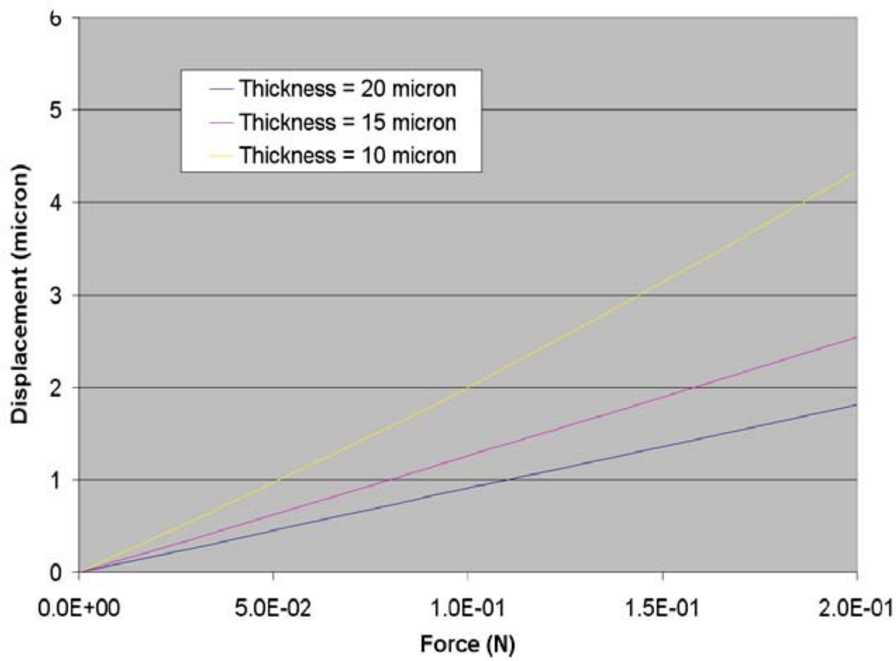

Lateral Displacement vs. Lateral Force with a Fixed Normal Displacement

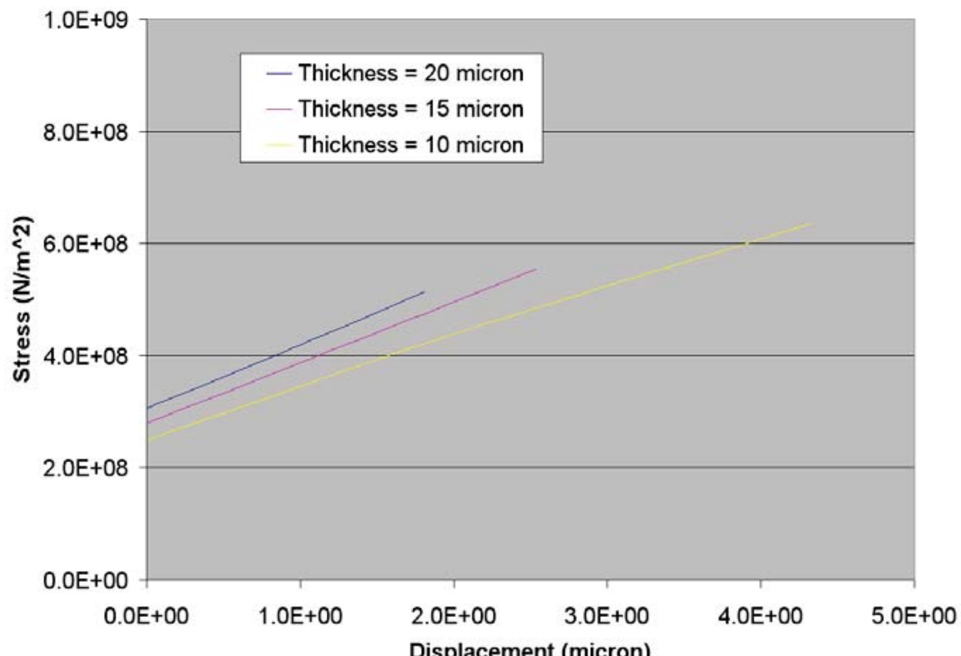

Maximum-Stress vs. Lateral Displacement with a Fixed Normal Displacement

Assembly Sequence

Driver fabrication | **Rail fabrication** | **Slider fabrication**

↓

Slider insertion

↓

Individual comb drive actuation test

↓

Epoxy attachment with PMN-PT

↓

Wire bonding to Rail

↓

Mount on PCB, wiring with Ag-epoxy

↓

Actuation test

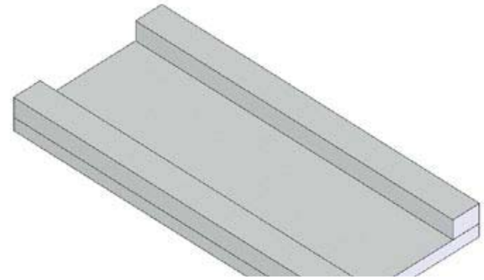

1. Fabricate rail guides.

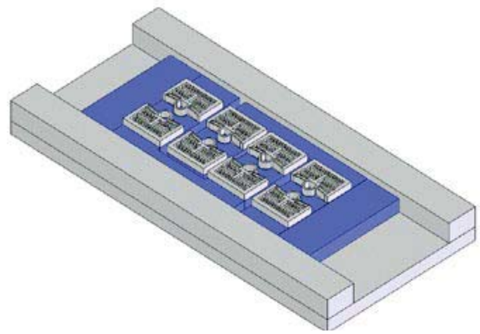

2. Attach driver.

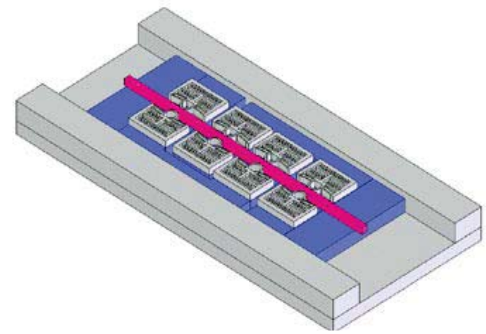

3. Insert slider.

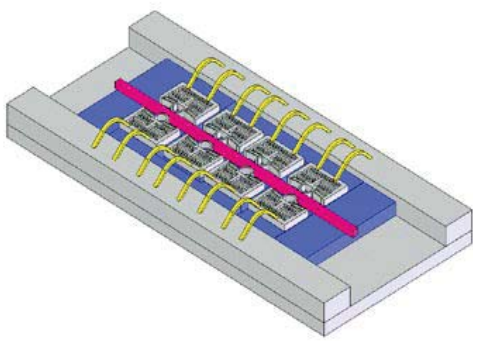

4. Bond Au wires.

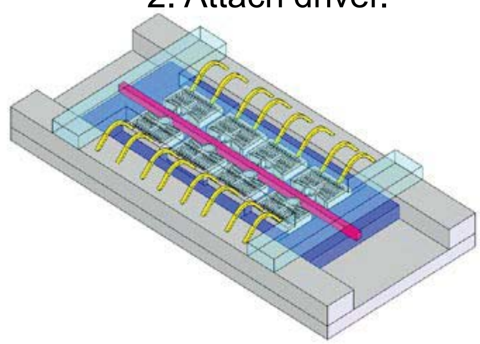

5. Attach the lid.

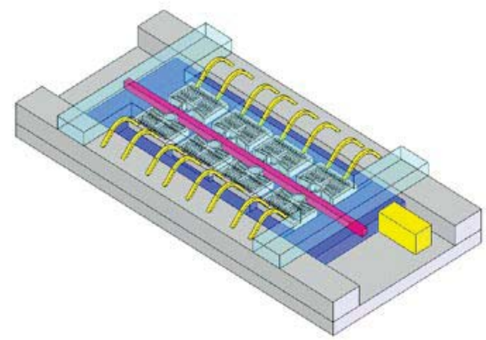

6. Attach the PMN-PT to driver and rail.

Non-linearity: Why?

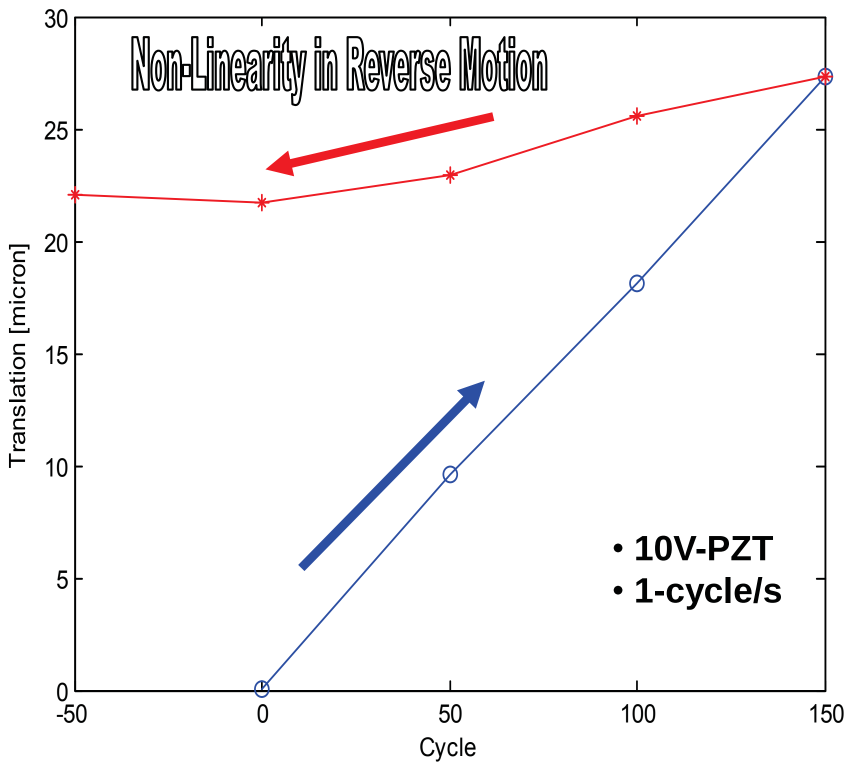

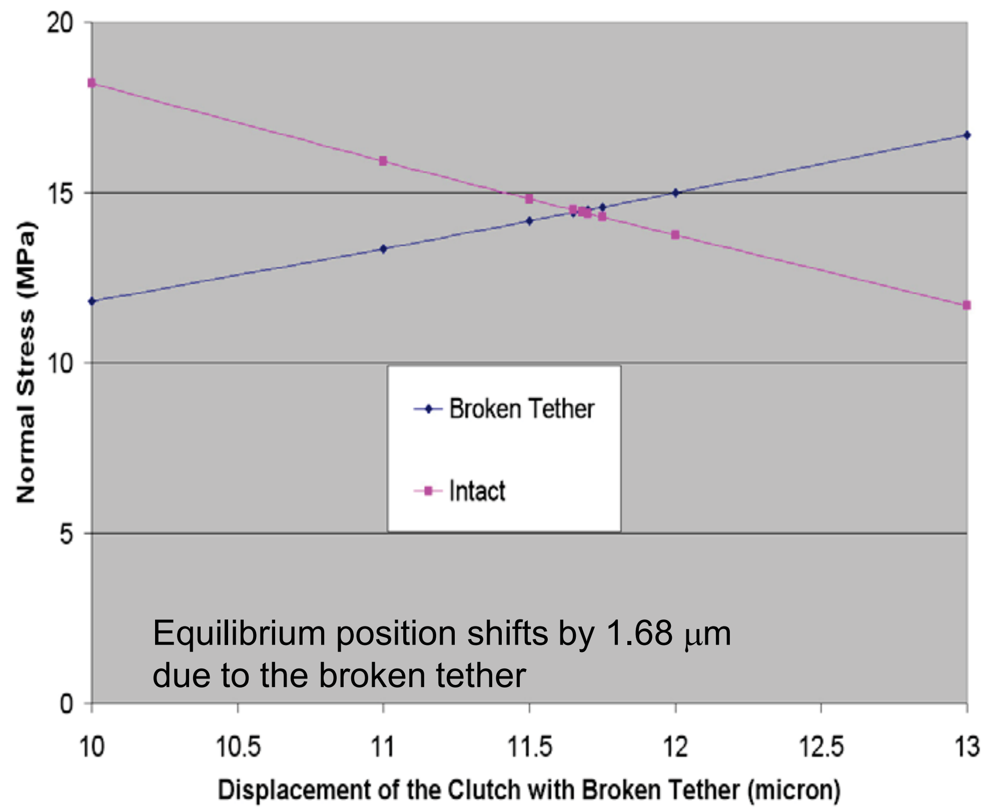

National Aeronautics and Space Administration
Jet Propulsion Laboratory
California Institute of Technology

Non-linearity: Why?

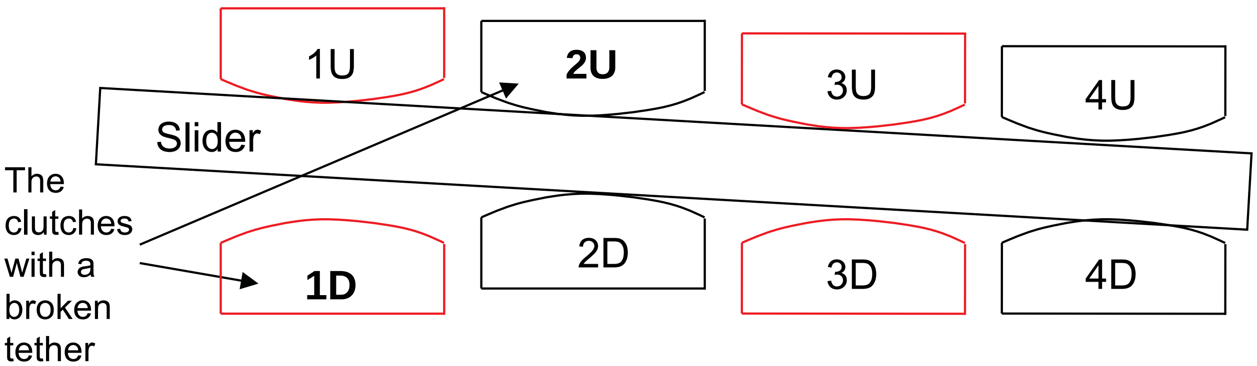

It is more difficult for the clutches to move to the right, because both 1U and 3U are against the movement. In the mean time, there is no resistance against the clutches to move to the left.

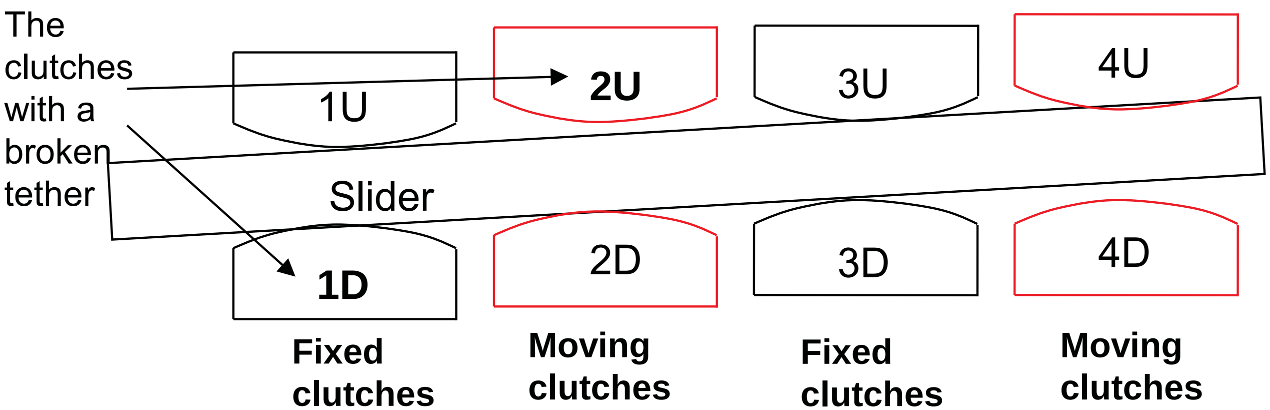

It is about the same for the clutches to move to the right or left, because 2D is against the movement to the right, while 4U is against the movement to the left.

- When the moving clutches are in the clamping position, they have uneven resistance for moving to the left or to the right.
- When the moving clutches are in the releasing position, they have about the same resistance for moving in both directions.

Comparison with SOAs

Requirements	Buleigh (conventional)	Sandia (MEMS)	JPL Demonstrated Performance
Push force, N	15	0.00005	0.05
Speed, mm/s	1	4	*0.08 → 3*
Travel, mm	100	0.1	0.5 / 130-cycle
Size, mm^3	25x25x70	0.6x0.2x?	14x7x0.6
Mass, g	10	-	0.1
Position resolution, nm	1	10	50
Maximum motor frequency, KHz	1	Failed at 46	*0.02 → 1*
Force density (force x speed/mass) W/Kg	1	-	*0.04 → 1.5*
Glitch, nm	<50	-	-
Self-Latching	No	No	Yes

Actuator Max. Force of a 10 μN?

National Aeronautics and Space Administration
Jet Propulsion Laboratory
California Institute of Technology

- Calculated maximum step of an actuator with a 100-μN-force to actuate a structure (with a rod stiffness of 10^4 N/m) is on the order of a 100 angstrom, while the maximum step of an actuator with a 10-mN-force is on the order of 1 μm.

- There are other drastic consequences using actuators with a 100 μN force limit:

  - The structure will not be able to support it's own weight on earth.
  - Any movement will take about a 100 times longer because the maximum step is about a 100 times smaller.
  - Navigating the low force path will be much more difficult since the control precision will need to be 100 times better.
  - The system will be 100 times more unstable.
  - If it is made very soft to accommodate the low forces, it will have a large number of low frequency modes (easily excited and difficult to damp out.)

Comb Drive Motion

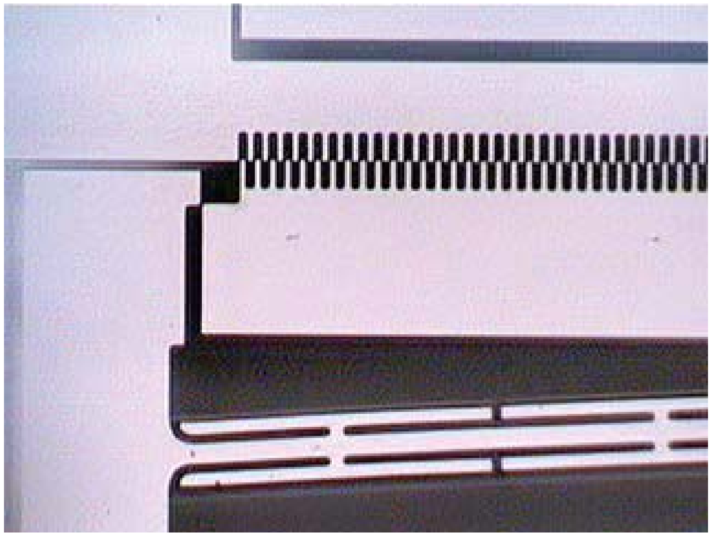

(from Unit B)

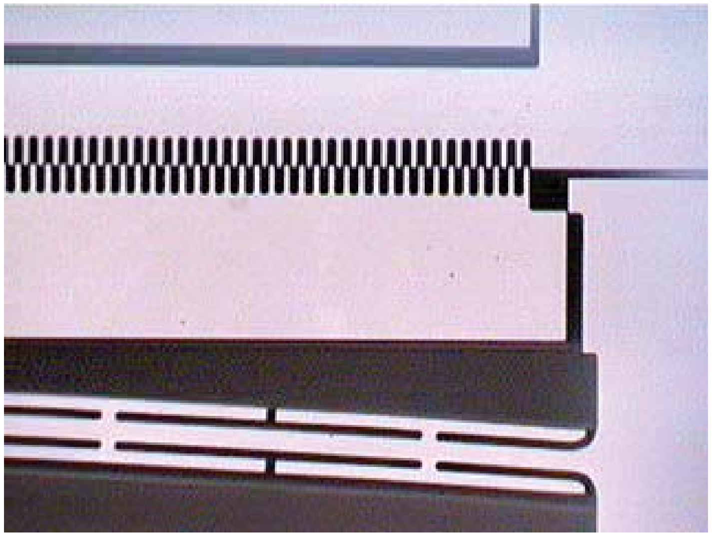

(from Unit A)

Challenge and Other Approaches

Challenge

• Demonstrate leak-tight, low power, high-pressure microvalve technology for integration with micropropulsion systems.

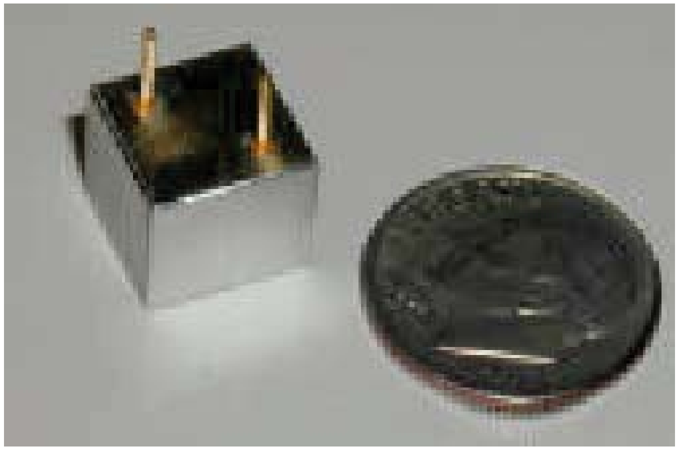

Moog Micro Valve prototype
➔ 4 W to open

Other approaches

• Conventional microvalve technologies: mass/volume, power consumption

➔ *Ex: Moog, VACCO μ-valves: 3-8 W to operate*

• Typical MEMS-based valves: leak or narrow pressure range

➔ *Ex: Redwoods microvalve: 400 ms, 0.2 sccm (20 psi), 2 W*

Microvalve Design

National Aeronautics and Space Administration
Jet Propulsion Laboratory
California Institute of Technology

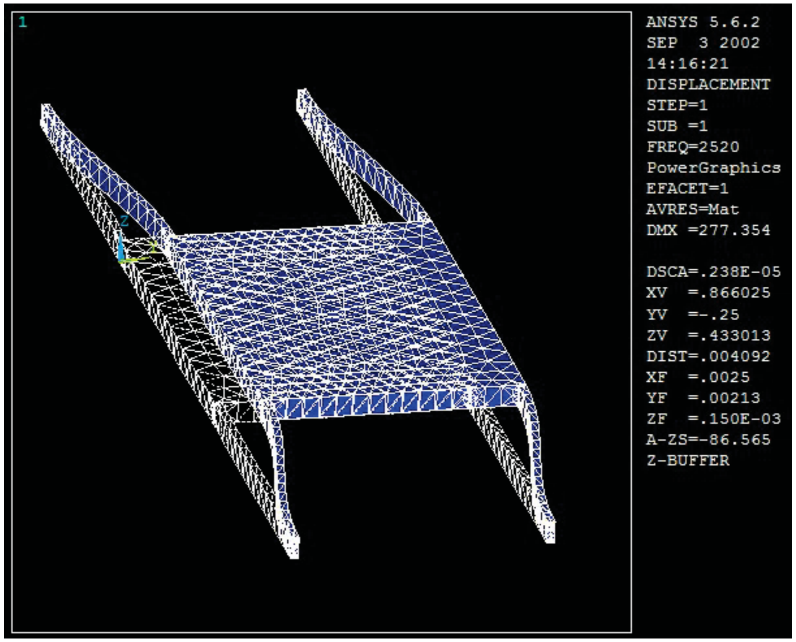

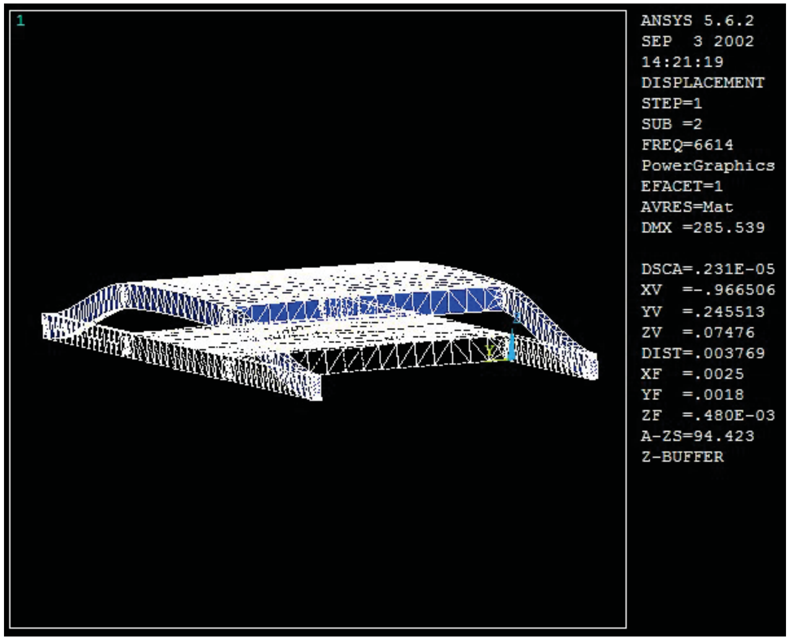

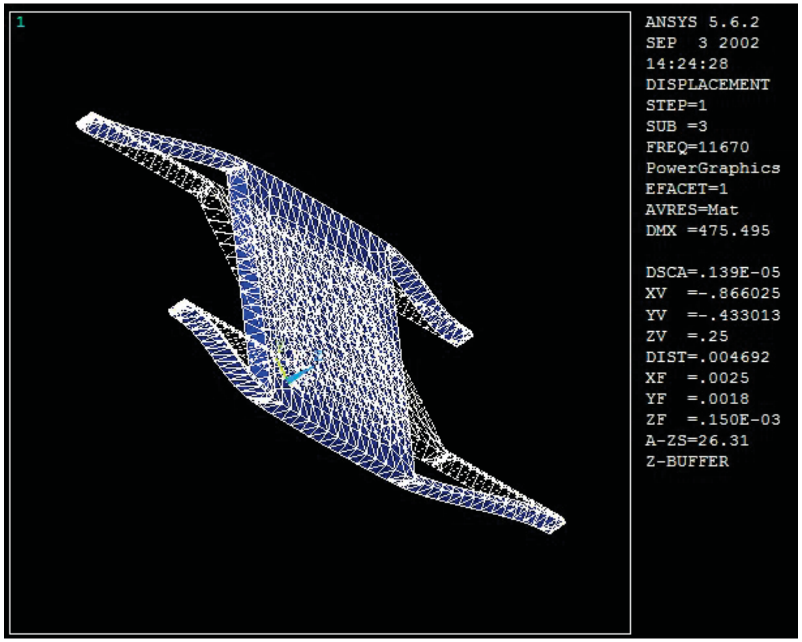

Modal analysis results

Available Data Sets:

Set	Frequency	Load Step	Substep	Cumulative
1	2519.5	1	1	1
2	6614.3	1	2	1
3	11670.	1	3	1
4	21043.	1	4	1

Read Next Previous

Microvalve Design

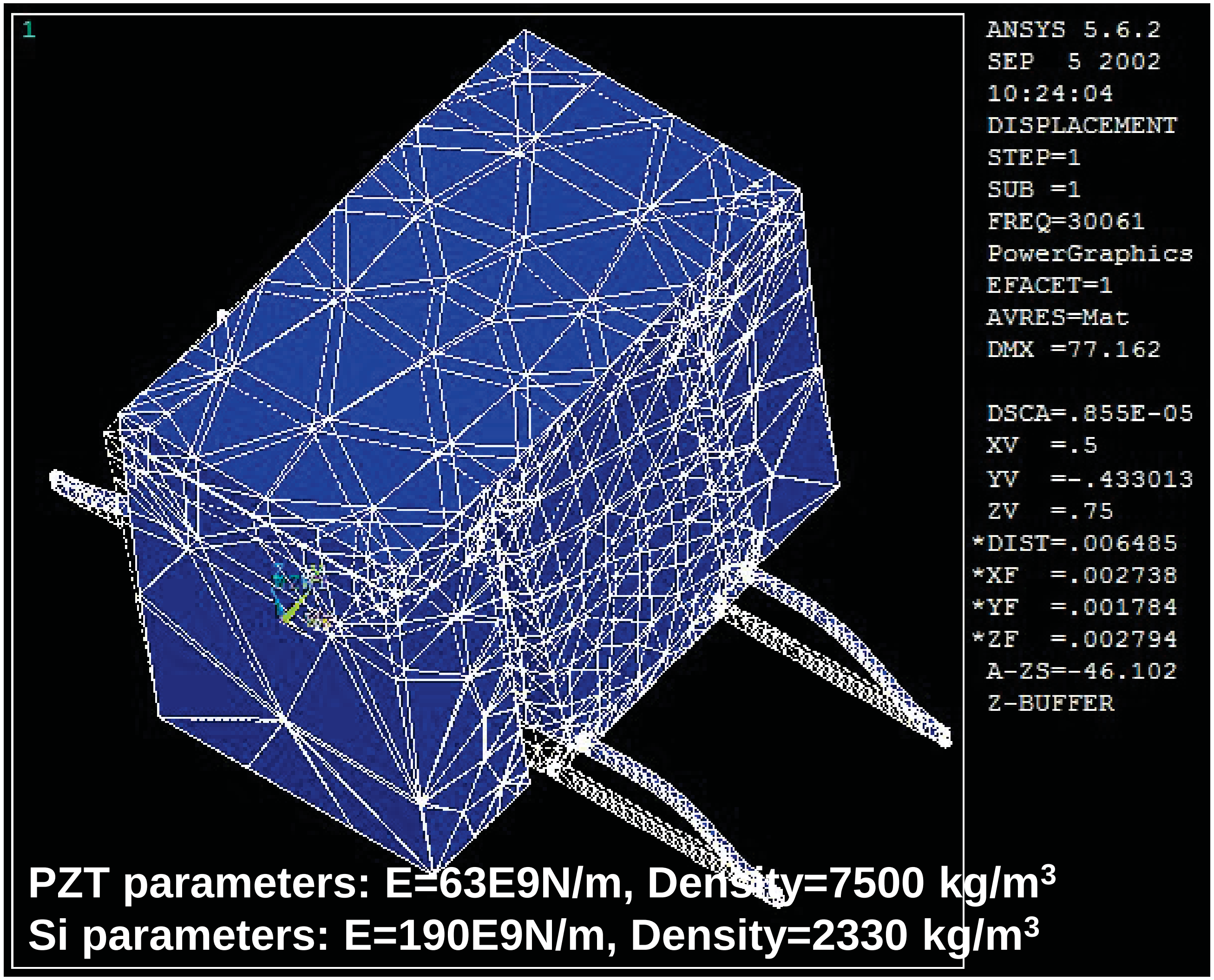

Microvalve with PZT (1st mode, f_0=30kHz)

PZT-Stack: Working Principle

National Aeronautics and Space Administration
Jet Propulsion Laboratory
California Institute of Technology

- Displacement of PZT = f(electric field, piezoelectric coefficient, size)
- Material properties is described by d_{ij} [m/V](piezoelectric coefficient)

Displacement of PZT: $\Delta L = S \cdot L = (+/-)\, E \cdot d_{ij} \cdot L_o$

Direction of poling
Direction of expansion

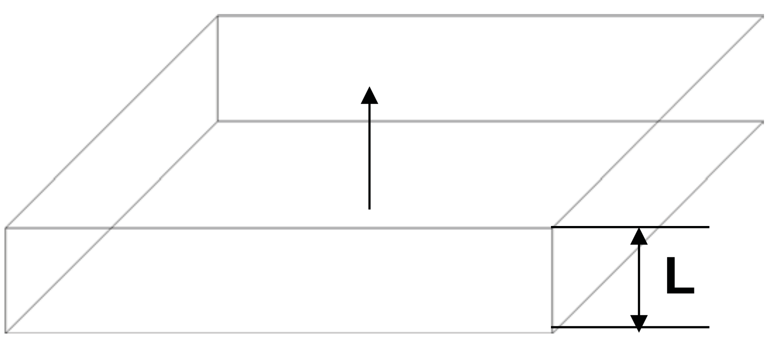

d33 mode

Direction of poling

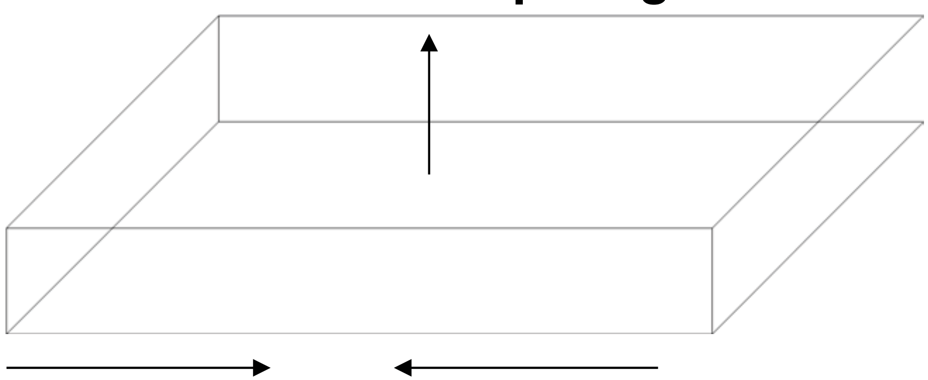

Direction of contraction
d31 mode

Surface Roughness of Seat Materials

National Aeronautics and Space Administration
Jet Propulsion Laboratory
California Institute of Technology

- Surface roughness of PECVD SiO_2 and thermal SiO_2

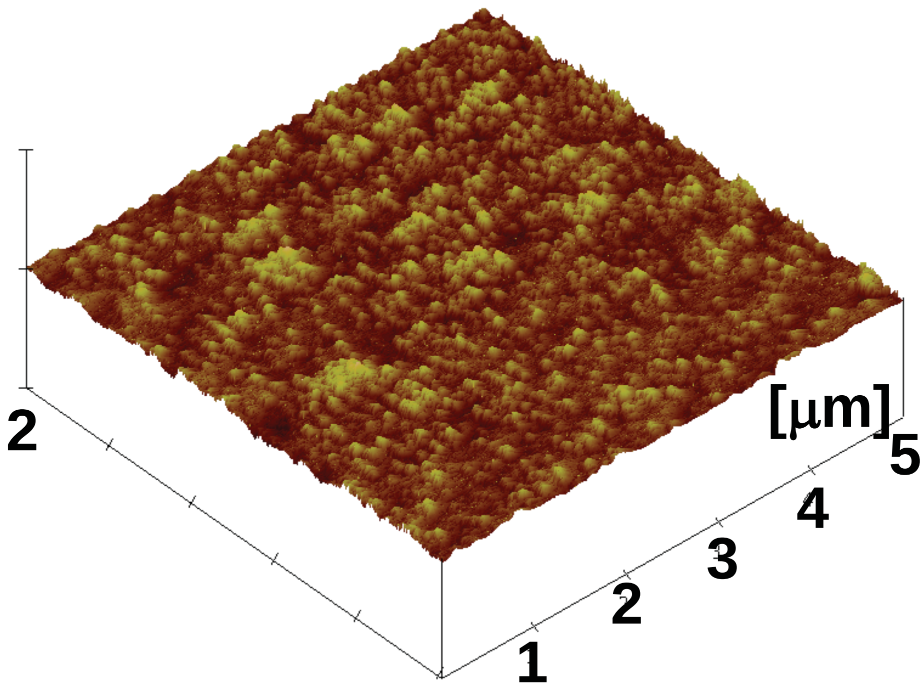

< PECVD SiO_2 >

- rms roughness: 2.6 nm

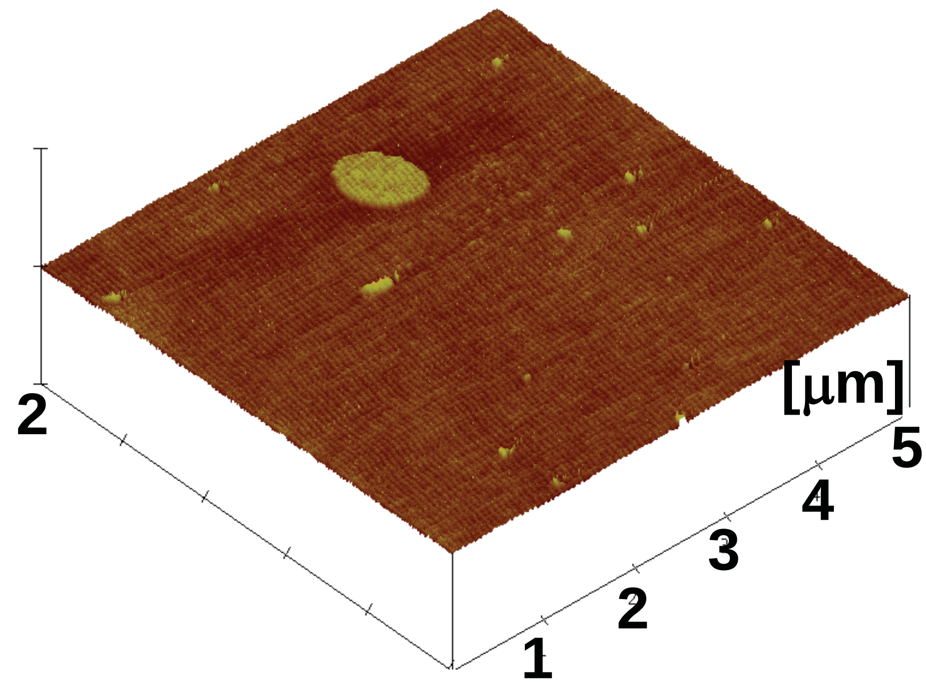

< Thermal SiO_2 >

- rms roughness: 0.3 nm

Test Setup

National Aeronautics and Space Administration
Jet Propulsion Laboratory
California Institute of Technology

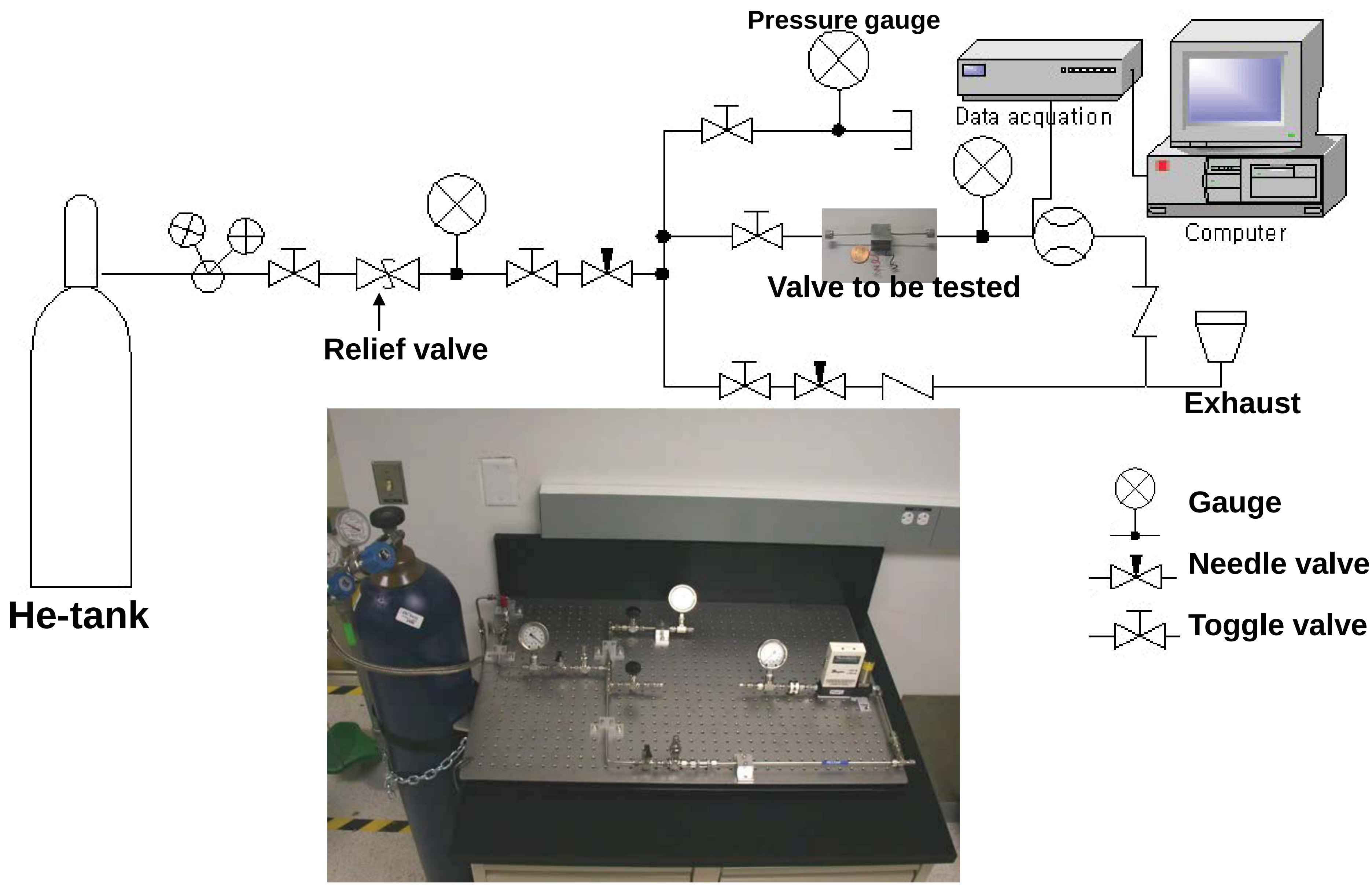

Dynamic Power Consumption

National Aeronautics and Space Administration
Jet Propulsion Laboratory
California Institute of Technology

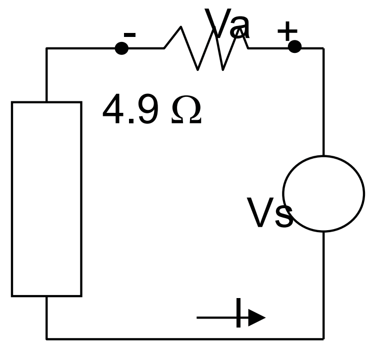

$P = 1/2 VI\cos\theta = V_{rms} I_{rms} \cos\theta$

θ: phase difference between V and I

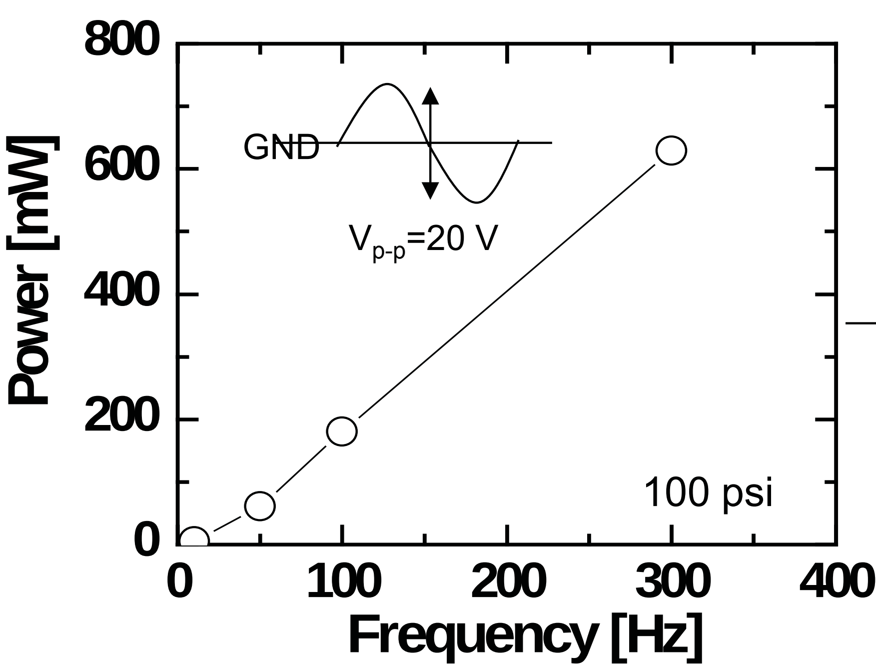

Example; @ 50 Hz

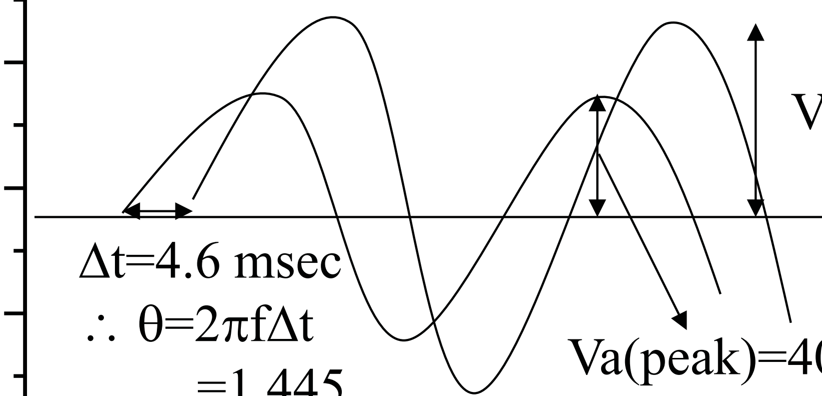

Vs(peak)=10V

Δt=4.6 msec

$\therefore\ \theta = 2\pi f \Delta t$

$= 1.445$

Va(peak)=400 mV

$\therefore$ I(peak)=Va(peak)/R

= 81.6 mV

$\therefore$ PZT power consumption: ~61 mW